Dark Energy & Galaxy Clusters

Stefano Ettori
(INAF-OA Bologna)

OUTLINE

1. Galaxy Clusters in a cosmological context: an introduction
2. Galaxy Clusters: how and what we observe
3. From observed GC to Cosmology: the mass proxies & constraints on DE

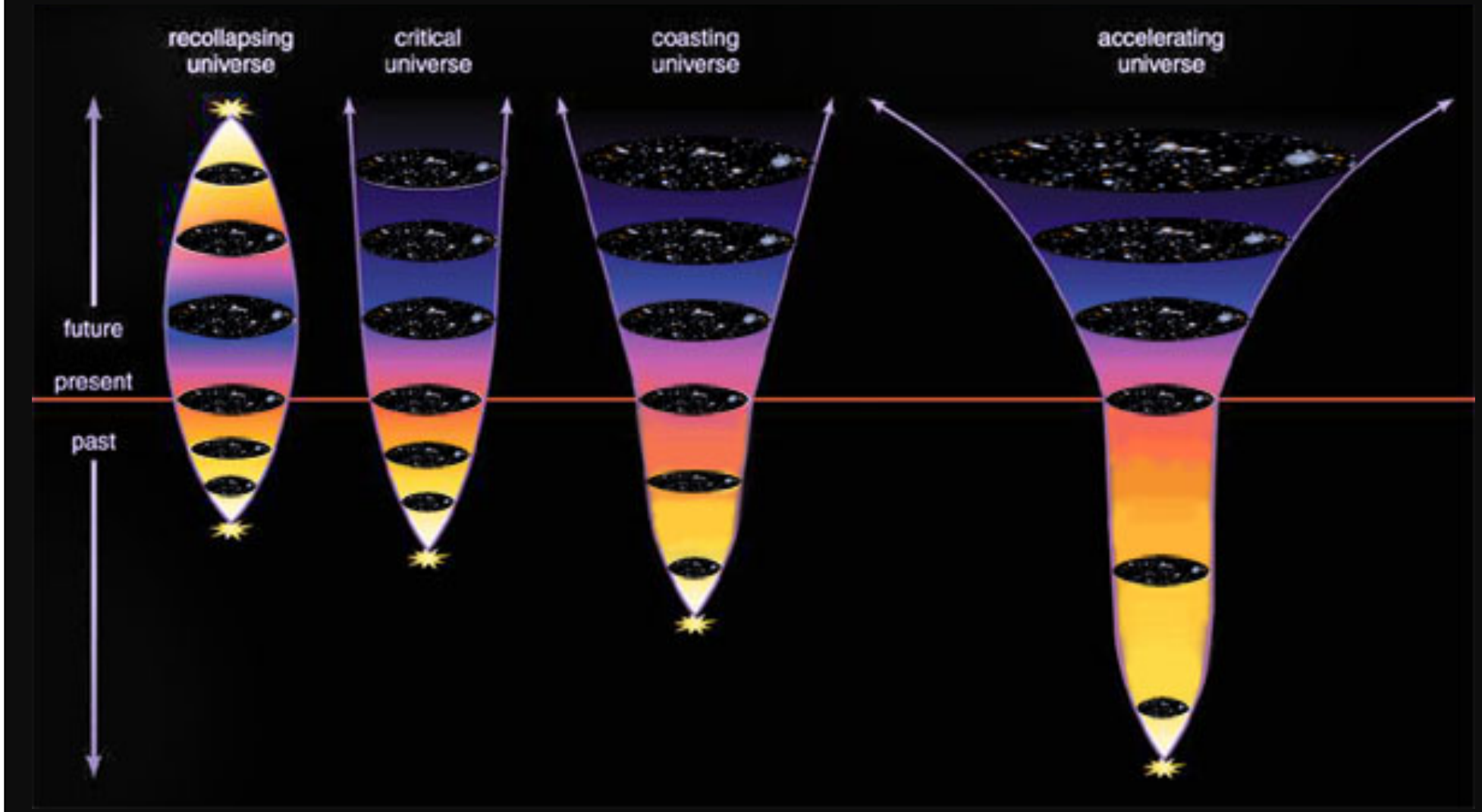
recollapsing universe
critical universe
coasting universe
accelerating universe
future
present
past

Dark Energy
& Dark Matter

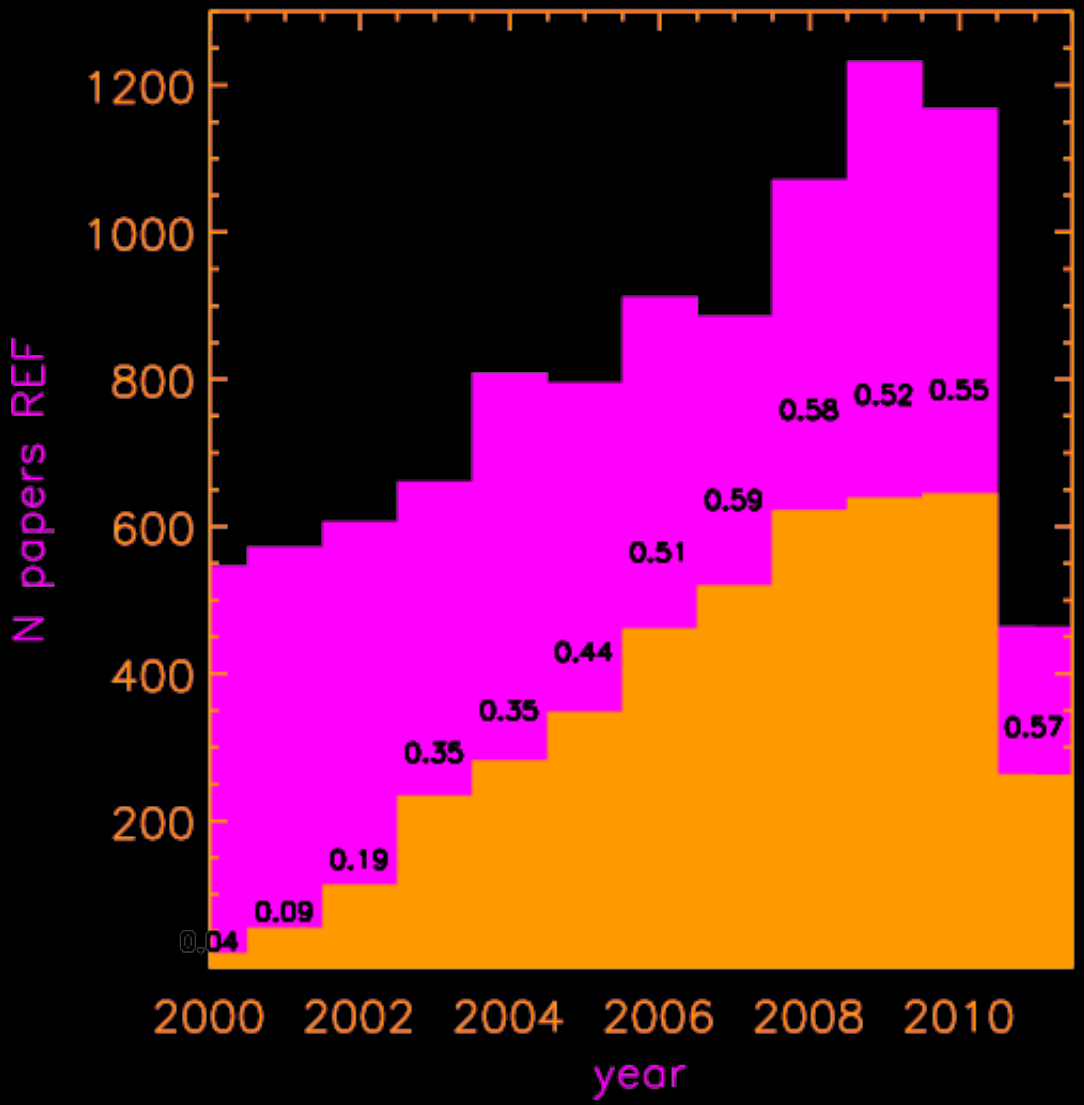

Dark Energy & Galaxy Clusters

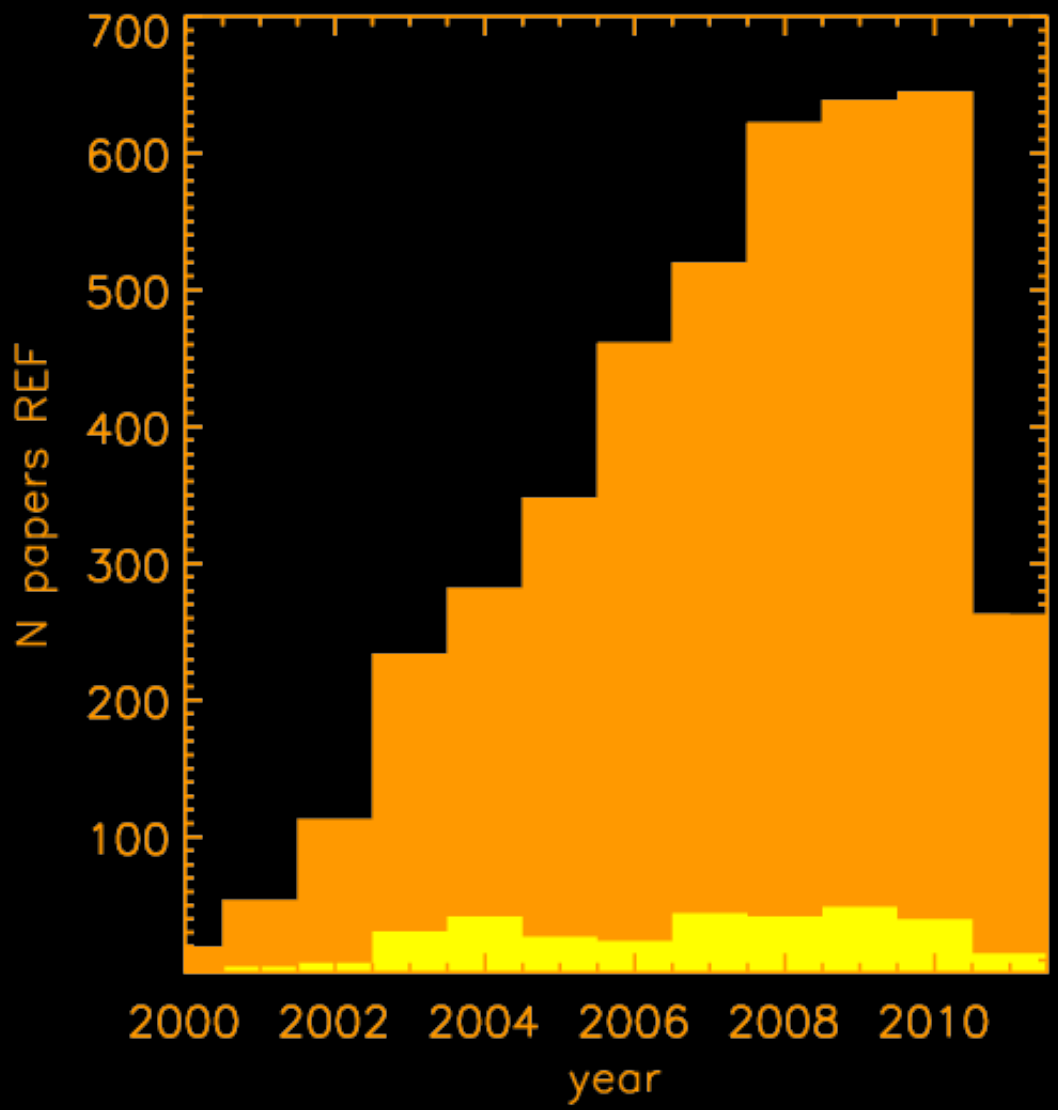

Dark Energy & Galaxy Clusters

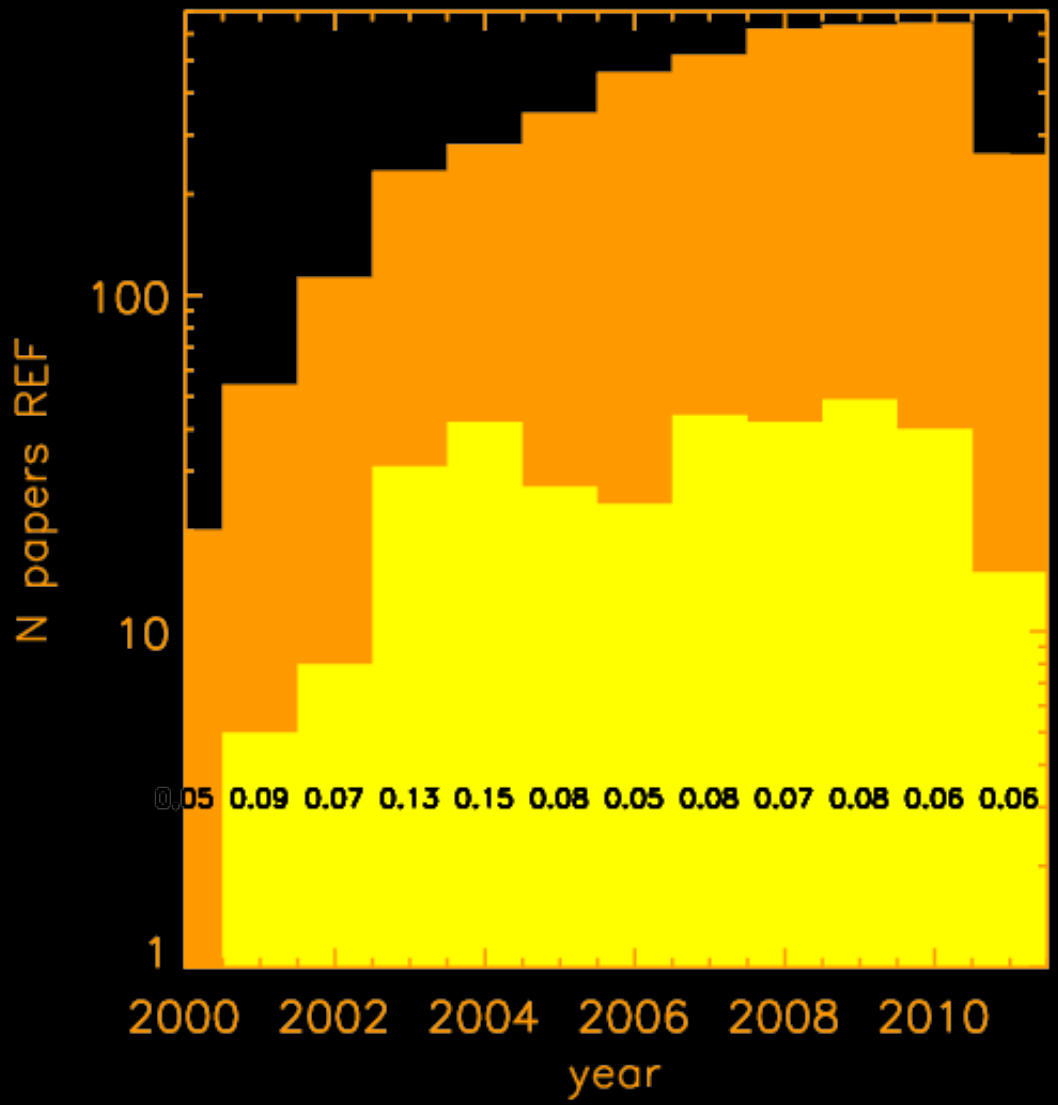

Galaxy Clusters in a cosmological context: an introduction

Stefano Ettori
(INAF-OA Bologna)

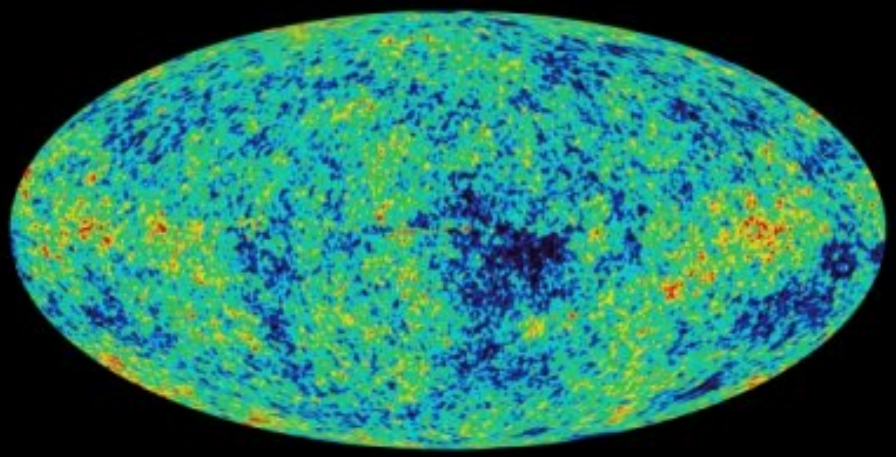

WMAP

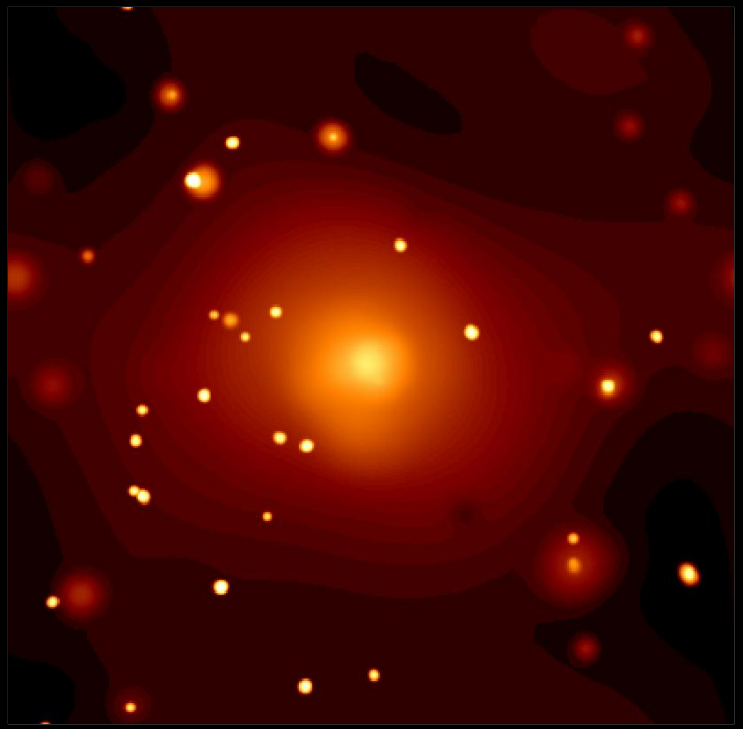

rxj1252 (z=1.24)

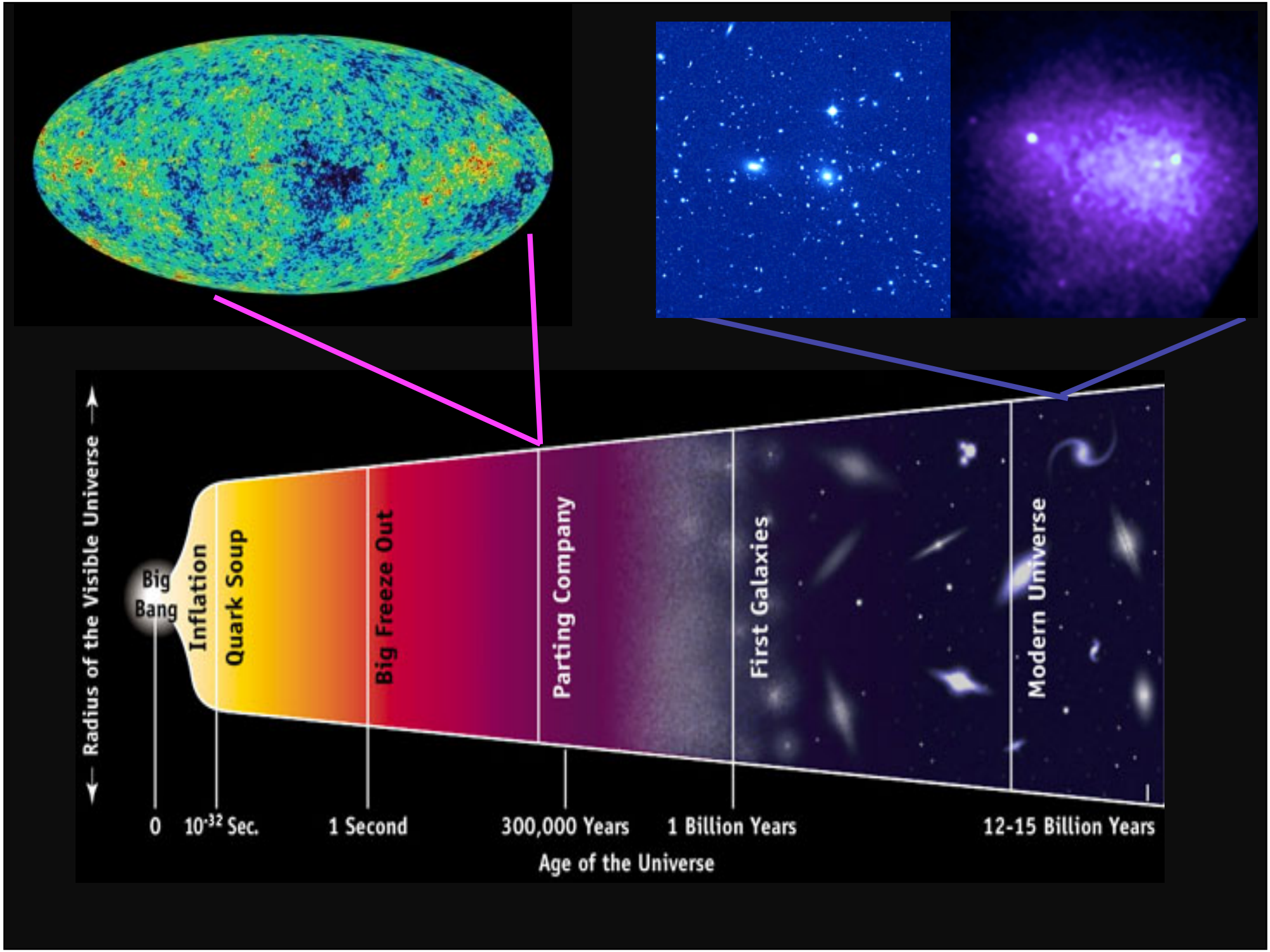
Radius of the Visible Universe
Big Bang
Inflation
Quark Soup
Big Freeze Out
Parting Company
First Galaxies
Modern Universe
0
10-32 Sec.
1 Second
300,000 Years
1 Billion Years
12-15 Billion Years
Age of the Universe

Galaxy clusters & cosmology

Friedmann model: the simplest model of the Universe based on the **cosmological principle** that the matter distribution is isotropic (the same in all directions) ➔ homogeneous (independent of location)

$$H^2 = \left(\frac{\dot{a}}{a}\right)^2 = \frac{8\pi G}{3}\rho - \frac{kc^2}{a^2} + \frac{\Lambda c^2}{3}$$

$$\dot{H} + H^2 = \left(\frac{\ddot{a}}{a}\right) = -\frac{4\pi G}{3}\left(\rho + \frac{3P}{c^2}\right) + \frac{\Lambda c^2}{3}$$

These equations determine the time evolution of the cosmic scale factor $a(t)/a(0) = (1+z)^{-1}$

To solve this system of equations, we need to specify the equation of state $w=P/(\rho c^2)$: the Universe starts as dominated from relativistic particles (w=1/3) and ends as filled with cold matter (w=0)

Galaxy clusters & cosmology

Expansion rate & mass-energy densities

$$\Omega = \frac{\rho}{\rho_c}, \quad \rho_c = \frac{3H^2}{8\pi G}$$

$$\Omega_0 = \Omega_M + \Omega_\Lambda + \Omega_R = 1 - \Omega_k$$

$$\Omega_R \approx 4.16e-5 \ (T_{CMB}/2.726K)^4$$

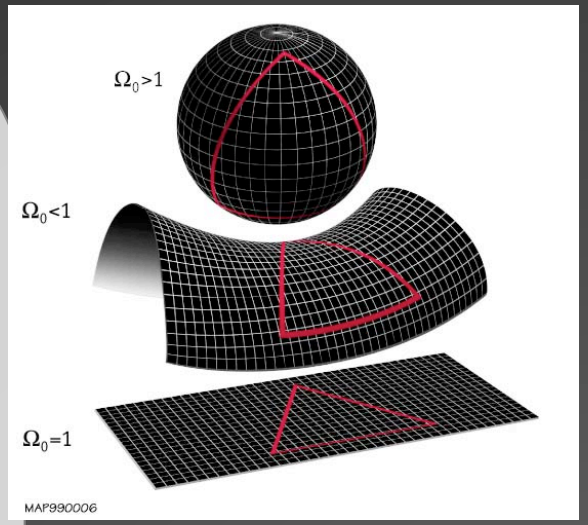

$$\left(\frac{\dot{a}}{a}\right)^2 = H_z^2/H_0^2 = \Omega_R a^{-4} + \Omega_M a^{-3} + \Omega_k a^{-2} + \Omega_\Lambda$$

$$= \Omega_0 (1+z)^{3(1+w)} + (1-\Omega_0)(1+z)^2$$

$$= \Omega_k (1+z)^2 + \Omega_M (1+z)^3 + \Omega_\Lambda \lambda(z)$$

$$\lambda(z) = \exp\left(3\int_0^z \frac{1+w(z)}{1+z} dz\right)$$

Galaxy clusters & cosmology

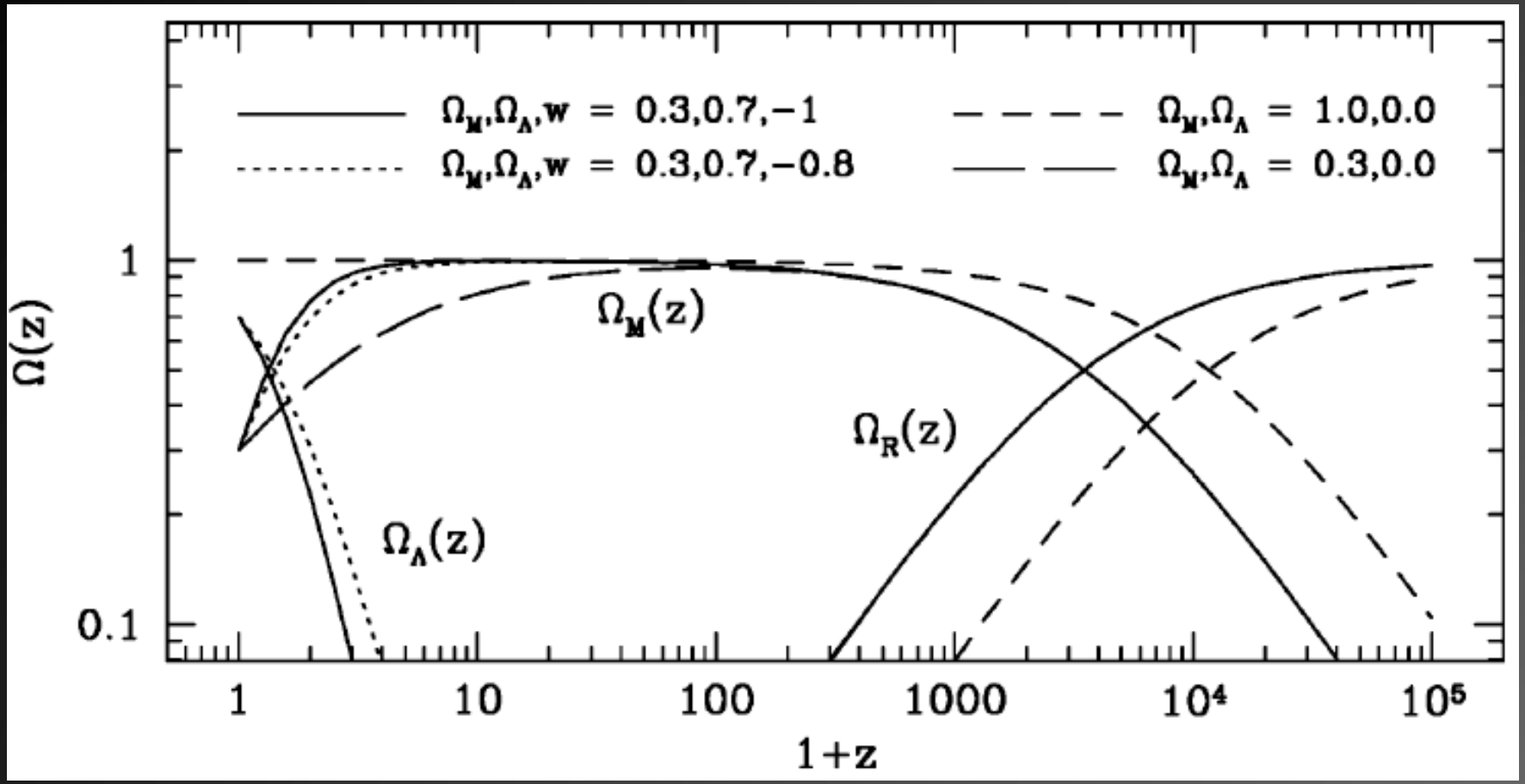

Voit 05

Matter dominates the dynamics at z>1

Dark energy becomes relevant at z<2

Radiation was the most important component before $z_{eq}=2e4\Omega_m$

Galaxy clusters & cosmology

But we are in Bertinoro … the Universe is not perfectly homogeneous and the density perturbations begin to grow accreting materials from the neighboring underdense regions

$$\delta = \frac{\rho_m - \langle\rho\rangle}{\langle\rho\rangle} \quad \ldots \; P(k) = \langle |FFT(\delta)|^2 \rangle$$

$\sigma^2 = \langle | \delta M/M |^2 \rangle = \int\{P(k)\, d^3k\}$

σ_8^2 = power spectrum variance on 8/h Mpc

$$\ddot{\delta} + 2\frac{\dot{a}}{a}\dot{\delta} = 4\pi G \rho_m \delta$$

$$d(\ln\delta) = \Omega_{m,z}^{\gamma} d(\ln a)$$

This approximation matches the evolution of δ with $\gamma \approx 0.55$

Galaxy clusters & cosmology

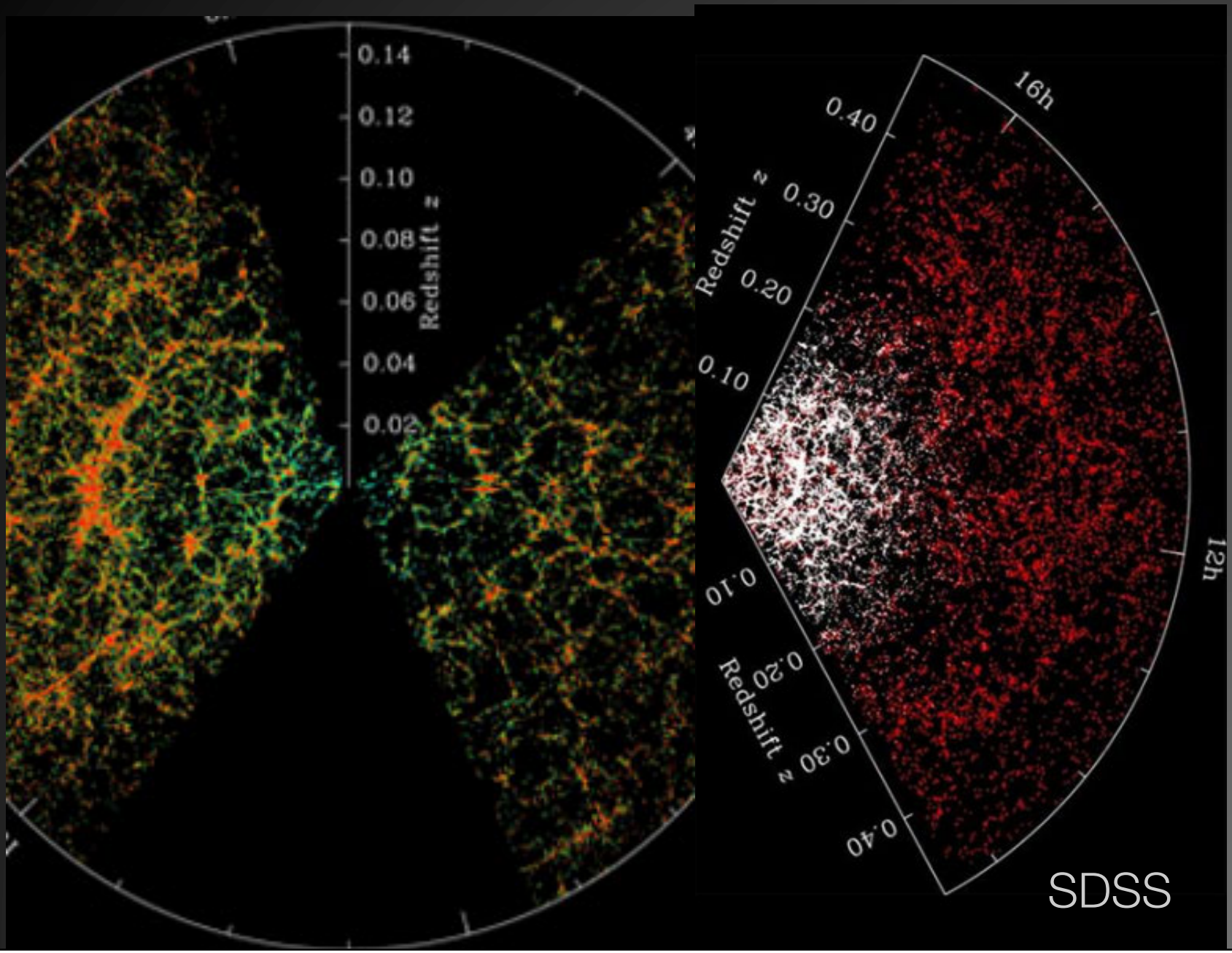

Dark Matter & galaxy clusters

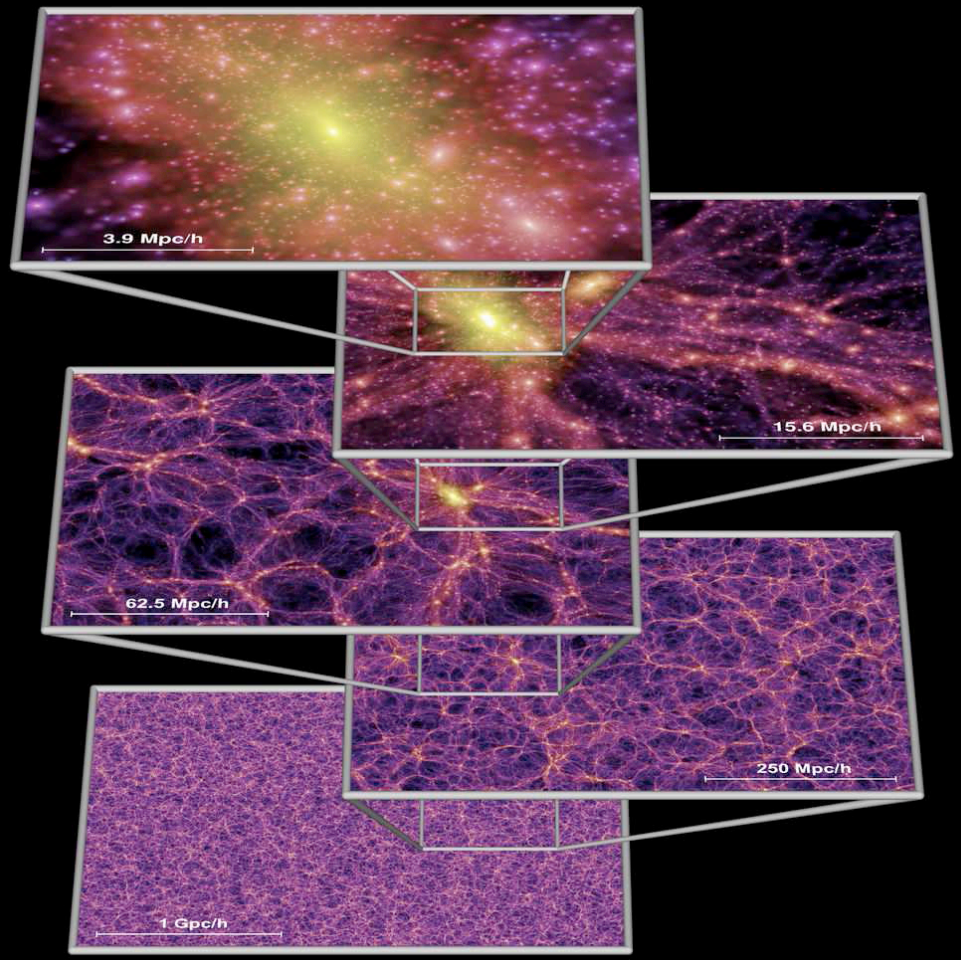

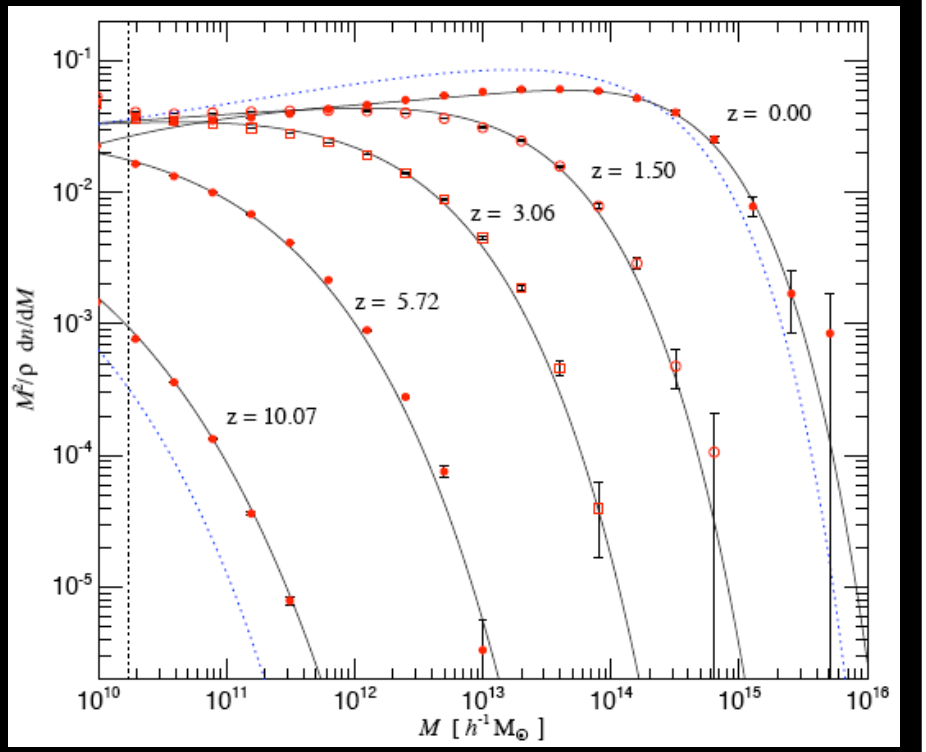

Ω_m=0.25=1- Ω_Λ
h=0.73
σ_8=0.9

L=500/h Mpc

(*Springel et al. 2005*) Millennium simulations:
10^{10} particles of ~9e8 /h $M_\odot$

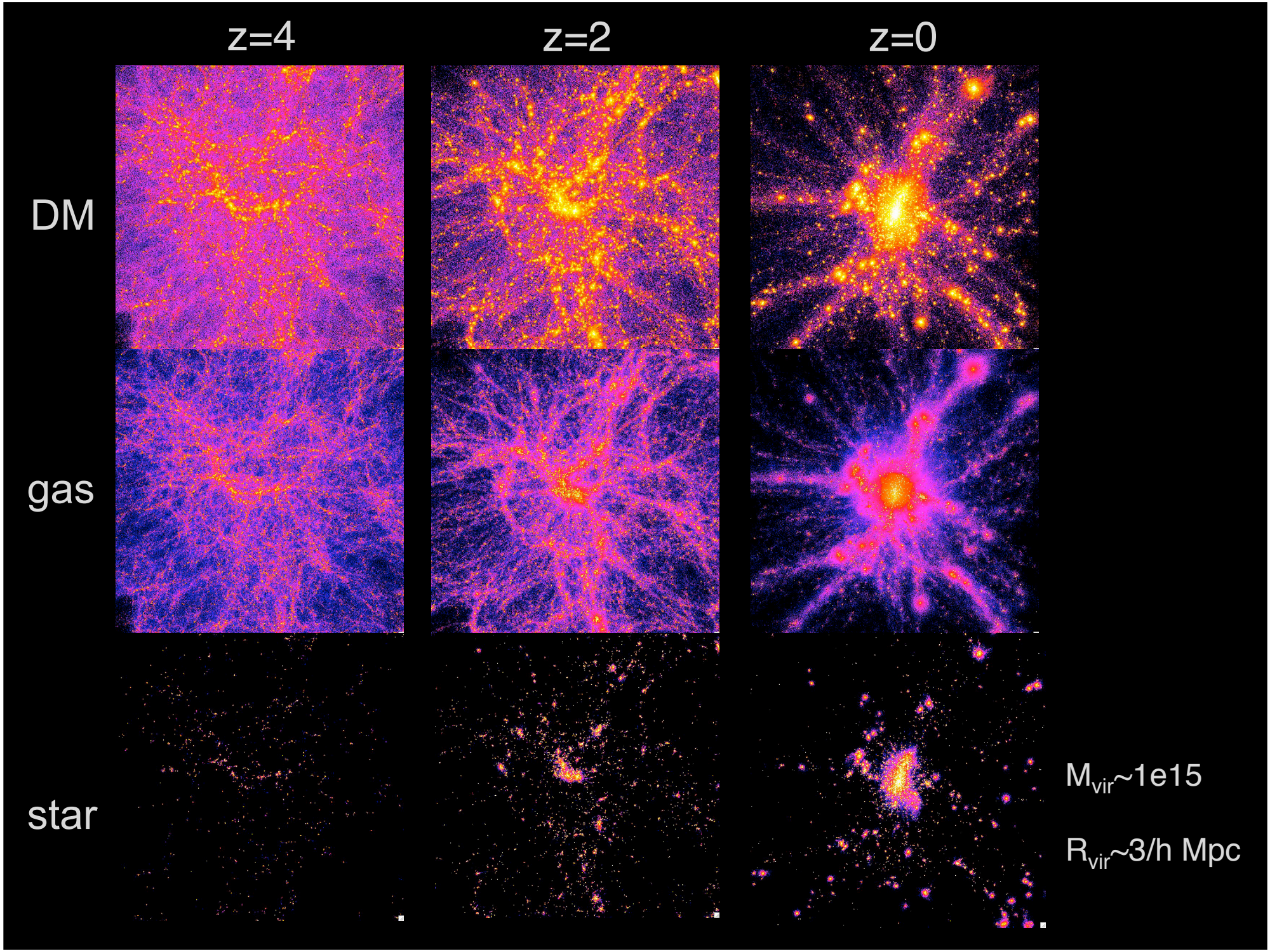
z=4
z=2
z=0
DM
gas
star
M_{vir}~1e15
R_{vir}~3/h Mpc

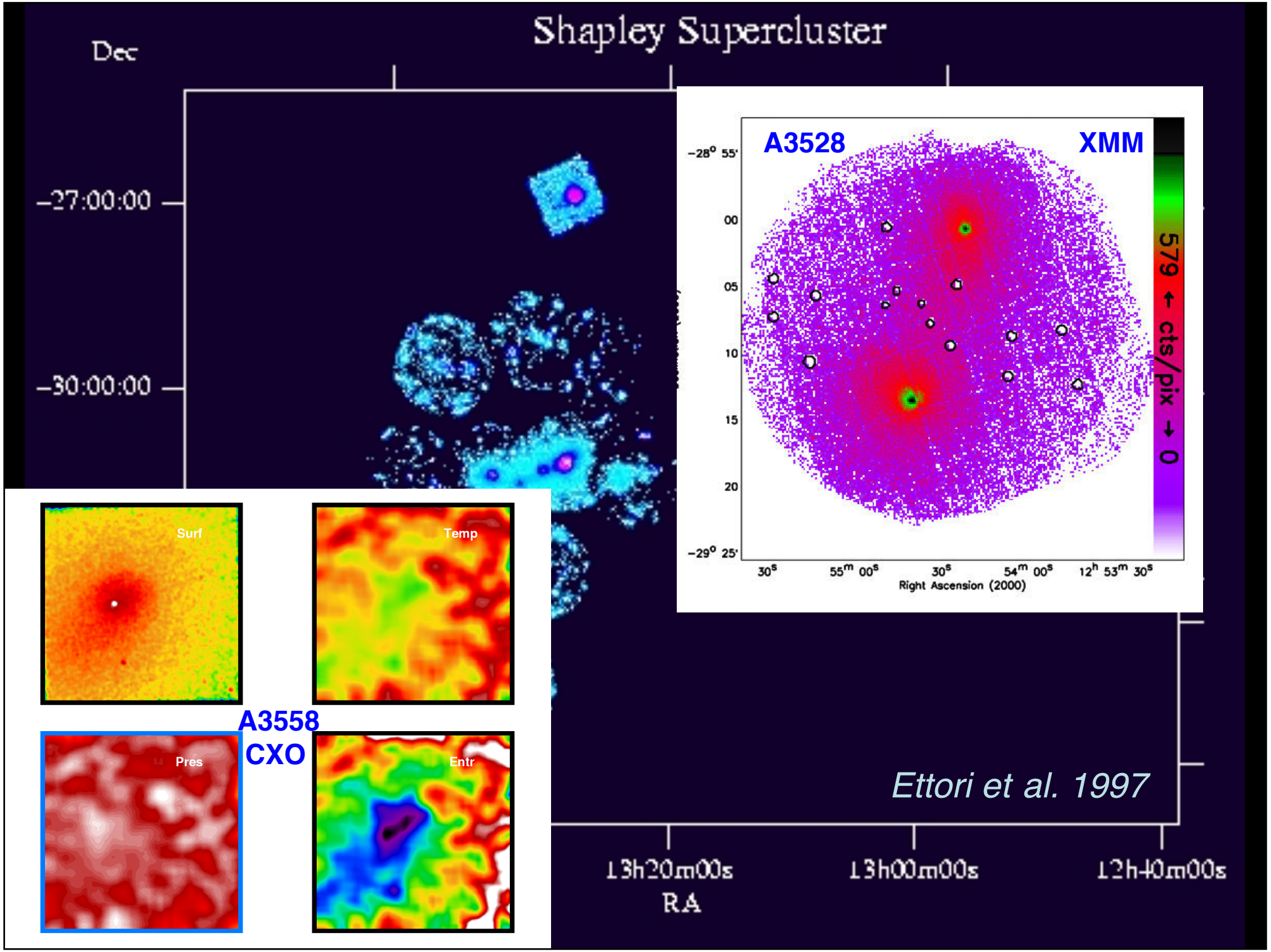
Shapley Supercluster
Dec
−27:00:00
−30:00:00
A3528
XMM
−28° 55'
00
05
10
15
20
−29° 25'
579 → cts/pix → 0
30s
55m 00s
30s
54m 00s
12h 53m 30s
Right Ascension (2000)
Surf
Temp
A3558
CXO
Pres
Entr
Ettori et al. 1997
13h20m00s
13h00m00s
12h40m00s
RA

Observable Properties of Clusters

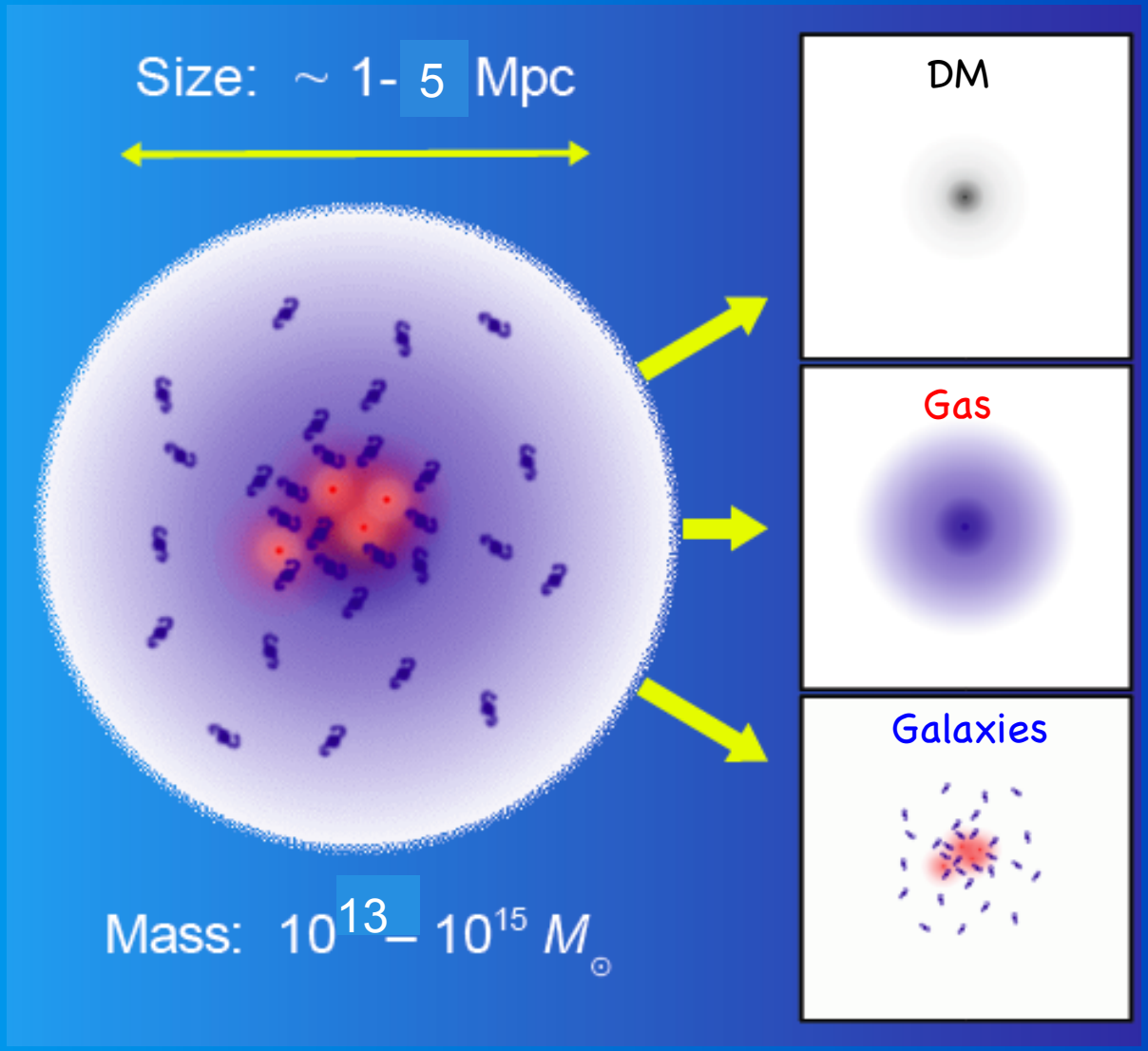

Composition of the Cosmos

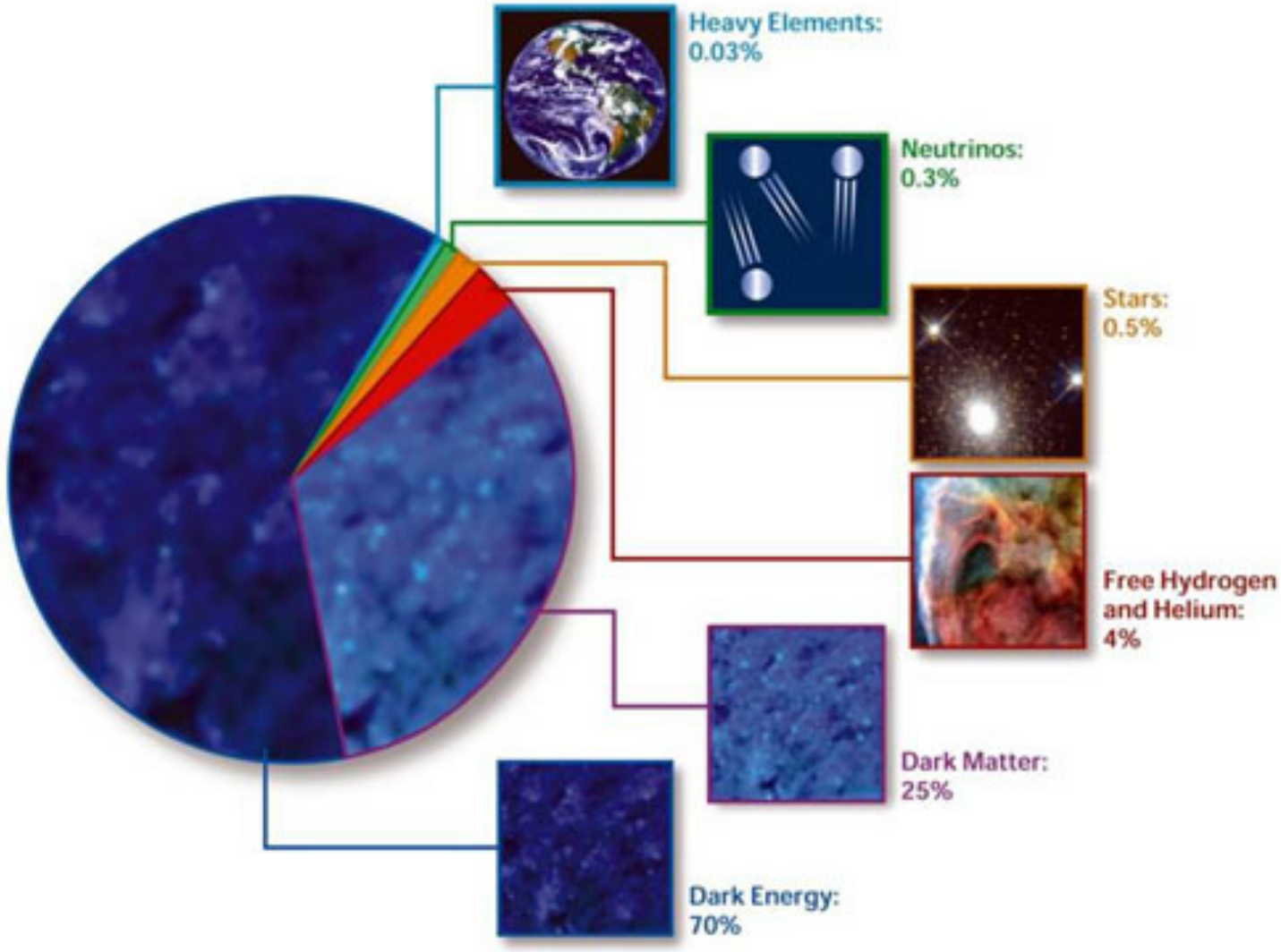

Galaxy clusters & cosmology

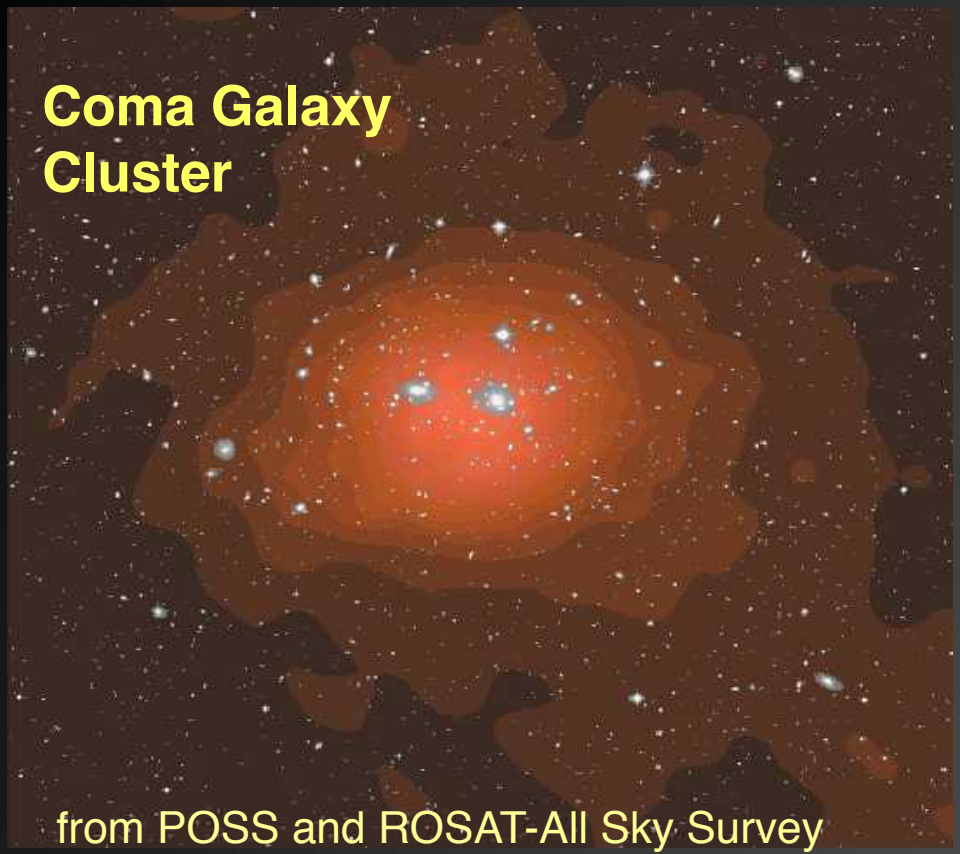

74 – 83% = Dark Matter
15 – 20% = *hot* ICM
2 - 6% = *cold* galaxies

Galaxy clusters & cosmology

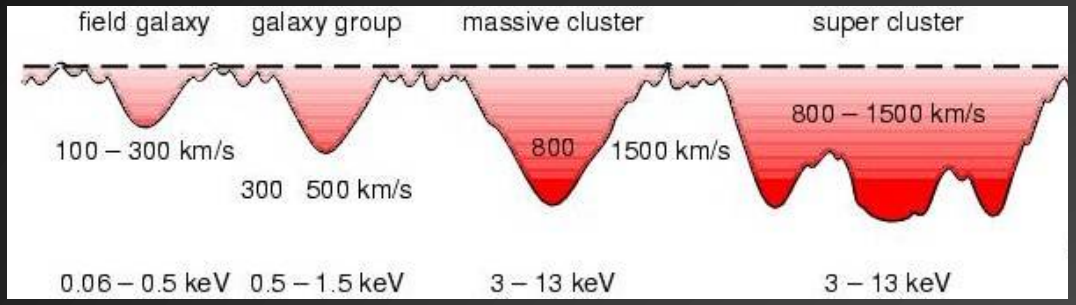

GCs are the largest gravitationally-bound structures in the Universe.
They form by hierarchical aggregation of smaller clumps in correspondence of the highest peaks of the primordial density field.

They are detached from Hubble flow and
have a total mass of ~10^{14}-10^{15} Solar masses (1 M = 2e33 g).
Their baryons are collected within regions of ~10 Mpc (3e25 cm).

Galaxy clusters contain only 4% of the cosmic mass,
but forming in correspondence of the highest density peaks trace the general properties of the Universe with their distribution in time (=redshift) and space.

Galaxy clusters & cosmology

Clusters are gravitationally-bound systems (otherwise, they'd disperse in a crossing time of 1 Gyr): $E=T+U < 0$

T [Kinetic energy] = $\frac{1}{2} \Sigma m_i v_i^2$

U [Potential energy]: $-\frac{1}{2} \Sigma G m_i m_j / r_{ij}$

Integrating the equation of galaxy motion: $\frac{1}{2} d^2I/dt^2 = 2T+U$

Assuming that the galaxy distribution is stationary ($d^2I/dt^2=0$), then: $2T+U = 0$

This is the **Virial theorem:** for gravitationally-bound systems in equilibrium, the total energy is ½ of the time-averaged potential energy U *OR* U=-2K, where K is time-averaged kinetic energy … $M_{tot} \sigma^2 = G M_{tot}^2 / R_G$ … $M_{tot} = R_G \sigma^2 / G$

Galaxy clusters & cosmology

- Concentration of 100-1000 galaxies
- Velocity dispersion (observed): $\sigma_v \sim 1000$ km s^{-1}
- Size: R ~ 1 Mpc $\Rightarrow$ the crossing time (lower limit to the relaxation time) is $t_{cross} = R/\sigma_v \sim 1$ Gyr < $t_H = 9.8\ h^{-1}$ Gyr
  $\Rightarrow$ clusters must be dynamically relaxed at the present
- **Mass:** assuming virial equilibrium $\Rightarrow$ $M \simeq \frac{R\sigma_v^2}{G} \simeq \left(\frac{R}{1}\right)\left(\frac{\sigma_v}{10^3}\right)^2 10^{15}\, h^{-1} M_\odot$
- Mass components: $f_{baryons} \approx$ 10-15%
  ($f_{gas} \approx$10%, $f_{gal} \approx$ a few%) $\Rightarrow$ $f_{DM} \approx$ 80-90%
- Intra-Cluster Gas: $T_X \approx$ 3-10 keV, $n_{gas} \approx 10^{-3}$ atoms/cm^3,
  Z ~ 0.3 solar $\Rightarrow$ **fully ionized plasma,** free-free bremsstrahlung + lines
  emission: $L_X \sim n_{gas}{}^2 \Lambda(T)\, V \sim 10^{43}$-$10^{45}$ erg/s

$$k_B T \simeq \mu m_p \sigma_v^2 \simeq 6 \left(\frac{\sigma_v}{10^3}\right)^2 \text{keV}$$

Dark Matter & X-ray clusters

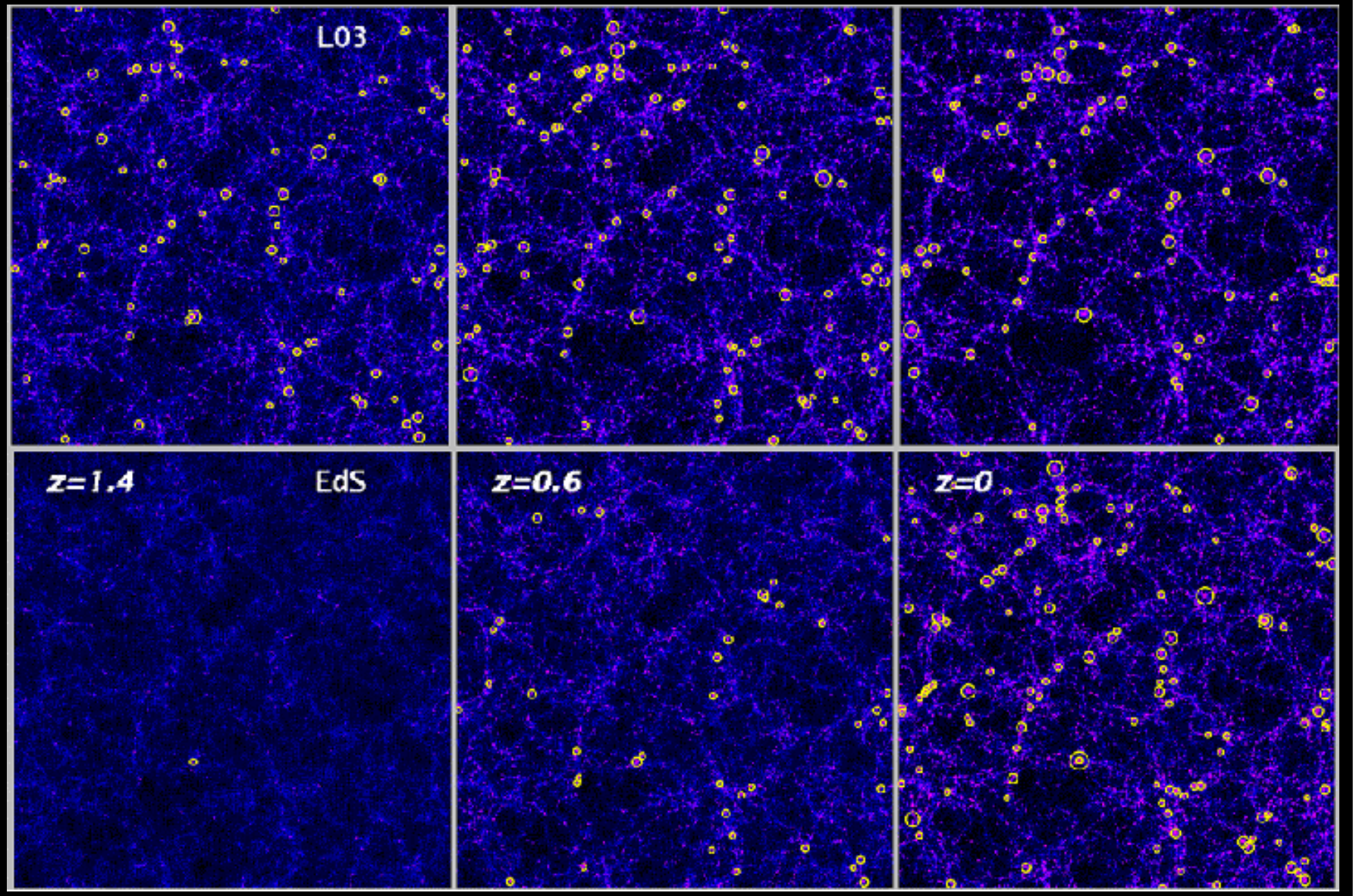

Ω_m=0.3
=1- Ω_Λ

EdS

(*Borgani & Guzzo 2001*) Normalized to space density at z=0;
circles: clusters with T>3 keV & $\propto$T

Galaxy clusters & cosmology

$$\frac{dN(X;z)}{dX\,dz} = \frac{dn(M,z)}{dM}\frac{dM}{dX}(z,p)\frac{dV}{dz}$$

$$\frac{dV}{dz}$$

Friedmann background: priors on cosmological parameters Ω_i

$$\frac{dn(M,z)}{dM}$$

Growth history: precisely calibrated with N-body Simulations. E.g. Jenkins et al. 00:
$=-0.315\ \rho_o/M\ 1/\sigma_M\ d\sigma_M/dM\ \exp[-|0.61-\log(D_z\sigma_M)|^{3.8}]$

$$\frac{dM}{dX}(z,p)$$

Astrophysics: priors on nuisance parameters p_j from follow-up observations and/or cosmological simulations

Galaxy clusters & cosmology

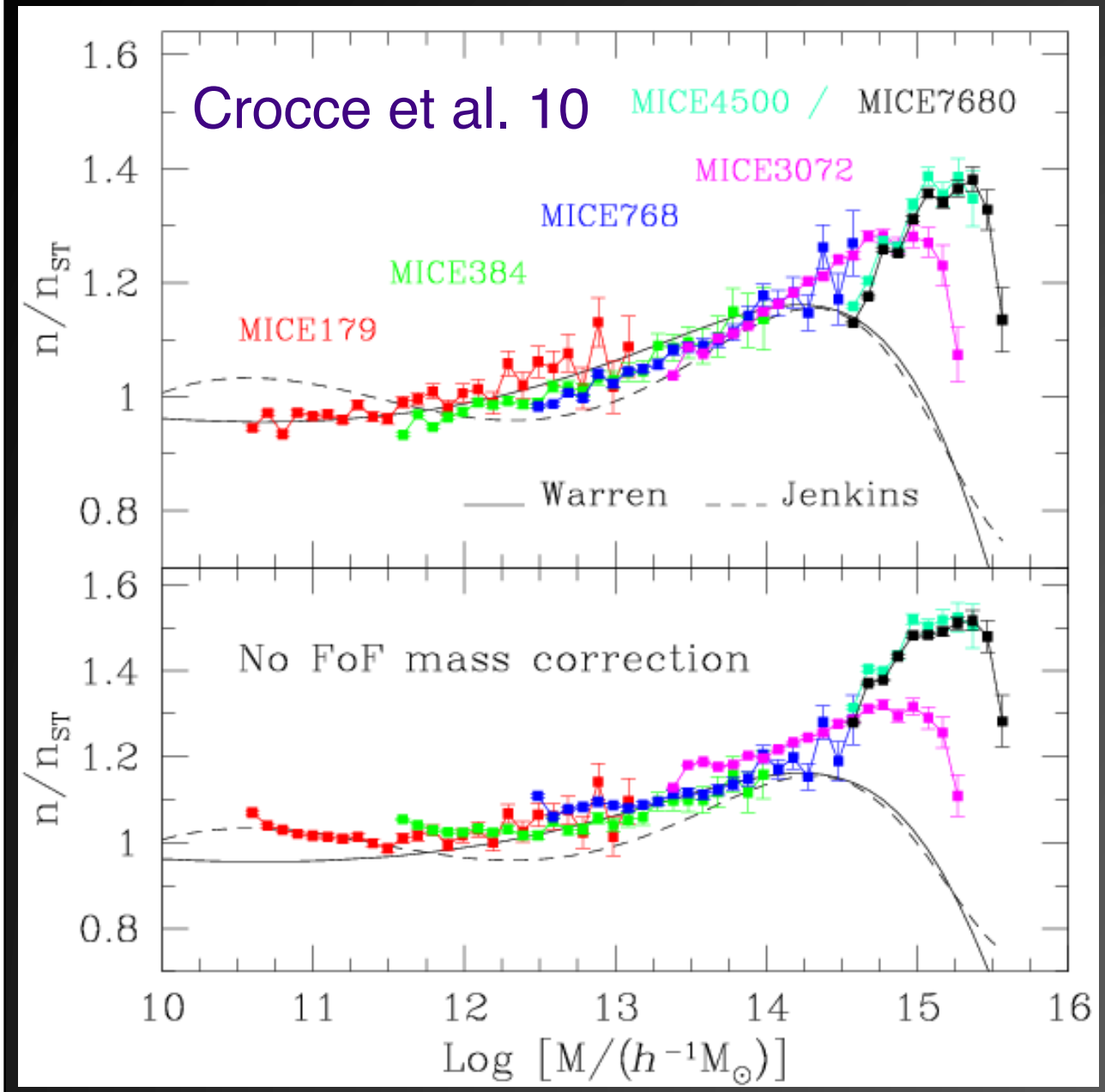

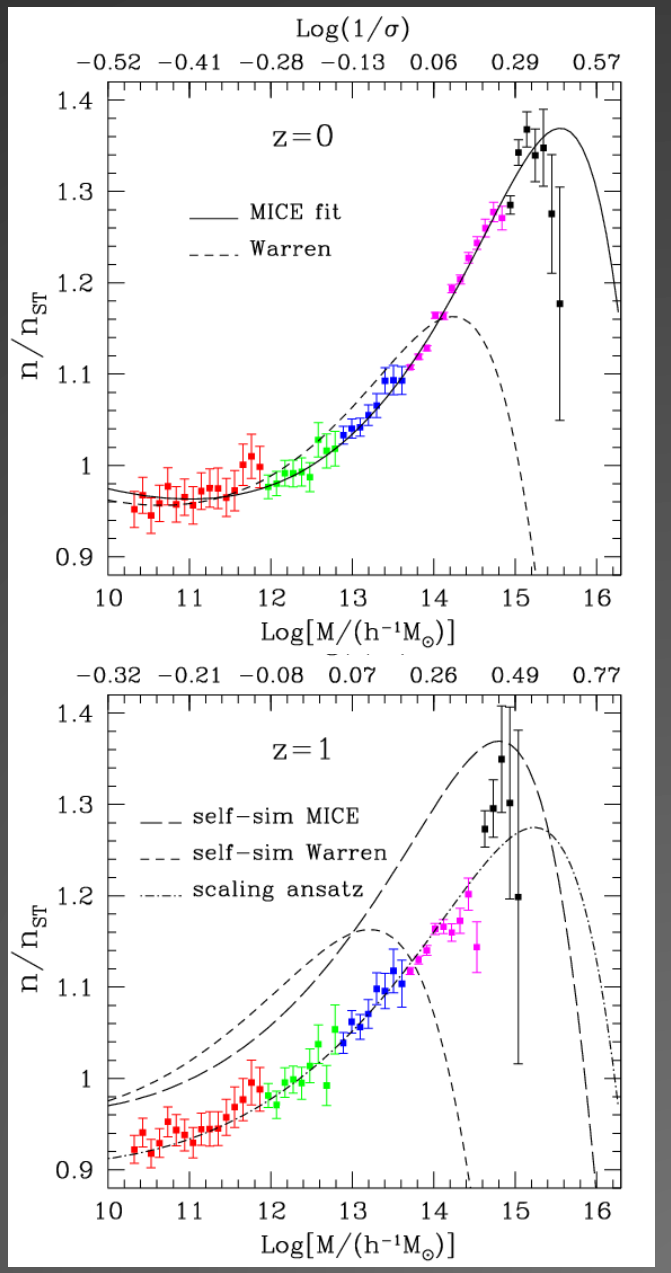

Galaxy clusters & cosmology

Changing Ω_m=0.27, 0.3, 0.33; w=-0.2, -0.6, -1

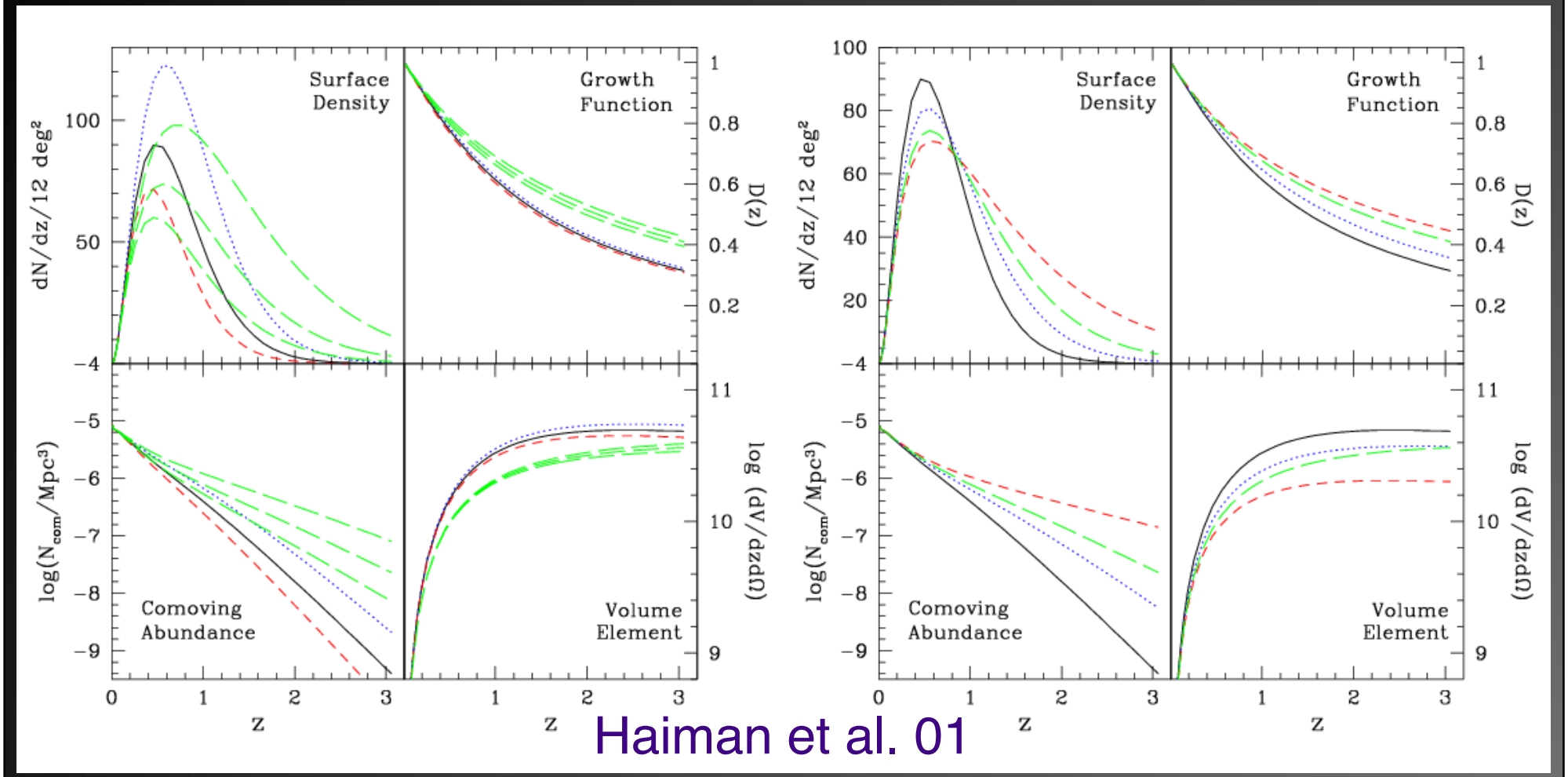

Haiman et al. 01

Galaxy clusters & cosmology

Number counts of clusters in a *given mass and redshift bin* is the most fundamental quantity in cluster cosmology.
The cosmological power of cluster number counts arises from their exponential sensitivity to the amplitude of the initial density perturbations.

However, to implement this experiment, the total mass of each cluster, which is dominated by dark matter, has to be inferred from available observables such as lensing, member galaxies, X-ray and the SZ effect.

$$\bar{n}_{i(b)} = \int_{z_{i,\min}}^{z_{i,\max}} dz \frac{d^2V}{dz d\Omega} \int_{M_{b,\min}}^{M_{b,\max}} dM_{\rm obs} \times \int dM \frac{dn}{dM} p(M_{\rm obs}|M) = \int dz \frac{d^2V}{dz d\Omega} \int dM \frac{dn}{dM} S_{i(b)}(M;z),$$

Galaxy clusters & cosmology

$$\bar{n}_{i(b)} = \int_{z_{i,\min}}^{z_{i,\max}} dz \frac{d^2V}{dz d\Omega} \int_{M_{b,\min}}^{M_{b,\max}} dM_{\rm obs} \times \int dM \frac{dn}{dM} p(M_{\rm obs}|M) = \int dz \frac{d^2V}{dz d\Omega} \int dM \frac{dn}{dM} S_{i(b)}(M;z),$$

$$d^2V/dzd\Omega = \chi^2/H(z)$$

$$\chi(z) = \int_0^z dz' \frac{1}{H(z')},$$

$$H^2(a) = H_0^2 \left[\Omega_M a^{-3} + \Omega_{\rm DE} a^{-3(1+w_0+w_a)} e^{-3w_a(1-a)}\right]$$

Galaxy clusters & cosmology

$$\bar{n}_{i(b)} = \int_{z_{i,\min}}^{z_{i,\max}} dz \frac{d^2V}{dz d\Omega} \int_{M_{b,\min}}^{M_{b,\max}} dM_{\rm obs} \times \int dM \frac{dn}{dM} p(M_{\rm obs}|M)$$

$$= \int dz \frac{d^2V}{dz d\Omega} \int dM \frac{dn}{dM} S_{i(b)}(M;z),$$

$$S_{i(b)}(M;z) \equiv \Theta(z - z_{i,\min})\Theta(z_{i,\max} - z) \times \frac{1}{2}\left[\mathrm{erfc}\{x(M_{b,\min})\} - \mathrm{erfc}\{x(M_{b,\max})\}\right]$$

$$p(M_{\rm obs}|M) = \frac{1}{\sqrt{2\pi}\sigma_{\ln M}} \exp\left[-x^2(M_{\rm obs})\right] \frac{1}{M_{\rm obs}},$$

where

$$x(M_{\rm obs}) \equiv \frac{\ln M_{\rm obs} - \ln M - \ln M_{\rm bias}}{\sqrt{2}\sigma_{\ln M}}.$$

Galaxy clusters & cosmology

$$\bar{n}_{i(b)} = \int_{z_{i,\min}}^{z_{i,\max}} dz \frac{d^2V}{dz d\Omega} \int_{M_{b,\min}}^{M_{b,\max}} dM_{\rm obs} \times \int dM \frac{dn}{dM} p(M_{\rm obs}|M) = \int dz \frac{d^2V}{dz d\Omega} \int dM \frac{dn}{dM} S_{i(b)}(M;z),$$

$$d^2V/dzd\Omega = \chi^2/H(z)$$

$$S_{i(b)}(M;z) \equiv \Theta(z - z_{i,\min})\Theta(z_{i,\max} - z) \times \frac{1}{2}\left[\mathrm{erfc}\{x(M_{b,\min})\} - \mathrm{erfc}\{x(M_{b,\max})\}\right]$$

$$p(M_{\rm obs}|M) = \frac{1}{\sqrt{2\pi}\sigma_{\ln M}} \exp\left[-x^2(M_{\rm obs})\right] \frac{1}{M_{\rm obs}},$$

where

$$x(M_{\rm obs}) \equiv \frac{\ln M_{\rm obs} - \ln M - \ln M_{\rm bias}}{\sqrt{2}\sigma_{\ln M}}.$$

$$N_{i(b)} = \Omega_s \bar{n}_{i(b)}$$

Galaxy clusters & cosmology

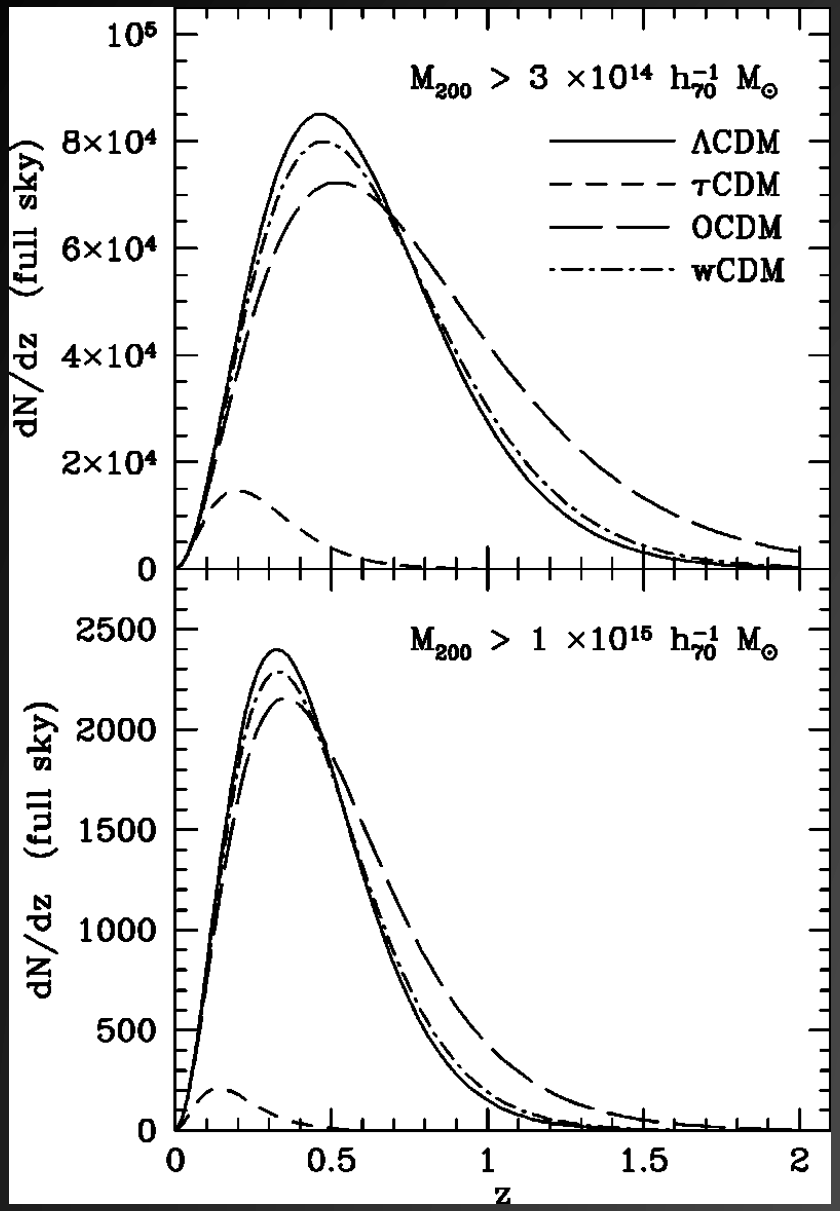

Predicted number of clusters on the sky as a function of redshift in different cosmologies.

Differences between models with Ω_M~0.3 but differing values of Ω_Λ and w should be detectable in large cluster surveys containing 10^4 clusters and extending to z~1.

Dark energy with X-ray GC

De Boni et al. (2011): influence of dark energy on structure formation, within five different cosmological models, using hydrodynamical simulations in a cosmological box of (300 Mpc/h)^3 including baryons and allowing for cooling and star formation.

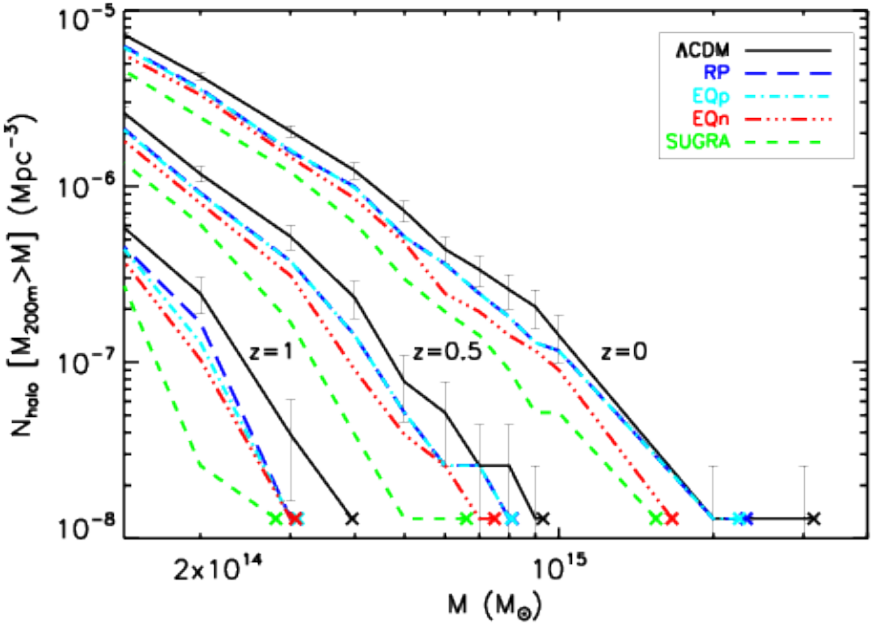

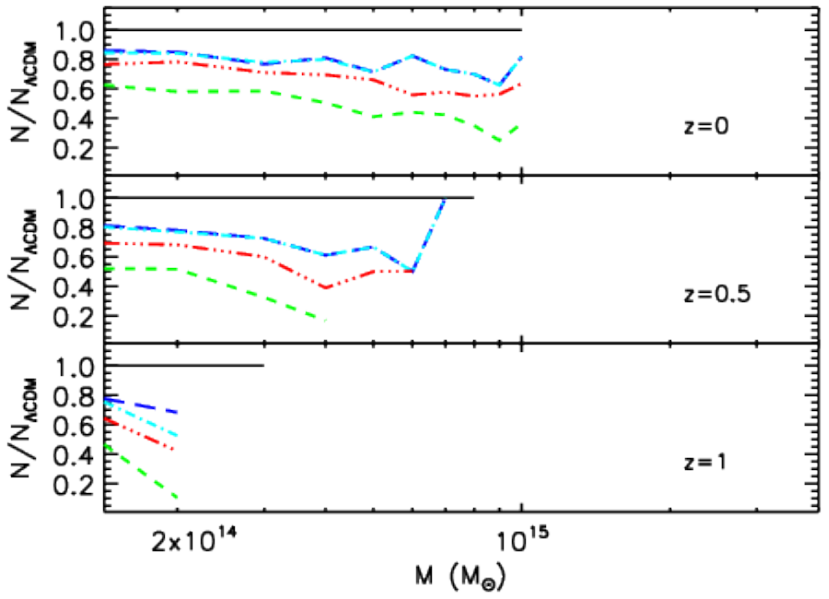

Galaxy clusters & cosmology

Cluster power spectrum are far weaker than those from dN/dz alone. Power spectrum (the Fourier-counterpart of the correlation function) has been widely used in galaxy surveys. The cluster power spectrum holds similar promise because clusters are highly biased when compared to galaxies, making it possible to obtain similar statistical uncertainties with far smaller samples.

Moreover, the bias b(M,z) for clusters can be determined from large scale N-body simulations and theoretical calculations (Mo & White 1996; Sheth & Tormen 1999). In addition, cluster masses are related to simple observables, making it possible to directly connect the bias of the cluster power spectrum to these same observables.

Galaxy clusters & cosmology

Cluster power spectrum are far weaker than those from dN/dz alone. Power spectrum (the Fourier-counterpart of the correlation function) has been widely used in galaxy surveys. The cluster power spectrum holds similar promise because clusters are highly biased when compared to galaxies, making it possible to obtain similar statistical uncertainties with far smaller samples.

$$C^{\rm hh}_{i(bb')}(\ell) = \int d\chi W^{\rm h}_{i(b)}(z) W^{\rm h}_{i(b')}(z) \chi^{-2} P^{\rm L}_m\left(k = \frac{\ell}{\chi}; z\right)$$

$$\frac{k^3}{2\pi^2} P^{\rm L}_m(k;z) = \delta^2_\zeta \left(\frac{2k^2}{5H_0^2\Omega_M}\right)^2 [T(k)D(a)]^2 \times \left(\frac{k}{k_0}\right)^{n_s - 1 + (1/2)\alpha_s \ln(k/k_0)};$$

$$W^{\rm h}_{i(b)}(z) \equiv \frac{1}{\bar{n}_{i(b)}} \frac{d^2V}{d\chi d\Omega} \int dM \frac{dn}{dM} S_{i(b)}(M) b_h(M;z)$$

Galaxy clusters & cosmology

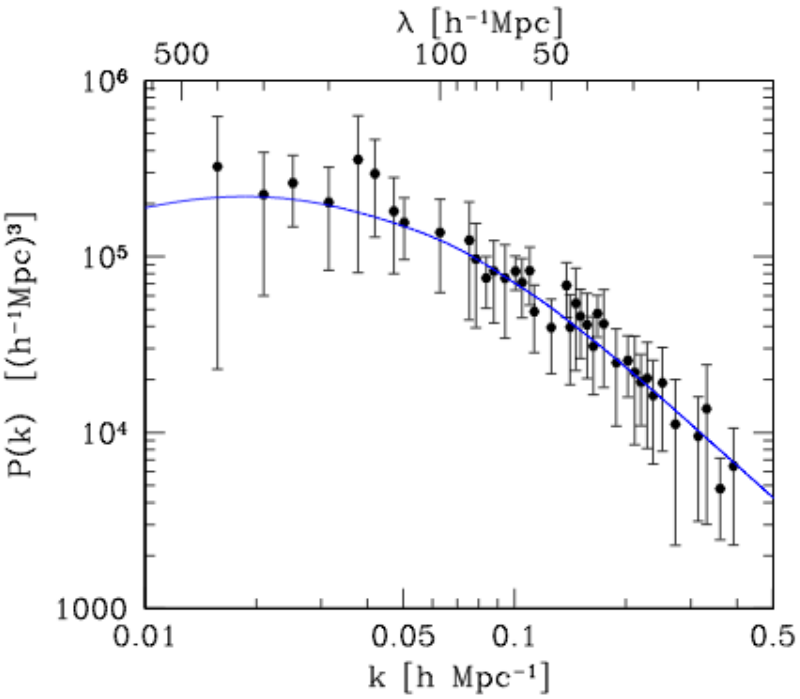

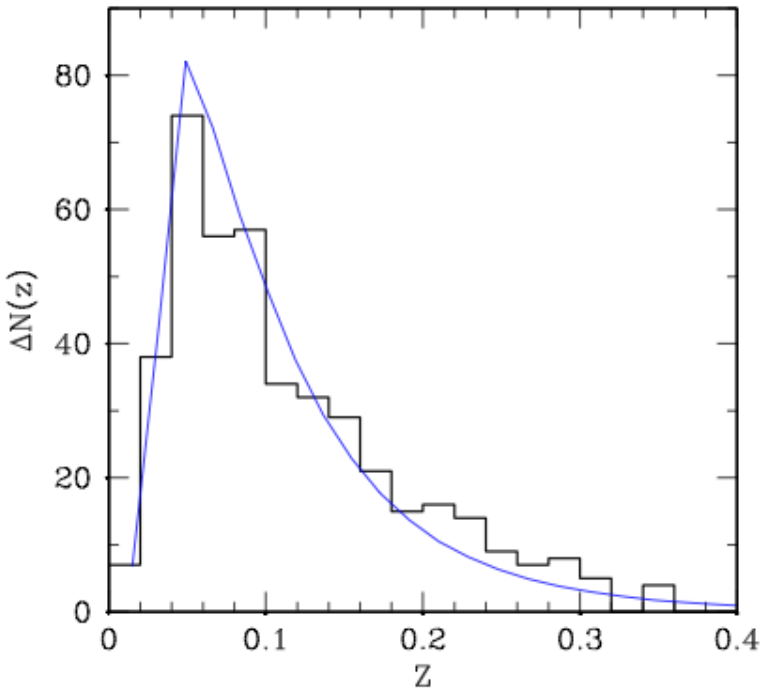

Fig. 8. Comparison of the reference KL solution ($\Omega_{\rm tot} = 1$, $\Omega_m = 0.341$, $\Omega_b h^2 = 0.020$, $h = 0.70$, $n_{\rm S} = 1.0$, $\sigma_8 = 0.711$, $\sigma_{\rm eff} = 25\%$, ST biasing) with REFLEX observations. **Left:** Power spectrum obtained with the flux-limited REFLEX sample (Paper I, points with 1σ error bars including cosmic variance) and the KL solution (continuous line). The theoretical model takes into account the effects of the different volumes covered by the present KL and the former Fourier analysis, includes the effects of the baryons, and is transformed into redshift space using the nonlinear model described in Paper I. In order to make the measured power spectrum less crowded adjacent power spectral densities and their errors were averaged. **Right:** Redshift histogram of the REFLEX subsample used here (steps) and the KL solution (continuous line).

Schuecker et al. 03

Galaxy clusters & cosmology

Wang & Steinhardt (1998) argue that a measurement of the changes of cluster number density or abundance with redshift would provide constraints on the dark energy equation of state parameter $w \equiv p/\rho$.

Haiman et al. (2001) show that with future large surveys it should be possible to obtain precise measurements of the amount Ω_E and nature w of the dark energy.

Majumdar & Mohr (2003, 2004) show that including the redshift averaged cluster power spectrum and direct mass-like measurements of ~100 (~1% of the survey sample) clusters (aka *self-calibration: solve for cluster structure and its evolution in addition to cosmology*) helps tremendously in reducing cosmological parameter uncertainties

Galaxy clusters & cosmology

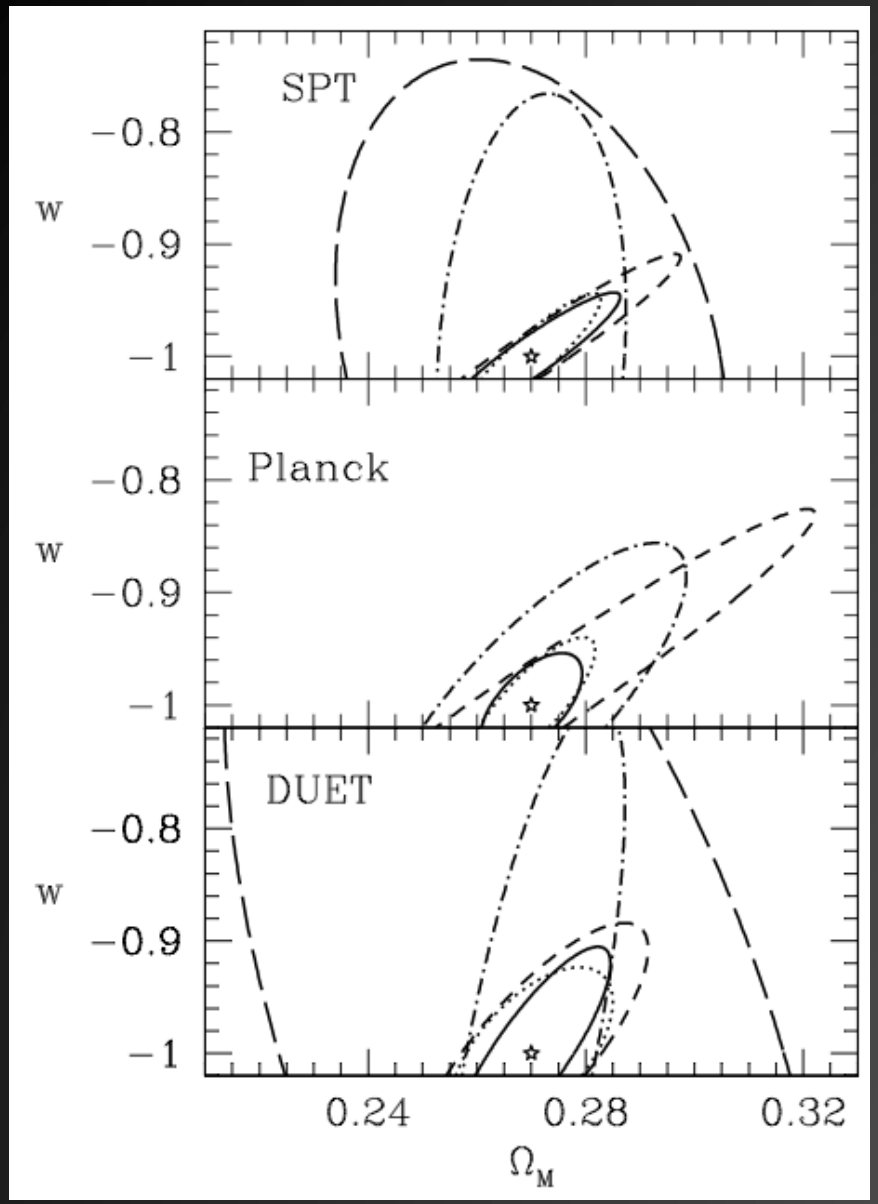

1 σ contours constraints for:

(***dotted line***) dN/dz for the only-cosmology case
(***long-dashed line***) dN/dz for the self-calibration case
(***dot-dashed line***) dN/dz + P_{cl}
(***short-dashed line***) dN/dz +100 cluster follow-up
(***solid line***) dN/dz + P_{cl} + 100 cluster follow-up

A flat universe is assumed.

Galaxy clusters & cosmology

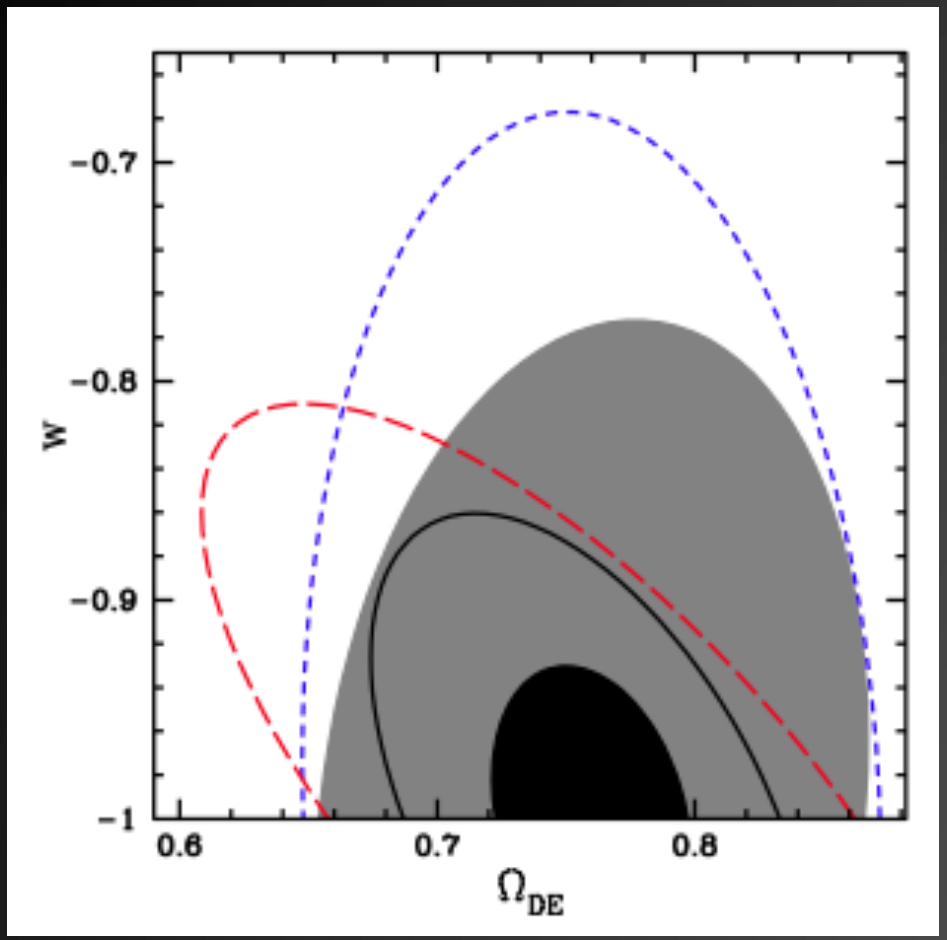

Cunha 09

The constraints from cross-calibration using only clusters detected simultaneously in optical and SZ (i.e. *partial cross-calibration:* M_{SZ} >1e14.2/h Msun, M_{opt}>1e13.5/h Msun @0 < z < 1) are represented by the ***filled gray ellipses***. The cross-calibration using all clusters (i.e. *full cross-calibration*) yields the ***filled black ellipses***.

long dashed red lines: constraints for the fiducial optical survey; *short dashed blue lines*: constraints for the fiducial SZ survey. Treating the optical and SZ surveys as independent and adding their Fisher matrices yields the ***solid black lines***.

Cosmology in the WMAP era

7-years results of the temperature anisotropies in the CMB from WMAP (Komatsu et al 11) put ***alone*** constraints on $\Omega_b h^2$, $\Omega_m h^2$ at <5% uncertainty at 1σ *via PL-CDM*

Class	Parameter	*WMAP* 7-year ML[a]	*WMAP*+BAO+H_0 ML	*WMAP* 7-year Mean[b]	*WMAP*+BAO+H_0 Mean
Primary	$100\Omega_b h^2$	2.270	2.246	$2.258^{+0.057}_{-0.056}$	2.260 ± 0.053
	$\Omega_c h^2$	0.1107	0.1120	0.1109 ± 0.0056	0.1123 ± 0.0035
	Ω_Λ	0.738	0.728	0.734 ± 0.029	$0.728^{+0.015}_{-0.016}$
	n_s	0.969	0.961	0.963 ± 0.014	0.963 ± 0.012
	τ	0.086	0.087	0.088 ± 0.015	0.087 ± 0.014
	$\Delta^2_{\mathcal{R}}(k_0)$[c]	2.38×10^{-9}	2.45×10^{-9}	$(2.43 \pm 0.11) \times 10^{-9}$	$(2.441^{+0.088}_{-0.092}) \times 10^{-9}$
Derived	σ_8	0.803	0.807	0.801 ± 0.030	0.809 ± 0.024
	H_0	71.4 km/s/Mpc	70.2 km/s/Mpc	71.0 ± 2.5 km/s/Mpc	$70.4^{+1.3}_{-1.4}$ km/s/Mpc
	Ω_b	0.0445	0.0455	0.0449 ± 0.0028	0.0456 ± 0.0016
	Ω_c	0.217	0.227	0.222 ± 0.026	0.227 ± 0.014
	$\Omega_m h^2$	0.1334	0.1344	$0.1334^{+0.0056}_{-0.0055}$	0.1349 ± 0.0036
	$z_{\rm reion}$[d]	10.3	10.5	10.5 ± 1.2	10.4 ± 1.2
	t_0[e]	13.71 Gyr	13.78 Gyr	13.75 ± 0.13 Gyr	13.75 ± 0.11 Gyr

Angular scale of 1st peak = curvature of the Universe
Ratio btw odd/even peaks = $\Omega_b h^2$
Amplitude of 3rd peak = constraints on $\Omega_{CDM} h^2$

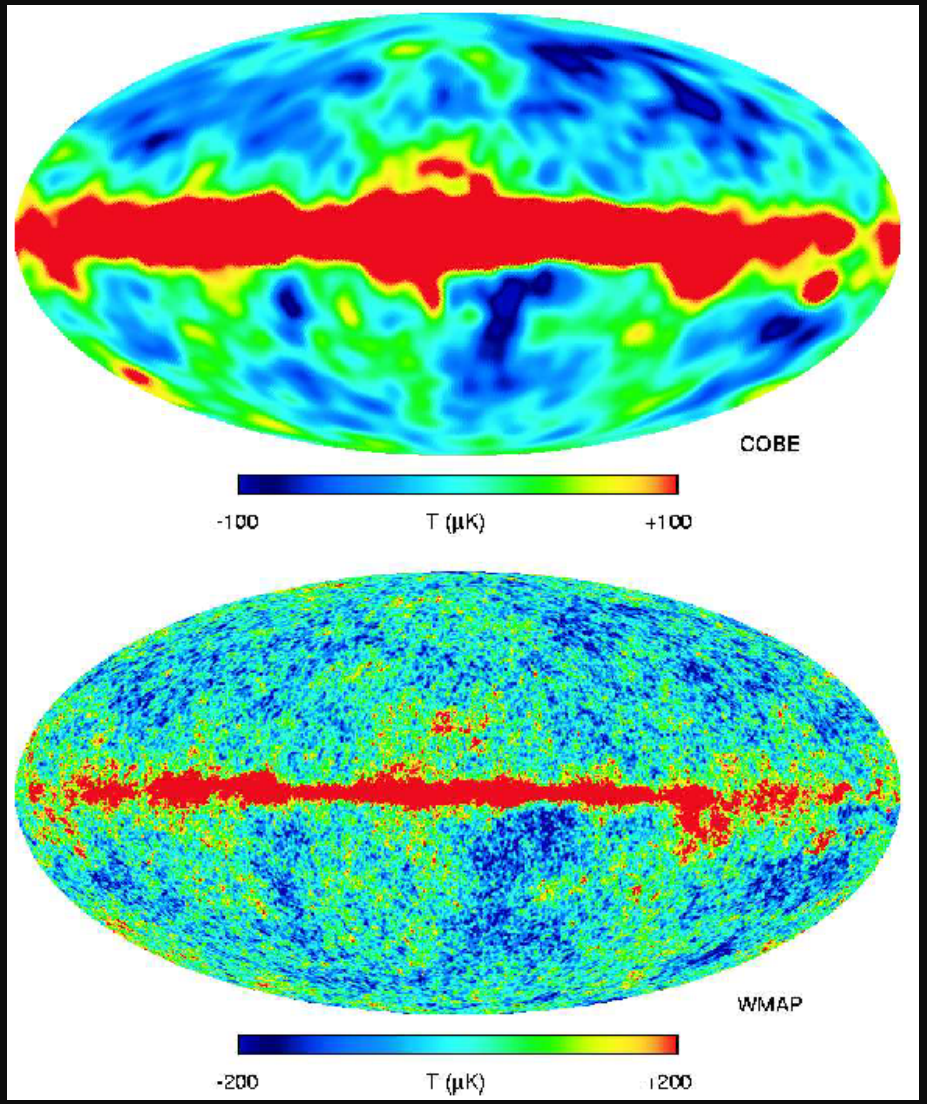

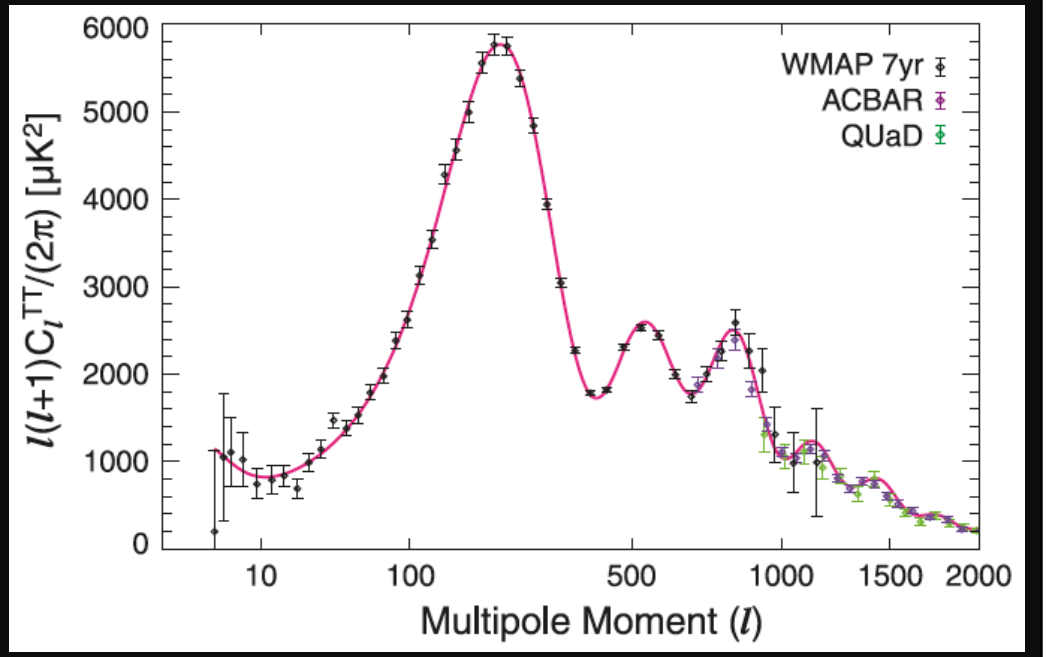

WMAP *(2001-Aug 20, 2010)*
measured fluctuations over >0.3° scale & constraints cosmological parameters at few % level

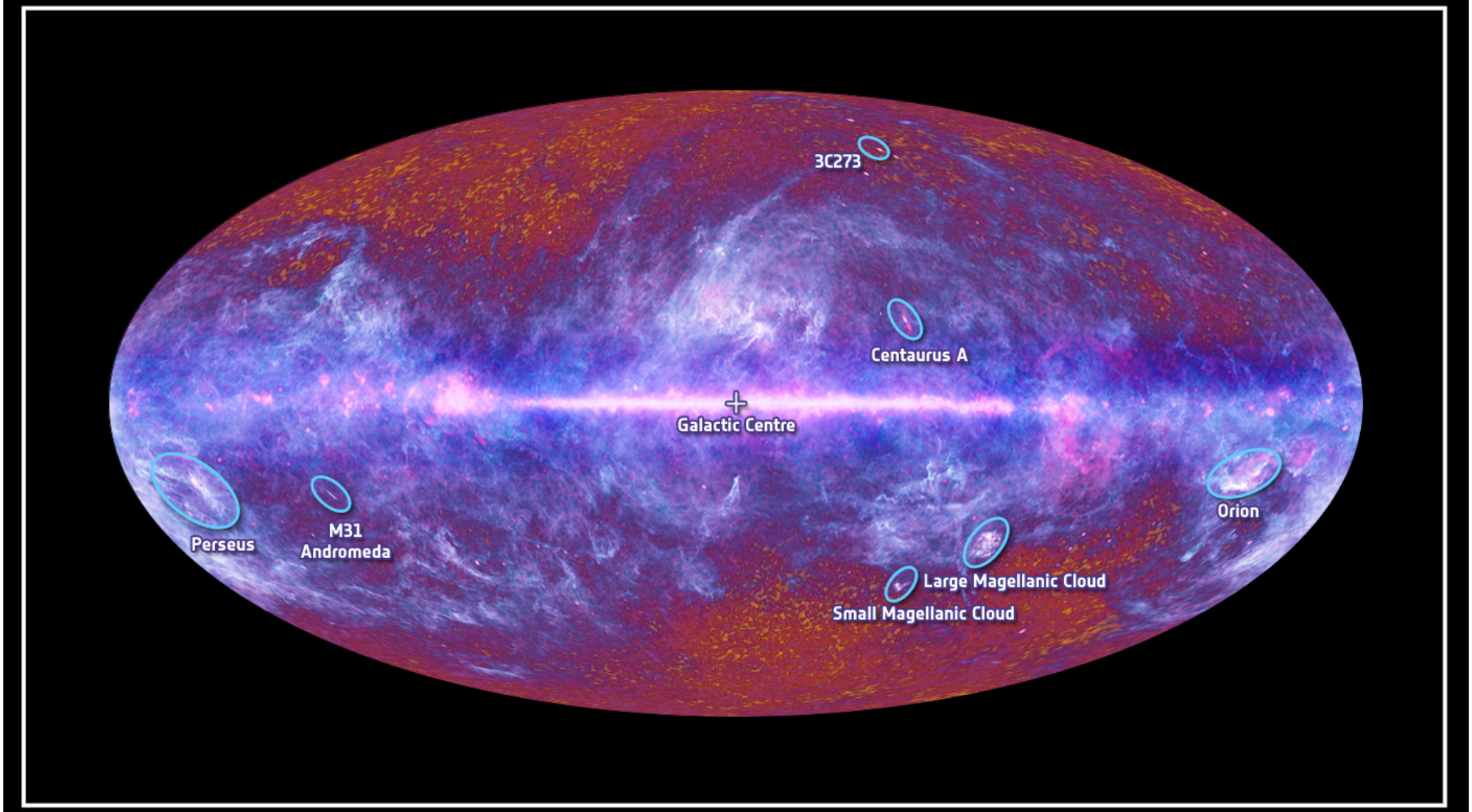

The Planck one-year all-sky survey

esa

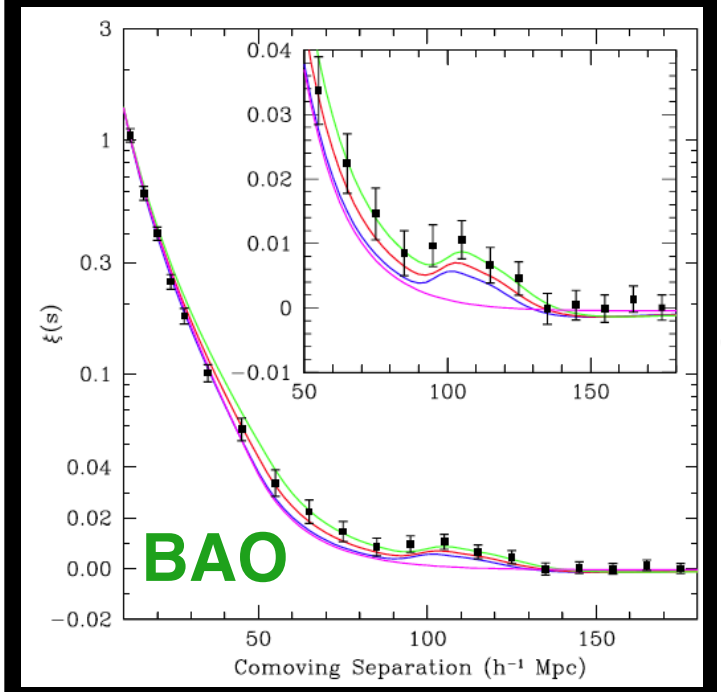
BAO
ξ(s)
Comoving Separation (h⁻¹ Mpc)

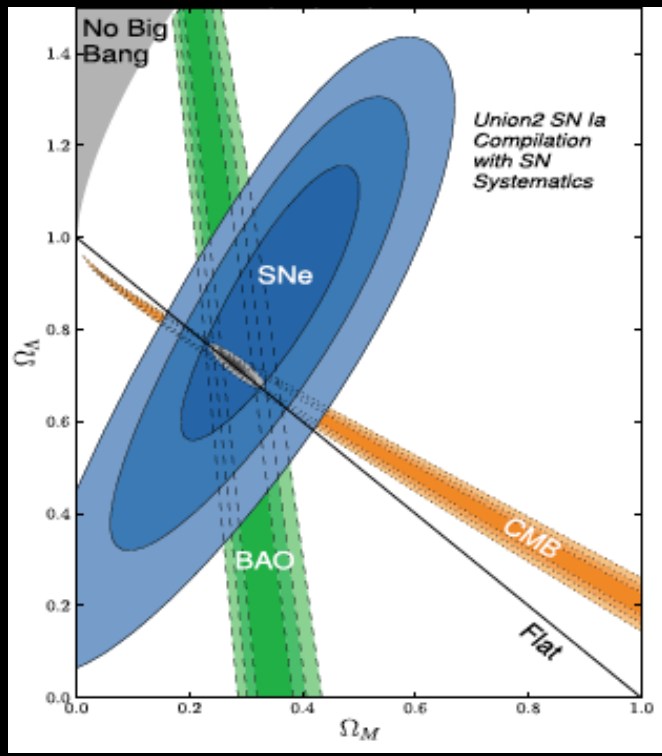
No Big Bang
Union2 SN Ia Compilation with SN Systematics
SNe
BAO
CMB
Flat
Ω_Λ
Ω_M

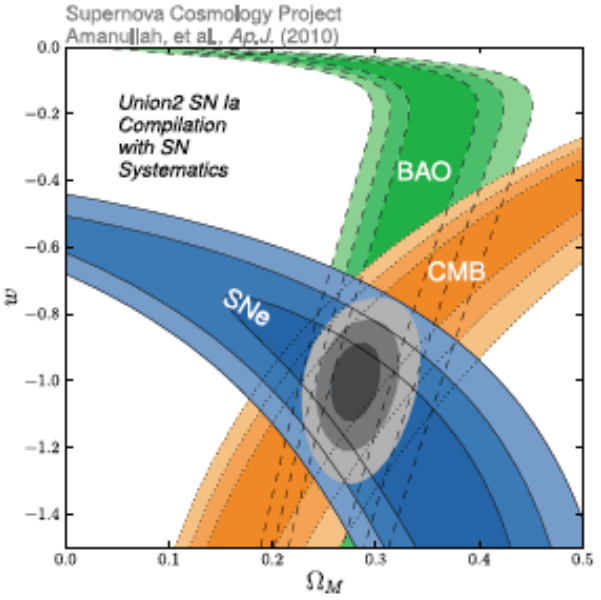
Supernova Cosmology Project
Amanullah, et al., ApJ (2010)
Union2 SN Ia Compilation with SN Systematics
BAO
CMB
SNe
w
Ω_M

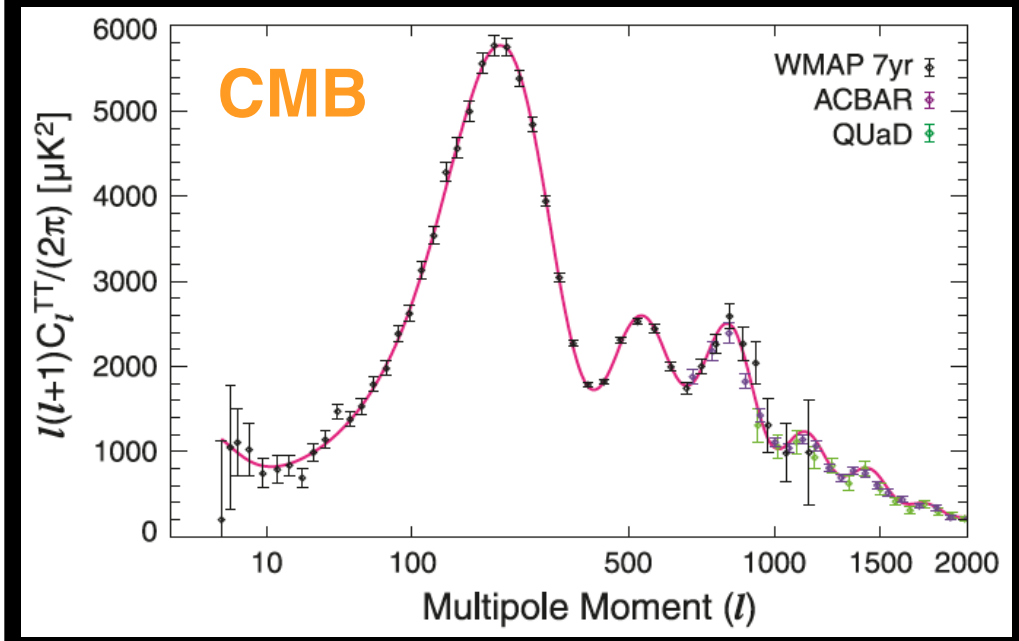
CMB
WMAP 7yr
ACBAR
QUaD
$l(l+1)C_l^{TT}/(2\pi)$ [μK²]
Multipole Moment (l)

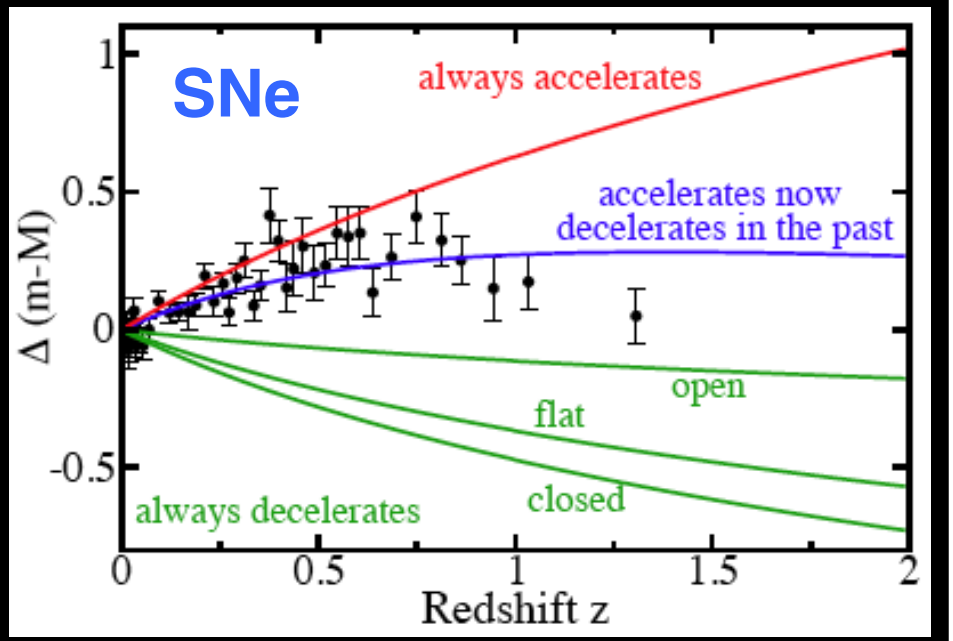
SNe
always accelerates
accelerates now
decelerates in the past
open
flat
closed
always decelerates
Δ (m-M)
Redshift z

Galaxy clusters & cosmology

- The ***amplitude of P(k)*** on cluster scale

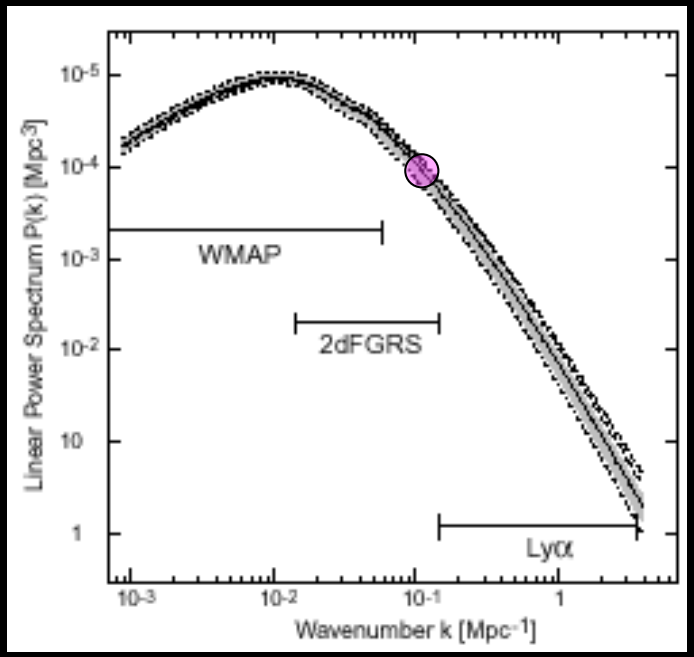

Galaxy clusters & cosmology

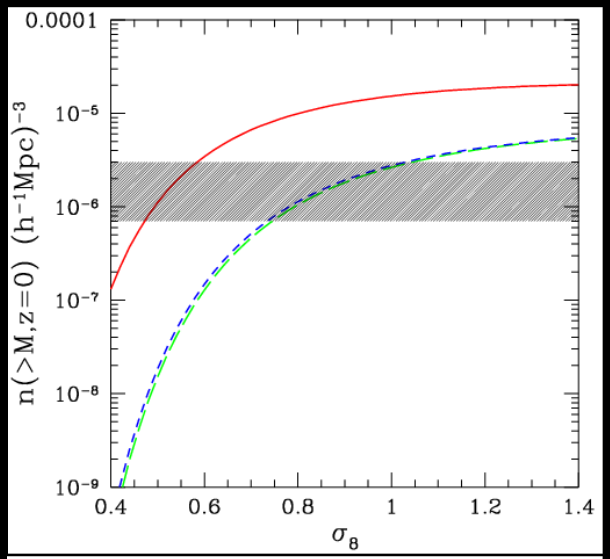

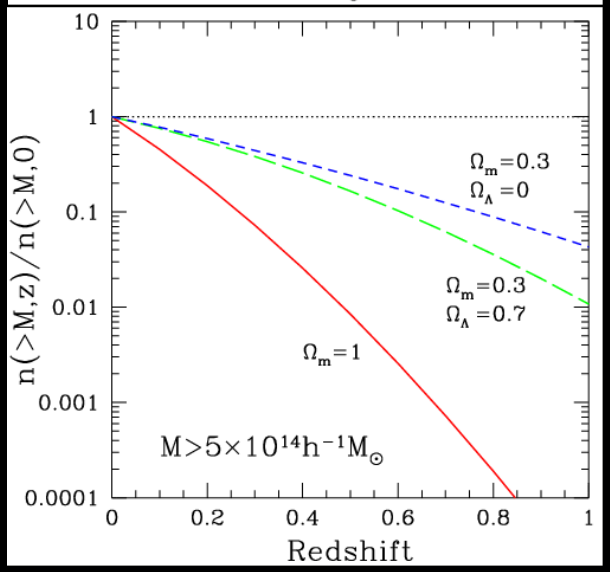

Locally one can determine $\sigma_8\Omega_m^{0.5} \approx 0.5$, because only the amplitude on a given scale $R \approx (M/\Omega_m)^{1/3}$ can be measured

The degeneracy can be broken looking at the evolution of N(M)

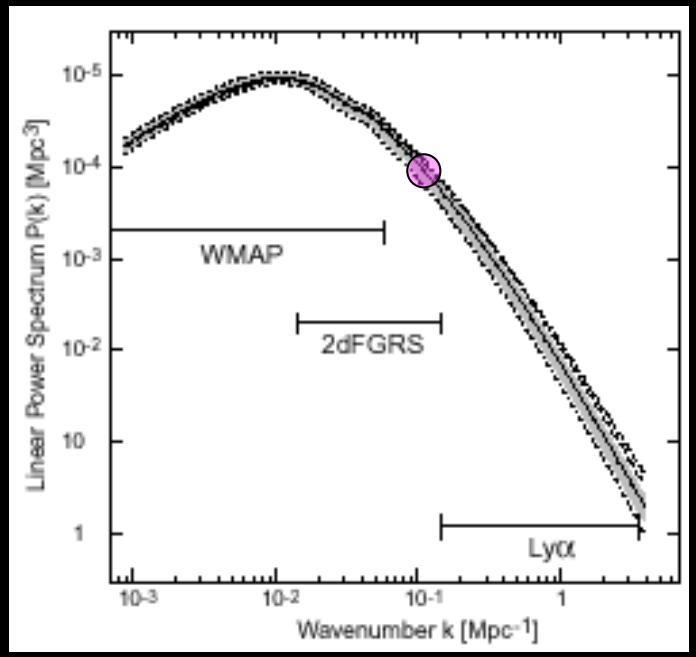

Galaxy clusters & cosmology

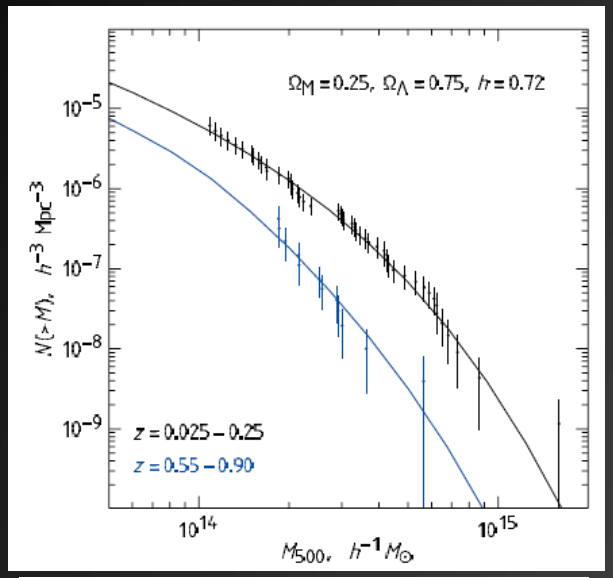

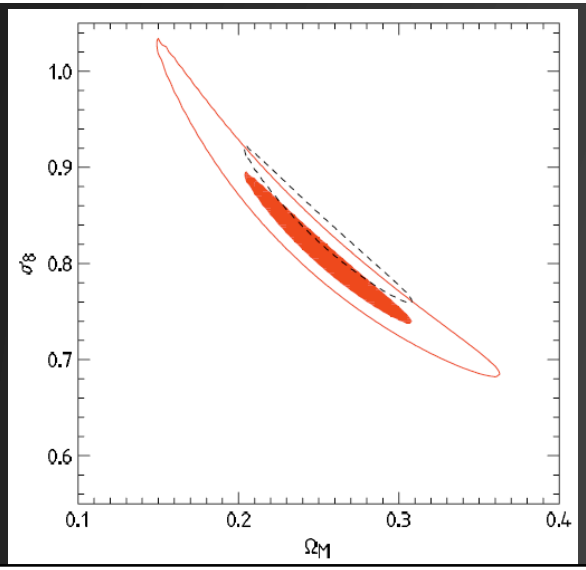

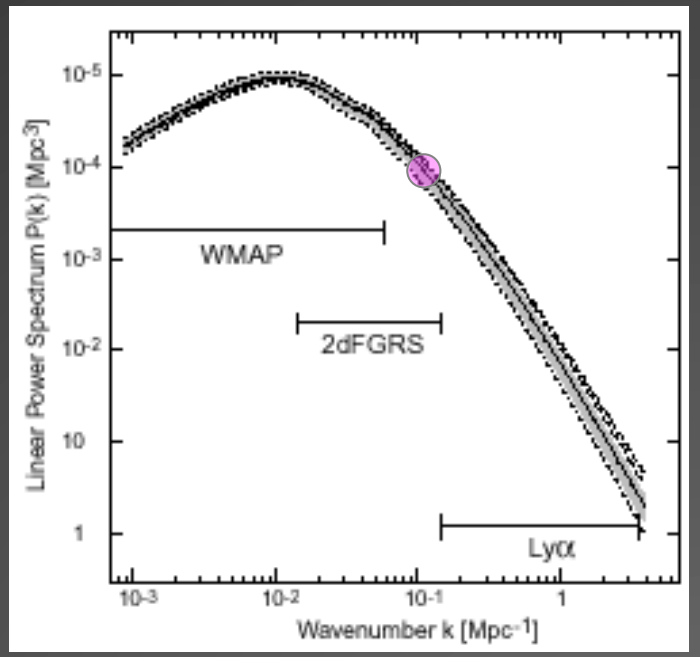

Galaxy clusters & cosmology

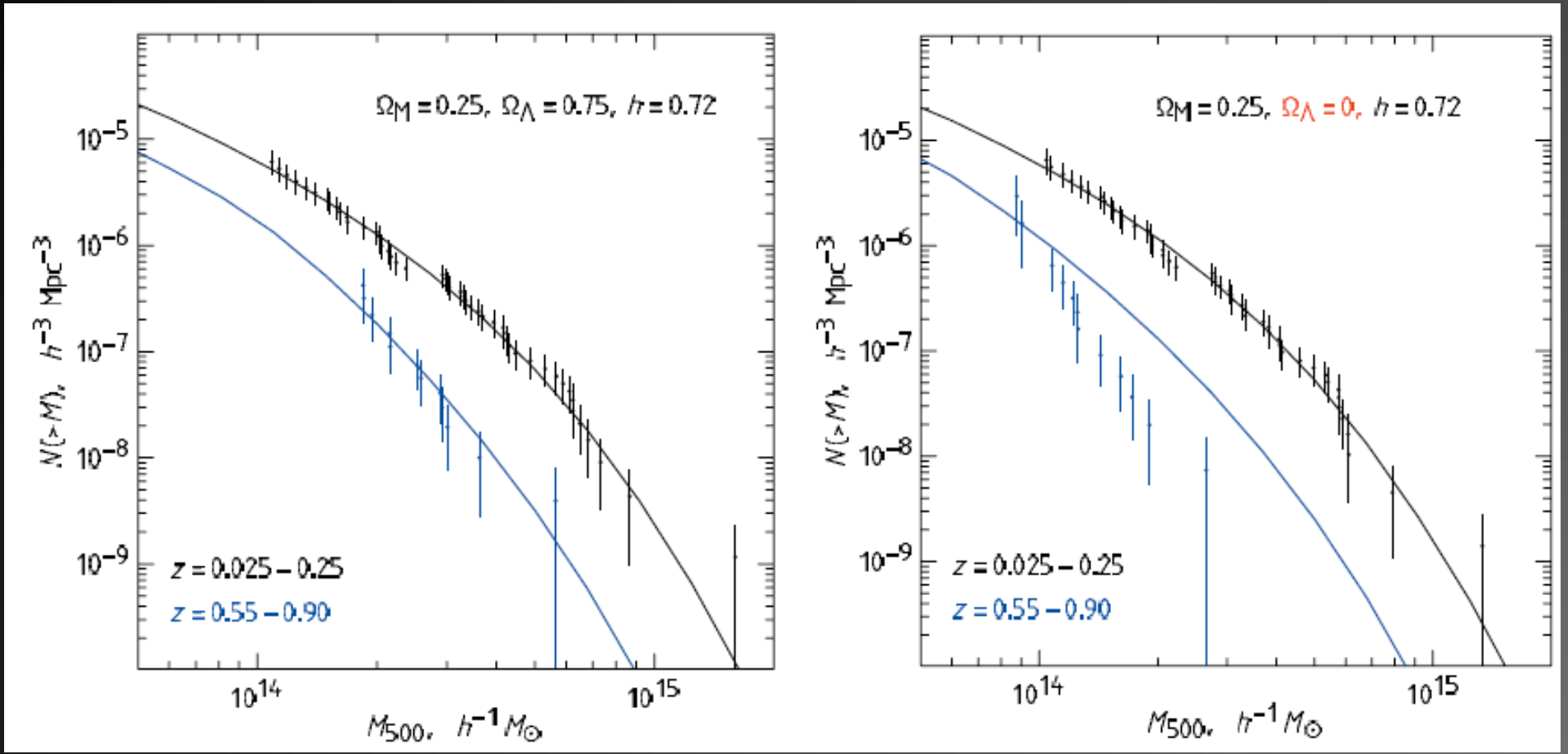

Vikhlinin et al. 09

Galaxy clusters & cosmology

- The ***amplitude of P(k)*** on cluster scale
- There is degeneracy in the determination of the cosmological parameters… ***complementarity***

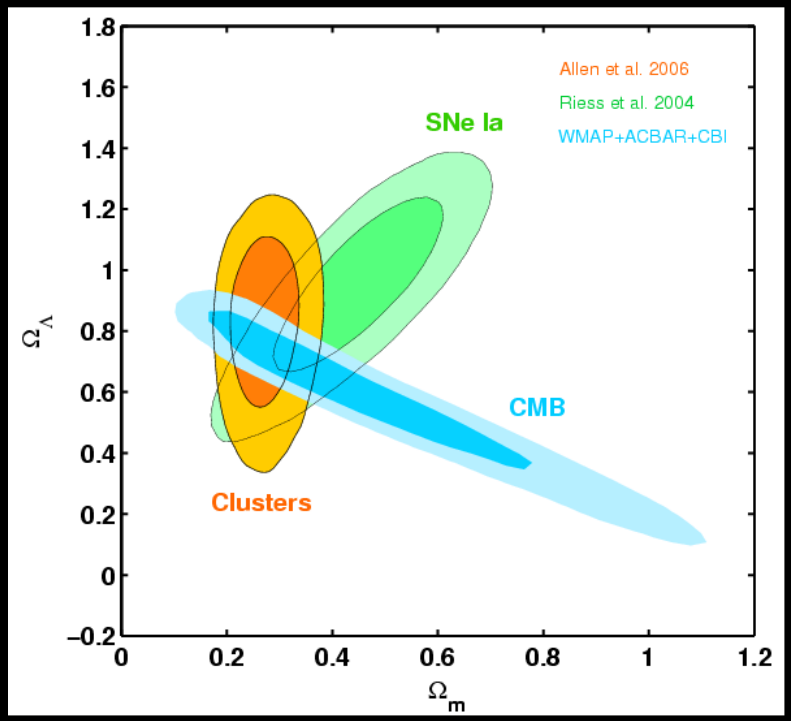

Galaxy clusters & cosmology

- The ***amplitude of P(k)*** on cluster scale
- There is degeneracy in the determination of the cosmological parameters… ***complementarity***
- The ***equation of state of the Dark Energy*** & its evolution with redshift is unknown

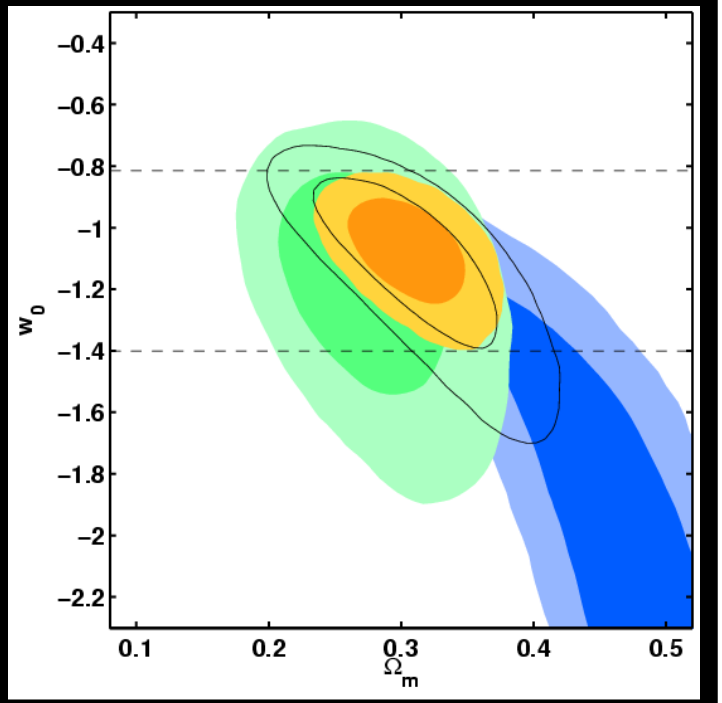

Galaxy clusters & cosmology

- The ***amplitude of P(k)*** on cluster scale
- There is degeneracy in the determination of the cosmological parameters… ***complementarity***
- The ***equation of state of the Dark Energy*** & its evolution with redshift is unknown

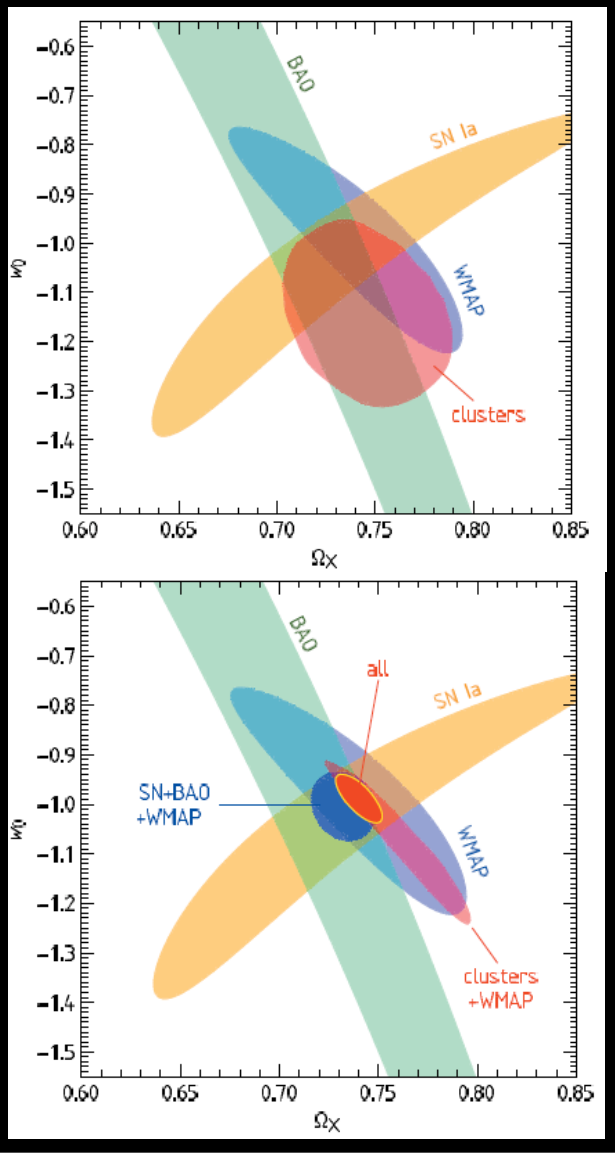

Galaxy clusters & cosmology

- The ***amplitude of P(k)*** on cluster scale
- There is degeneracy in the determination of the cosmological parameters… ***complementarity***
- The ***equation of state of the Dark Energy*** & its evolution with redshift is unknown
- Testing ***GR*** on GC scales

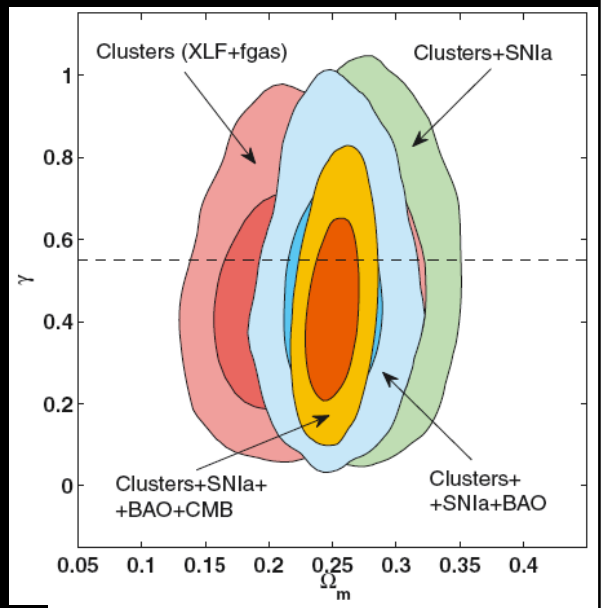

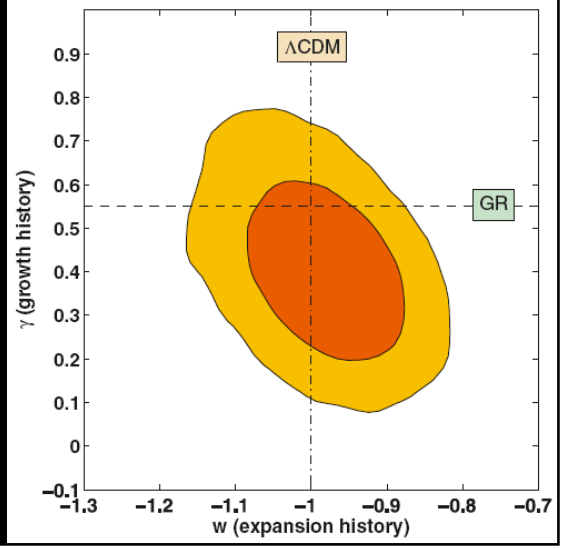

Galaxy clusters & cosmology

- The ***amplitude of P(k)*** on cluster scale
- There is degeneracy in the determination of the cosmological parameters… ***complementarity***
- The ***equation of state of the Dark Energy*** & its evolution with redshift is unknown
- Testing ***GR*** on GC scales
- The ICM physics can be investigated fixing the cosmology: the *reverse game*

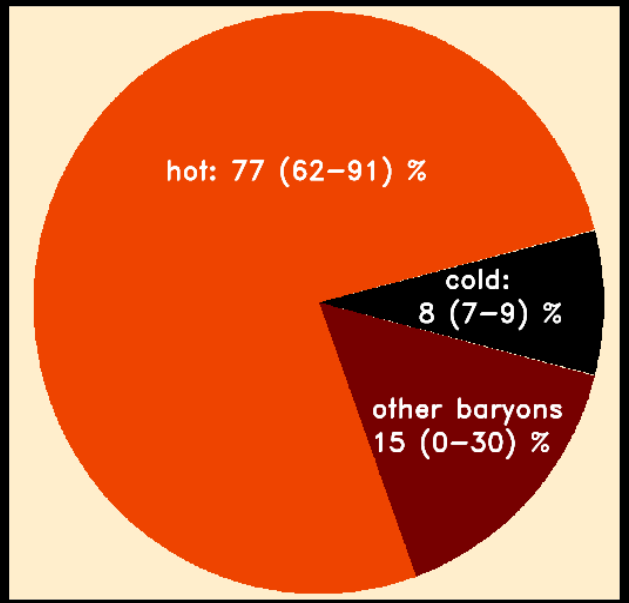

Galaxy Clusters: how and what we observe

Stefano Ettori
(INAF-OA Bologna)

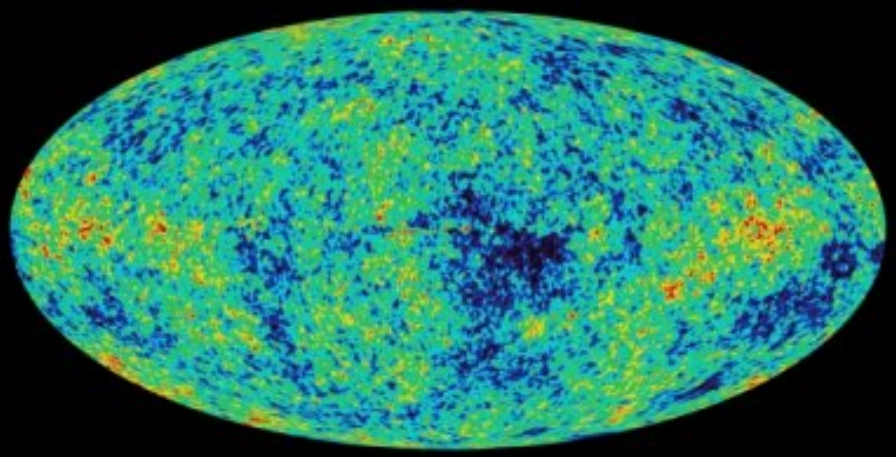

WMAP

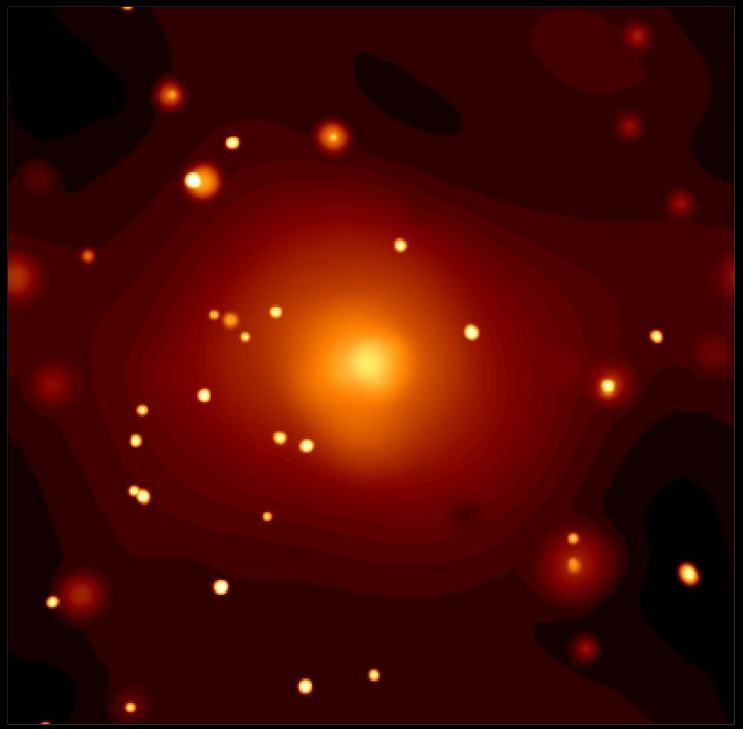

rxj1252 (z=1.24)

Theory vs Observations

- Current numerical simulation accurately reproduce the behaviour of the dominant (80-90% in mass) *dark component* (pure gravitational interactions)

- Current models finds it difficult to accurately predict the observed behaviour of the *baryonic component* (interactions are also hydrodynamical and thermodynamical)

- Galaxy formation alters the state of the cluster's ICM in a way difficult to model:
  - cold and hot phases of the baryonic component are interlinked via "feedback" from stellar and black hole accretion (AGN) processes
  - relations to derive *masses* from observations of baryons (hot gas, galaxies) are affected by this difficult physics

→ *Linking simulations to observations* is the main source of uncertainty when using clusters for precision cosmology

Observable Properties of Clusters used as cosmological probes

- Optical band:
  - "Richness", Total luminosity of cluster galaxies, L_{0pt}
  - Velocity dispersion of member galaxies, σ_V (dynamical state, virial eq.)
  - Gravitational lensing of background galaxies (shear, strong lensing features)
- Near-IR (rest-frame) band:
  - Total stellar mass
- X-ray band:
  - X-ray luminosity, L_X
  - Temperature (and metallicity) of the gas
  - Gas mass, gas fraction (M_{gas}/M_{tot})
- Microwave:
  - SZ effect (Compton scattering on the CMB photons), comptonization parameter Y

Methods for searching galaxy clusters

- Galaxies overdensities in the optical/near-IR:

  Since 1950s (Abell, Zwicki), extended to near IR and recently in IR

- X-ray selection:

  Started in the 60s, Einstein (80s), ROSAT (90s), Chandra, XMM

- Search for galaxy overdensities aorund high-z radio-gals & AGN

  Started in the 90s, recent successes out to z~4

- Sunyaev-Zeldovich (SZ) effect:

  Clear detection in late 90s, surveys are on-going

- Weak lensing shear:

  Started in late 90s, survey experiments underway

Optical/near-IR selection

- Classic work of Abell, Zwicky on photographic plates
- Abell, Corwin, Olowin (1989): 4073 (+1174) clusters (foundation of modern studies)
- Similar work with automated algorithms on digitized photograpgic plates (e.g. Edinburgh-Durham Southern Galaxy Catalog) (Lumsden et al. 1992, Maddox et al. 1990)
- First cluster search at high-z (z=0.8) with deep photographic plates (Gunn et al. 1986, Couch et al. 1991)
- Similar work on CCD imaging material (e.g. Postman et al. 1996)
- Problems with estimate accurately the selection function (completeness?)
- Projection effects increasingly severe at high redshifts, especially if only one band is used
- By *moving to redder bands and imaging in different bands* (up to near-IR bands) projection effects are mitigated and efficiency of cluster search is significantly boosted
  - This has been exploited in recent years using wide-field multicolor imaging, including IR (2-5μ with Spitzer satellite)

Distant clusters: blue/near-IR contrast

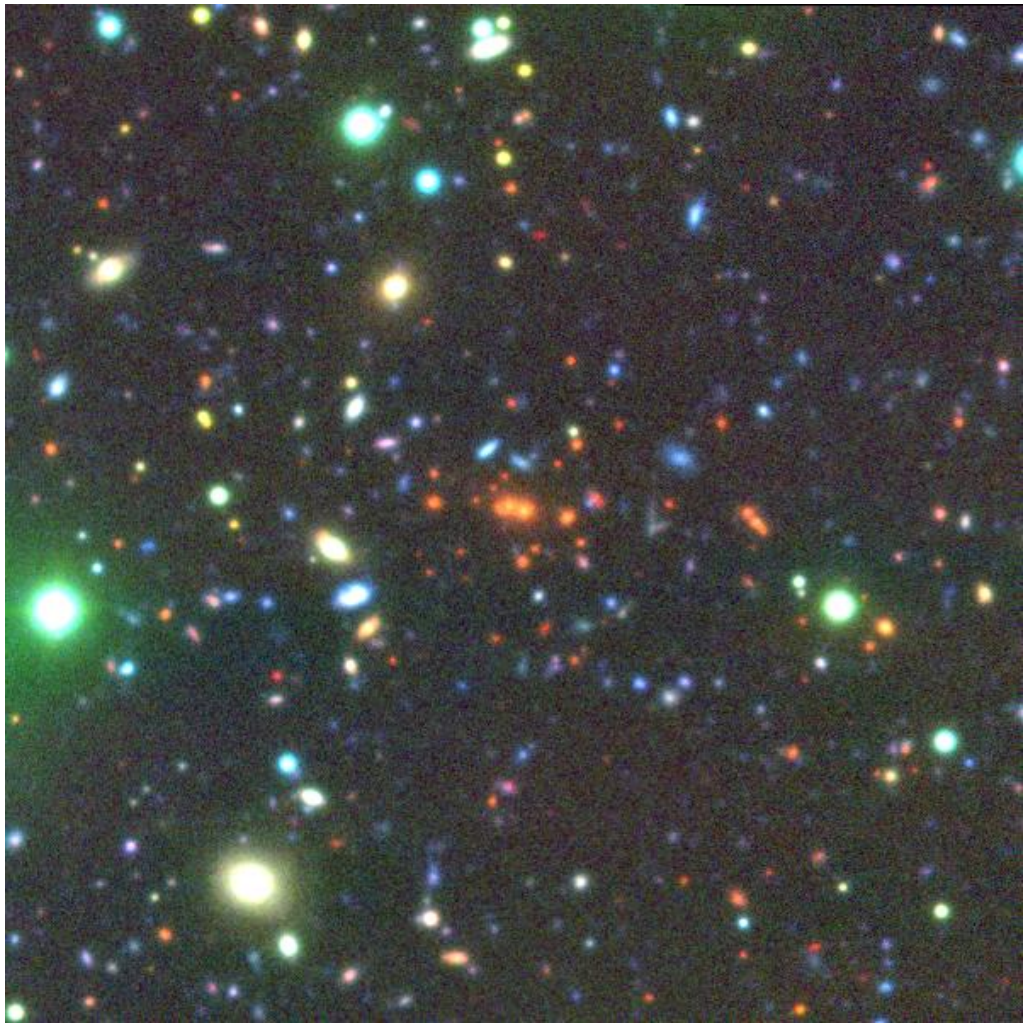

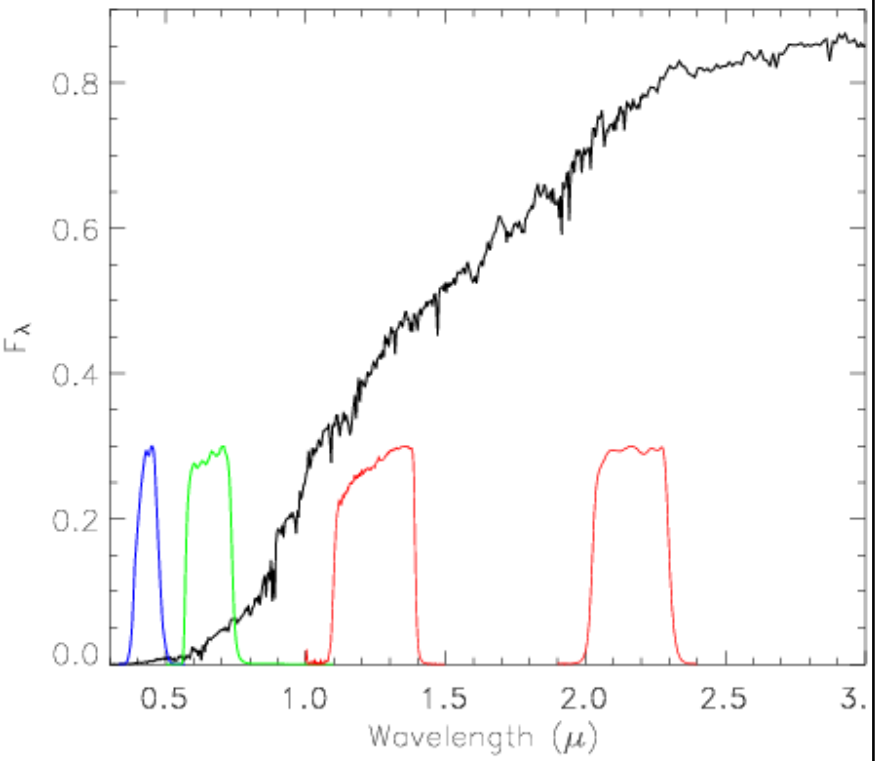

RDCS1252-29 @z=1.24 (Rosati et al.04)

Distant clusters: multi-band observations

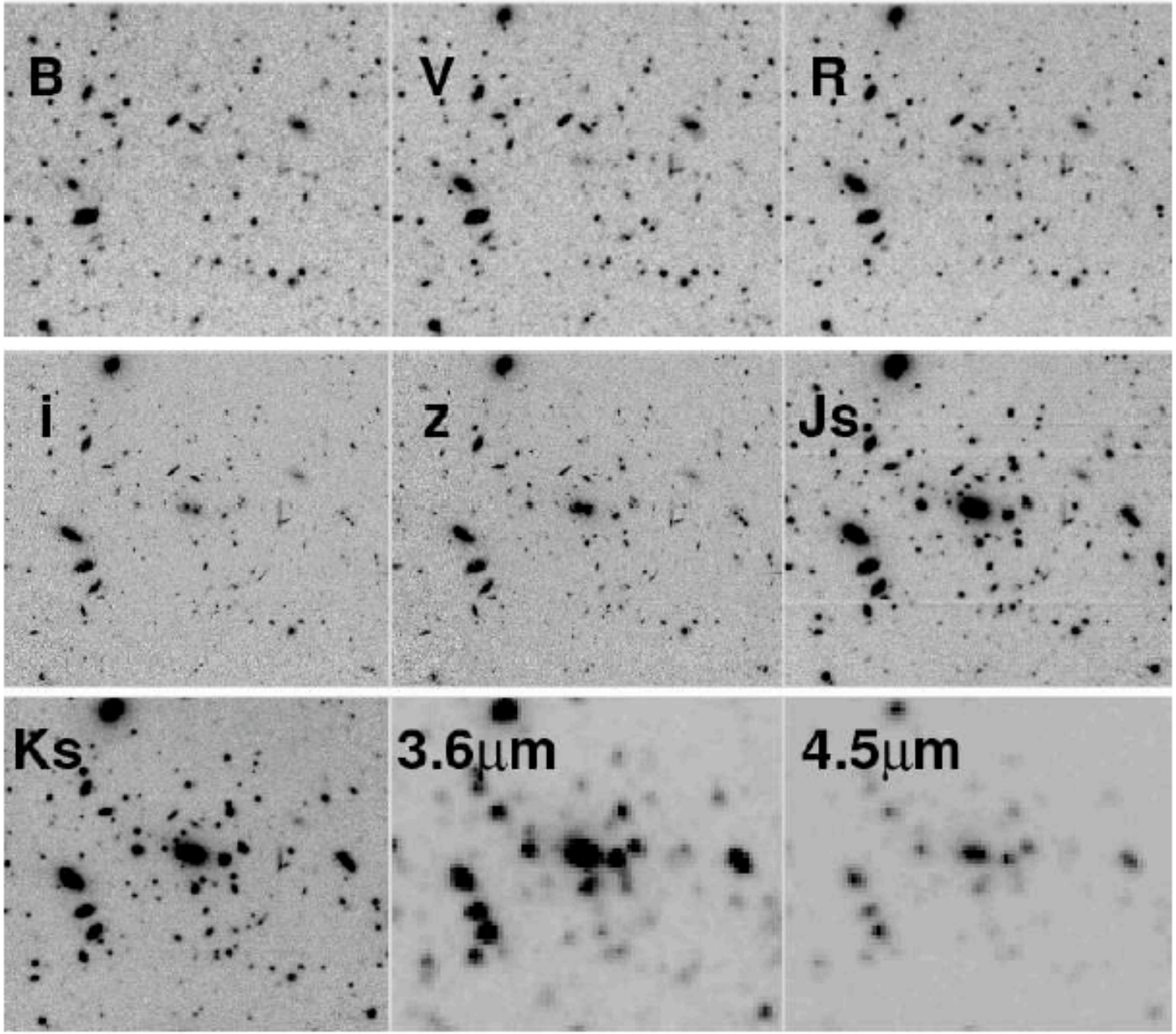

RDCS1252-29 @z=1.24

Red Sequence Cluster Survey
(Gladders et al. 00)

- RCS: 100 deg^2 surveyed in R and z bands with wide-field optical imagers (CFHT, CTIO)
- Relatively shallow (R~25, z~23.9) but capable to detect cluster candidates (concentrations of red galaxies) out to $z \approx 1.2$
- Simple R-z color allows a good photometric redshift with $\Delta z \approx 0.05$
- Selection function rather complicated (dependent on many parameters characterizing galaxy pop properties and their evolution)
- Very large area allows the discovery of rare massive systems (e.g. strong lensing features)

- **RCS2** is now complete over *1000 deg^2* in *g,r,i,z* bands ~1-2 mag deeper than SSDS: **10^4 candidates** (Gilbank et al. 11)

Red Sequence Cluster Survey

(Gladders et al. 00)

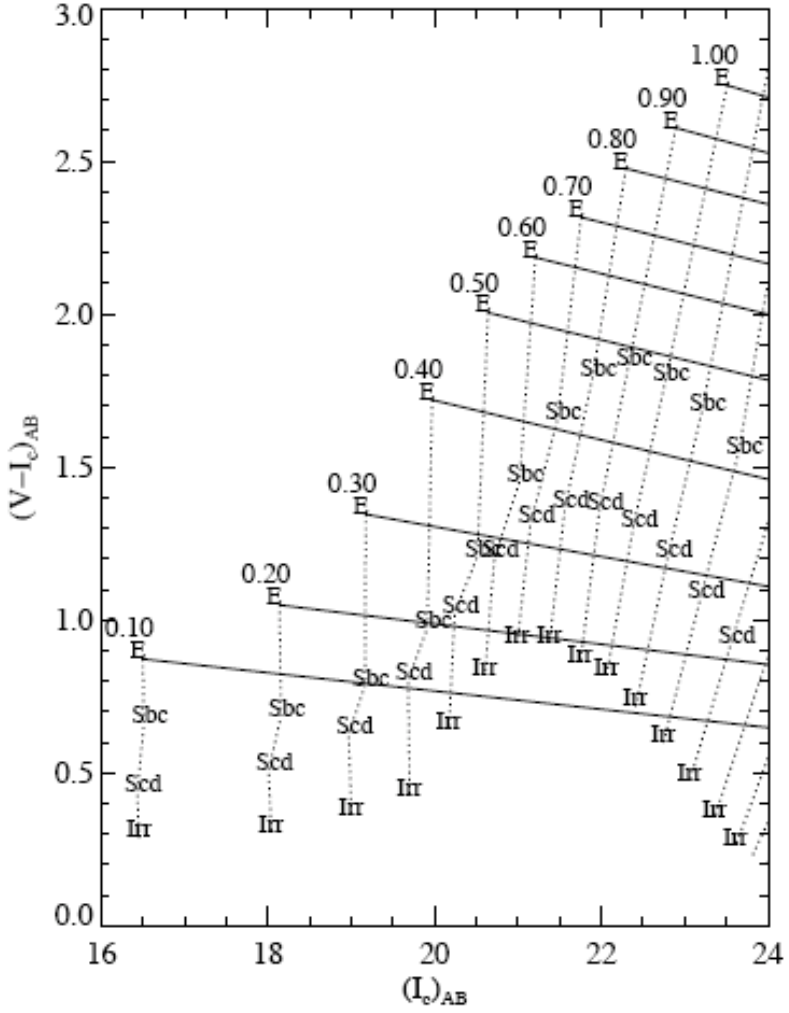

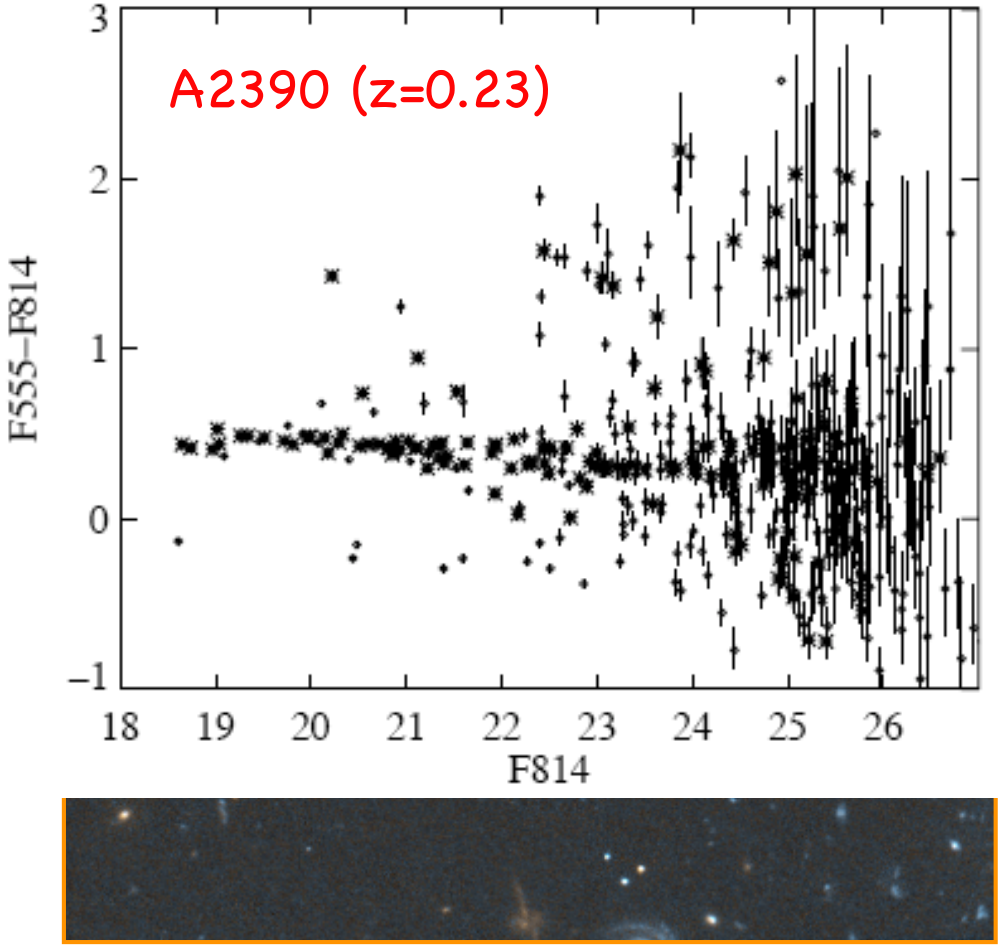

Weak Lensing method:
Example: MS1054 ar z=0.81

(Hoekstra et al 01)

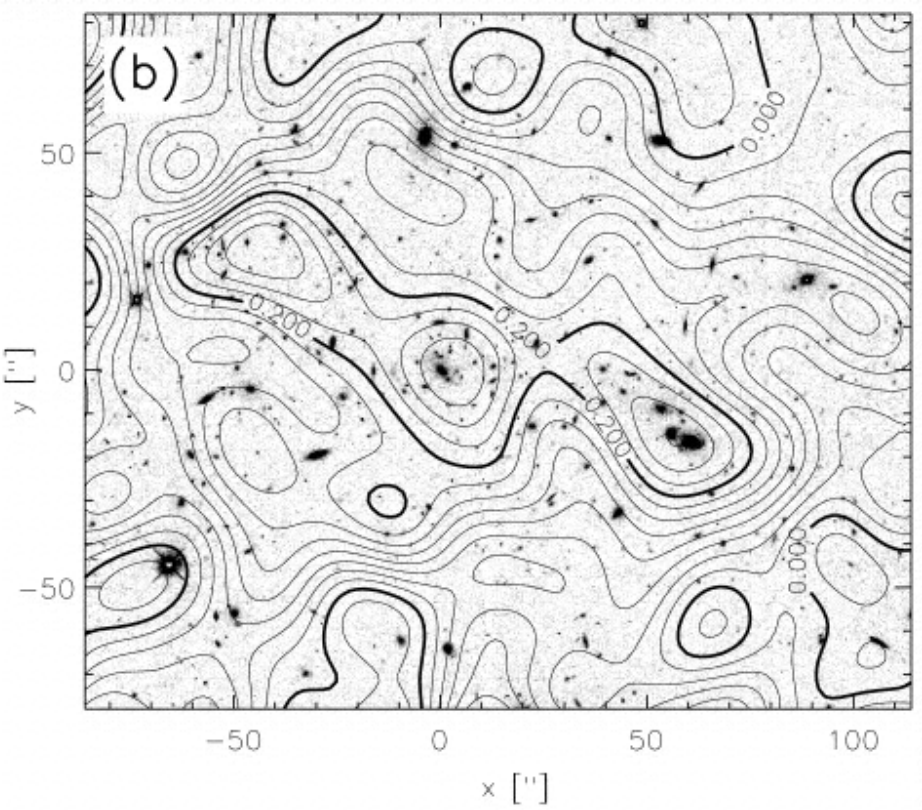

Mass map on HST image (F814W)

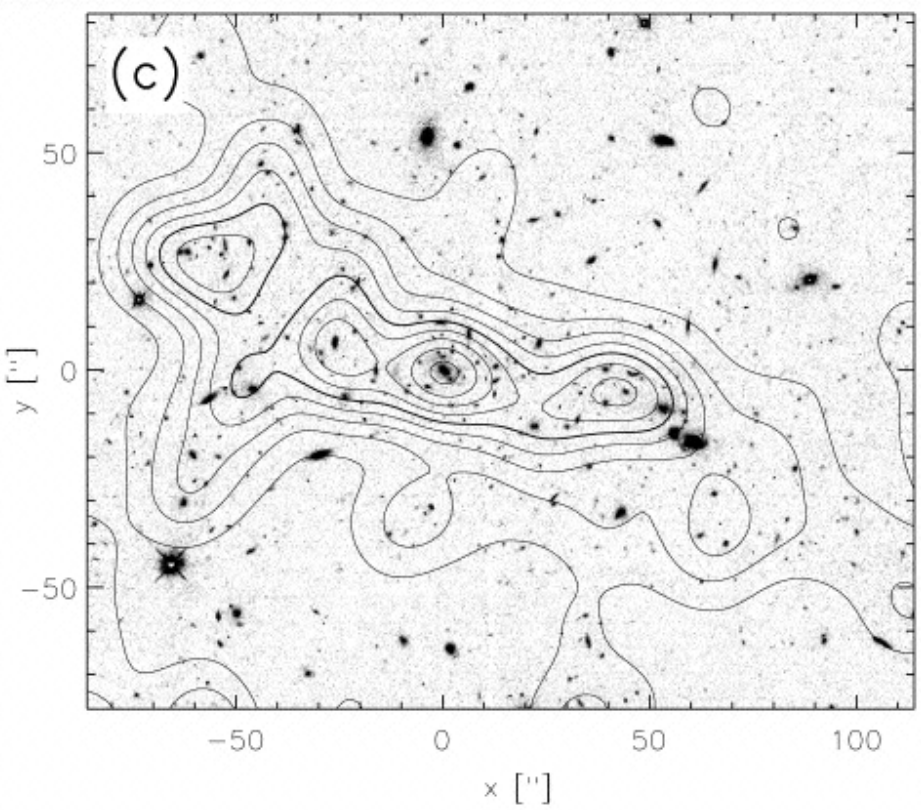

Light distribution on HST image

Serendipitous searches:

- best effort to date: Deep Lens Survey (DLS, Tyson, Dell'Antonio, et al.)
- selection based on mass only! (in theory…)
- difficult from the ground, it would be powerful from space..

Sloan Digital Sky Survey (SDSS) clusters

- 1 Million galaxy spectra
- 7500 square degrees in the northern sky
- based on 5-color CCD photometry (2.5m telescope)

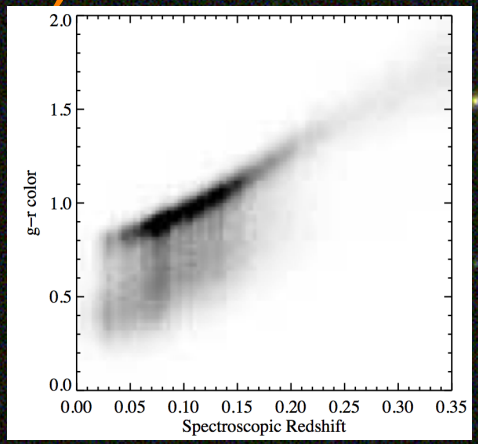

MaxBCG catalog (Koester et al.07)
13,823 clusters, each containing
ten or more E/S0 ridgeline galaxies
brighter than 0.4 L* (in the i-band)
within a scaled radius R200

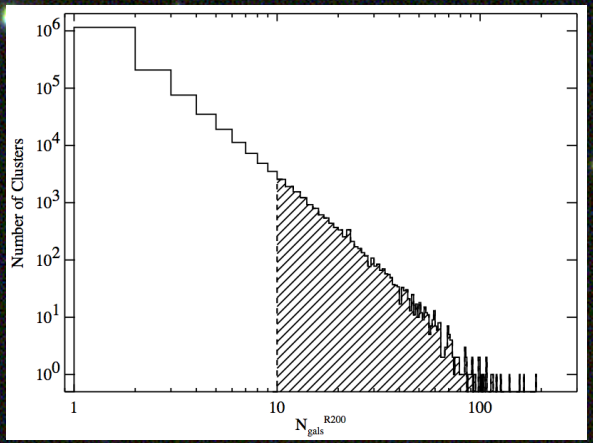

Optical Selected Clusters

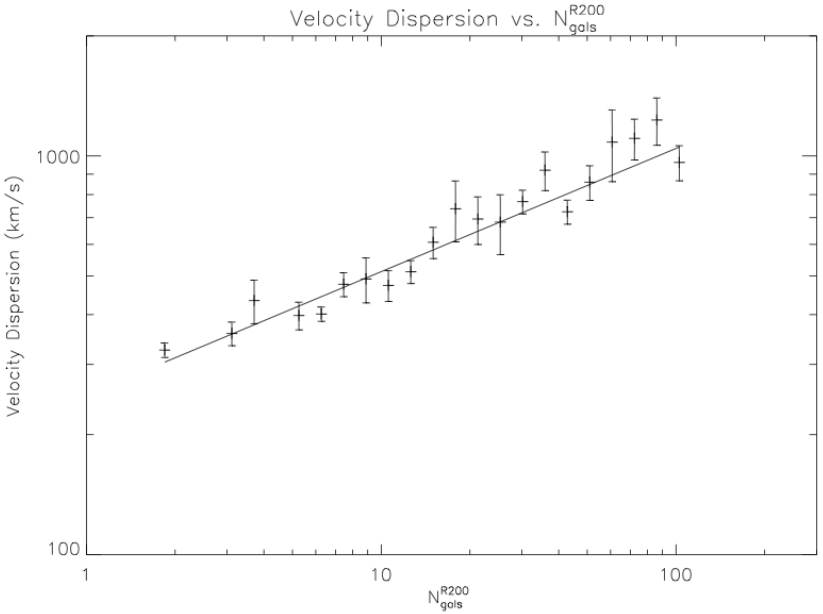

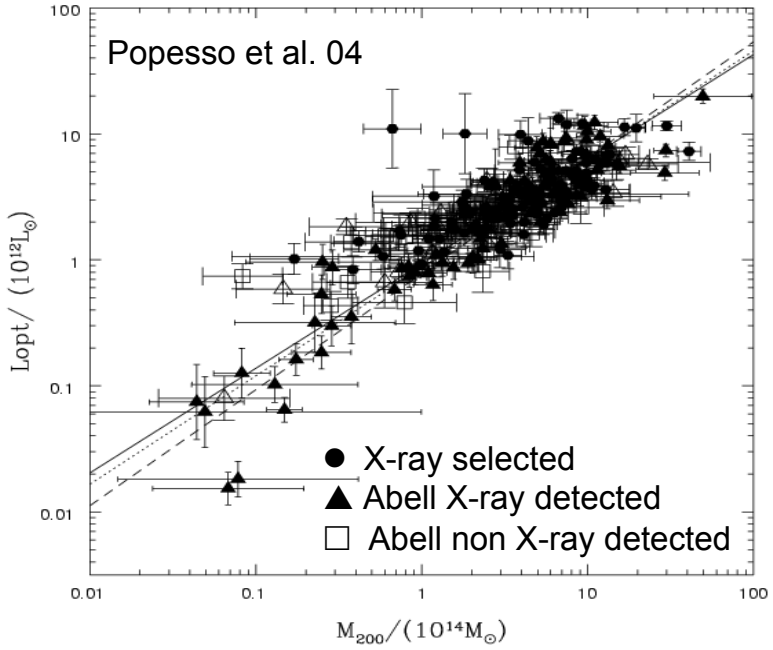

- Several refinements of the original Abell richness parameter have been proposed:
  - Given a Schechter luminosity function, $\phi(L) \sim L^{-\alpha}\exp(-L/L_*)$, for the cluster galaxies, $\Lambda_{CL}=N_{gal}(>L_*)$ is roughly correlated with M (Postman 96)
  - By combining two likelihood: (i) the bright end of $\phi(L)$ is dominated by galaxies occupying a narrow region of color-magnitude space (the E/S0 ridgeline="red gals"); (ii) clusters contain a brightest cluster galaxy (BCG) that is located near the center of the galaxy distribution and nearly at rest relative to the cluster center of M (Koester et al 07).
- To the extent that light traces mass, by summing the luminosity of all galaxies in a cluster one obtains an indication of its mass

X-ray Selected Clusters

- Uhuru satellite (1972): first X-ray all-sky survey
  - Revealed association between Abell clusters and luminous X-ray sources
  - Thermal nature of X-ray emission + Fe lines confirmed with X-ray spectra HEAO-1 A2 (1982)

- HEAO-1 satellite (1979): all-sky survey with much improved sensitivity
  - 30 out of 61 extra-gal sources identified as clusters (mostly Abell)
  - First flux-limited sample of clusters and estimate of local XLF
  - Sample further extended and improved using Ariel V and EXOSAT data (Edge et al. 90: 55 clusters, F_{lim}~1e^{-11} erg/cm^2/s)

- Einstein observatory with imaging X-ray optics opens a new era in X-ray astronomy (resolution <1', higher sensitivity)
  - **EMSS Cluster sample** (Gioia et al. 1990): 93 clusters from 700 deg^2 with F_{lim}~1e^{-13} erg/cm^2/s : first solid assessment of cluster evolution

- ROSAT satellite (1990-2000): great advances in cluster surveys
  - Higher sensitivity, low background, resolution~30"
  - **All-sky survey** (RASS): ~1000 clusters (BCS, NORAS, REFLEX), F_{lim}~1e^{-13}
  - **Serendipitous surveys**: (RDCS, WARPS, 160 deg^2, etc..) >~200 clusters with F_{lim}~1e^{-14}

X-ray Selected Clusters: advantages of X-ray selection

- Physically bound systems are selected (potential wells)
- L_x well correlated with the cluster mass
- Emissivity $\propto \rho^2$, more concentrated than optical gal distribution, since X-ray sources surf. density is low $\Rightarrow$ clusters are high contrast objects in the X-ray sky
- Flux-limited samples can be defined $\Rightarrow$ search volume is known (i.e. selection function is easy to model)
- ***Caveats***: surface brightness effects
- ***Limitation***: surface brightness dimming at high-z difficult to cover large areas..

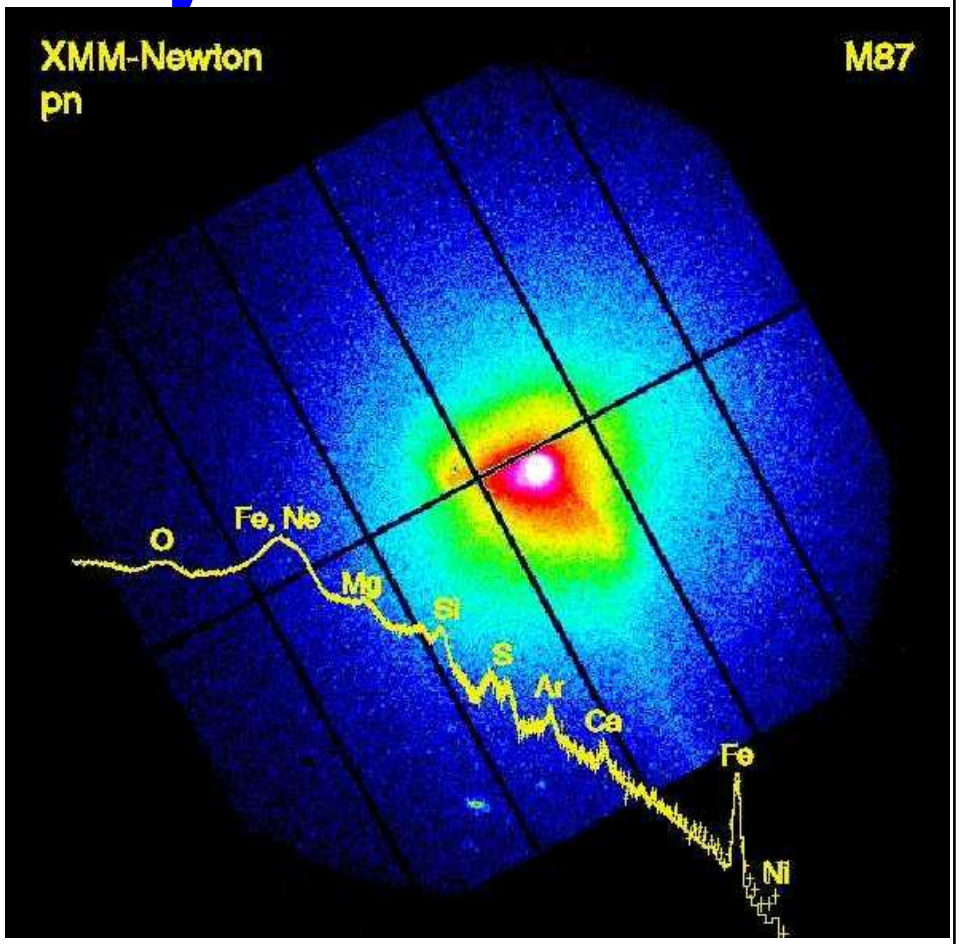

X-ray Follow-up observations reveals a wealth of information on physical properties and metallicity of the ICM

Galaxy Clusters in X-rays

Even if they contains only 4 per cent of the cosmic mass of the Universe, the importance of clusters in cosmological studies arises from the fact that they are the most massive relaxed systems, which, in standard scenarios, form from the highest primordial density peaks.

> The statistics of their distribution on large scales (detection)
> their abundance and its evolution with z (M_{tot})
> their gas composition (M_{gas})

are all functions of the cosmological parameters.

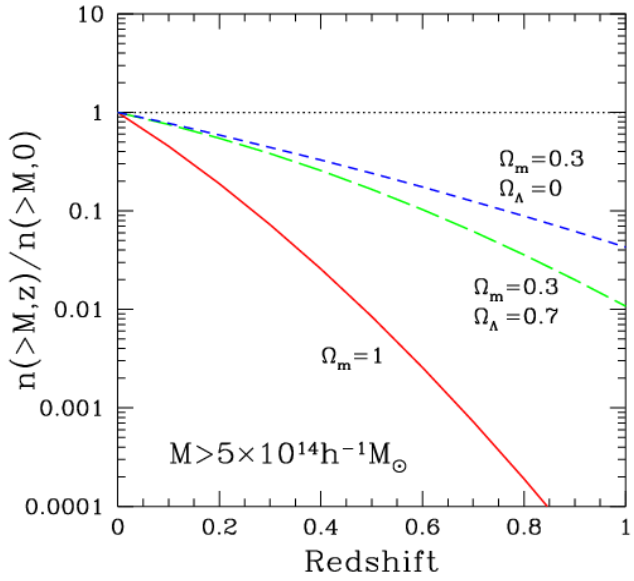

X-ray Cluster Surveys (1980 - present)

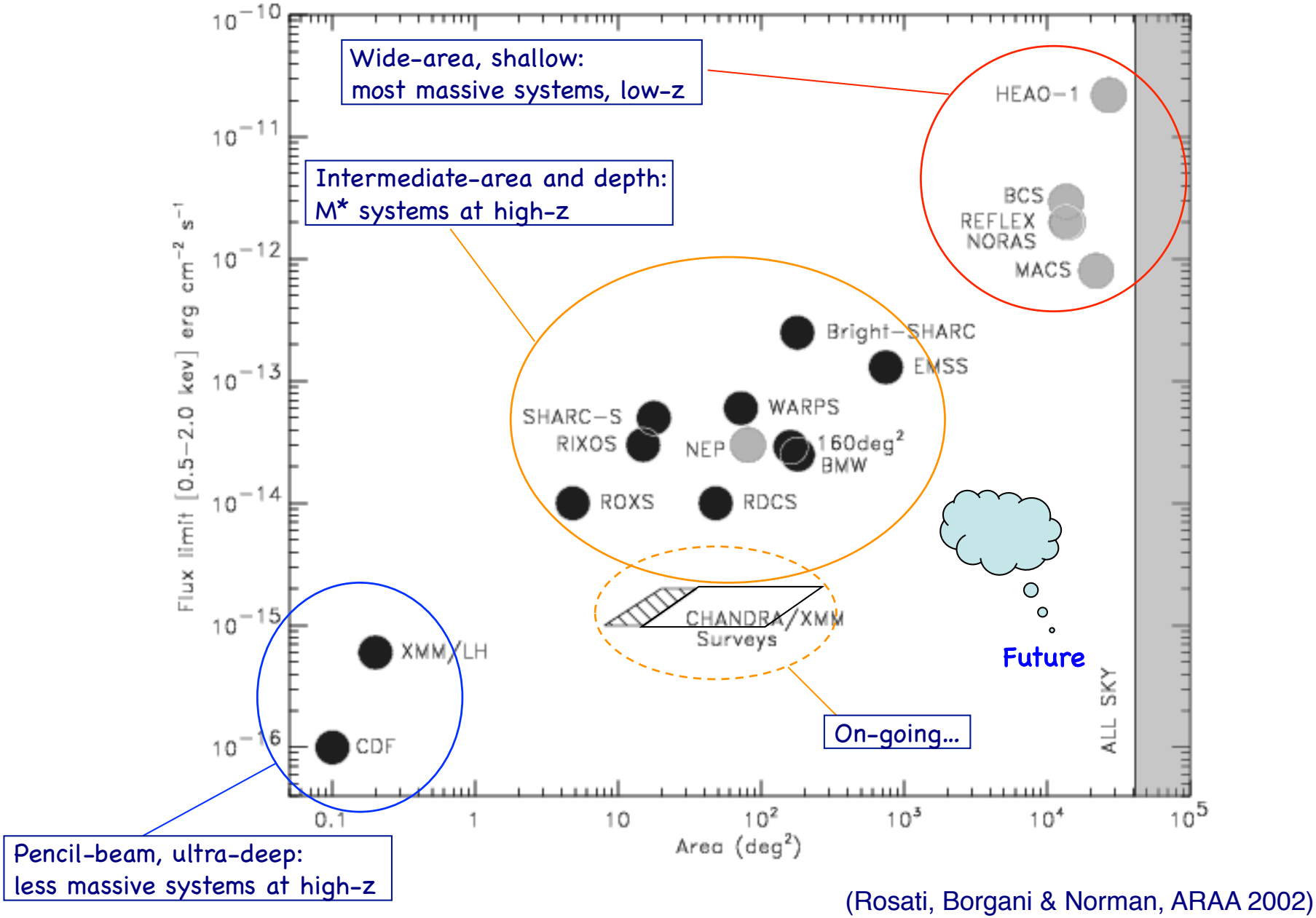

(Rosati, Borgani & Norman, ARAA 2002)

The search for clusters: XLF

Local (left) & high-z (right) XLF: no evolution evident below 3e44 erg/s, but present at 3σ level above it (i.e. more massive systems are rare at z>0.5)

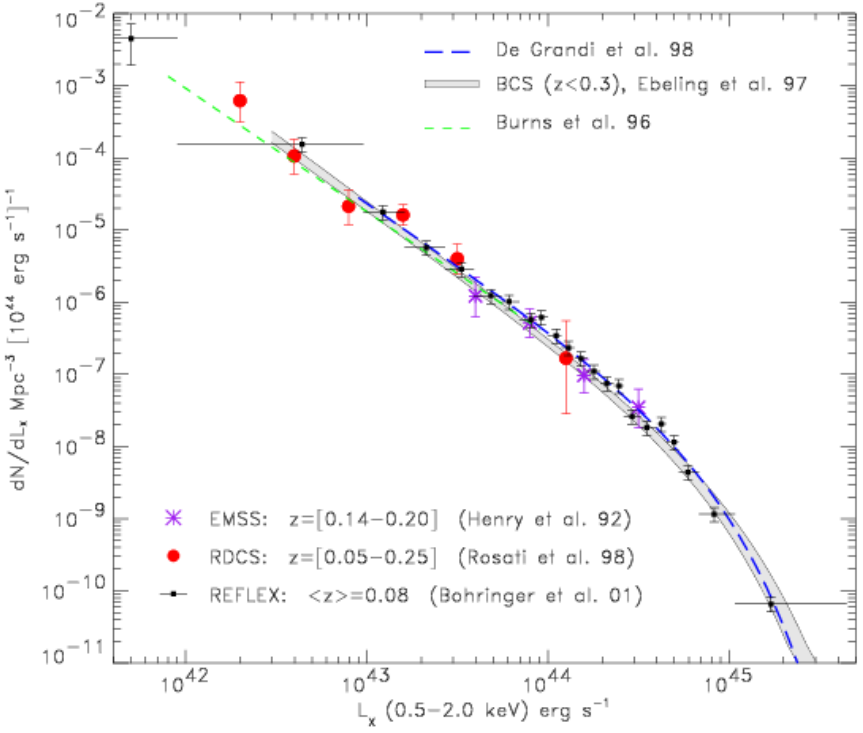

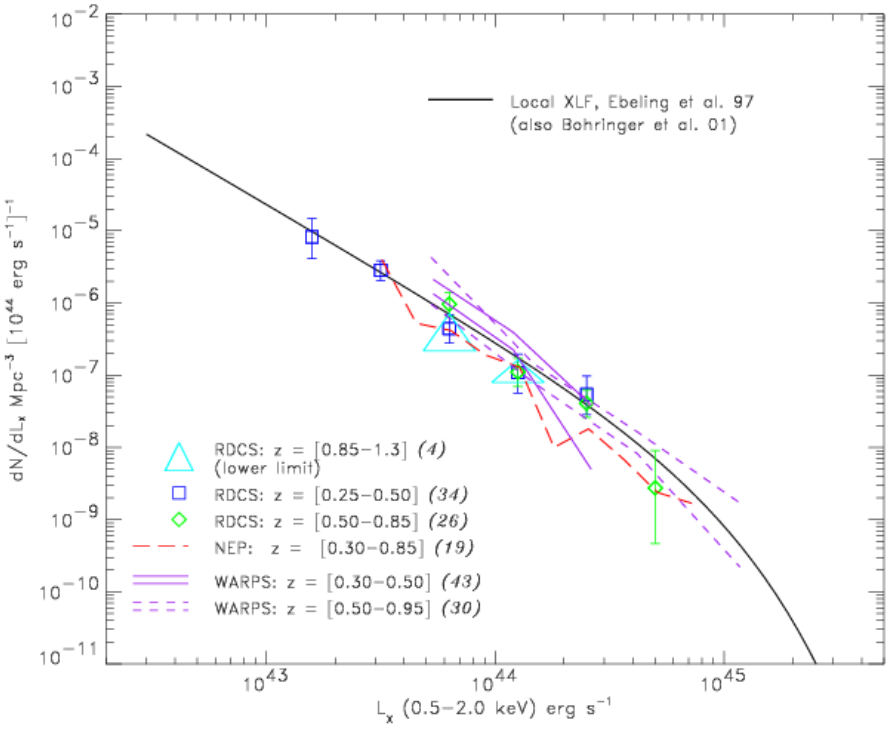

Rosati etal 03

Evolution of the *most massive* clusters

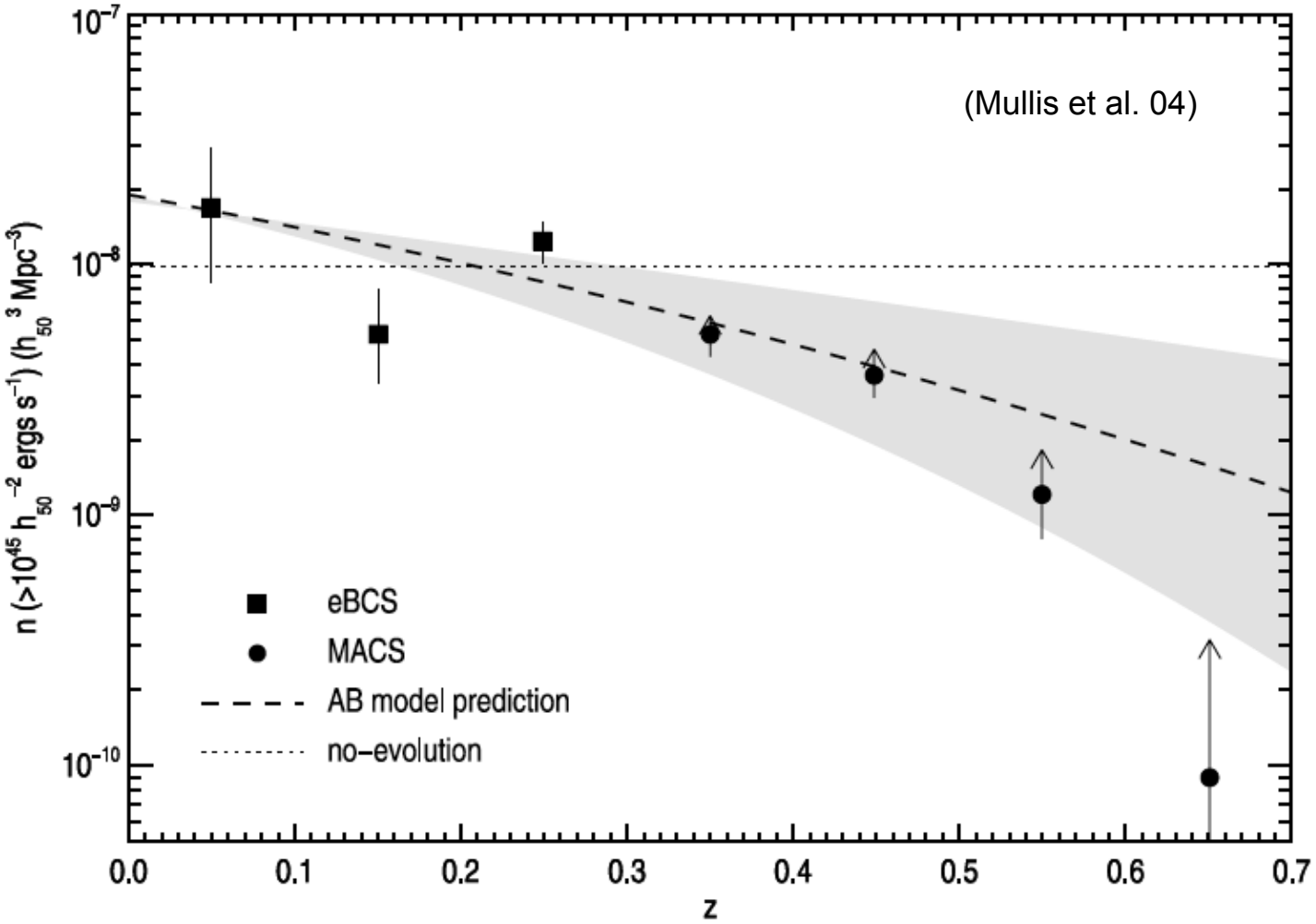

- Evolution from ROSAT serendipitous survey agrees with the one from wide-area ROSAT surveys

The search for clusters: XLF

The evolution in XLF provides cosmological constraints
once a L-(T)-M correlation is adopted & N(M) is recovered.

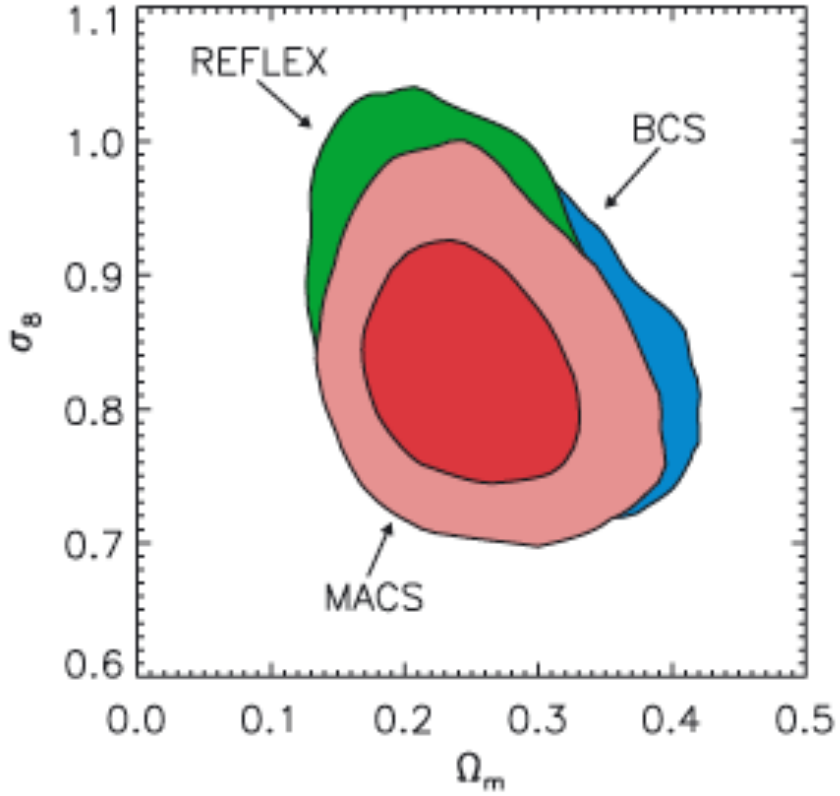

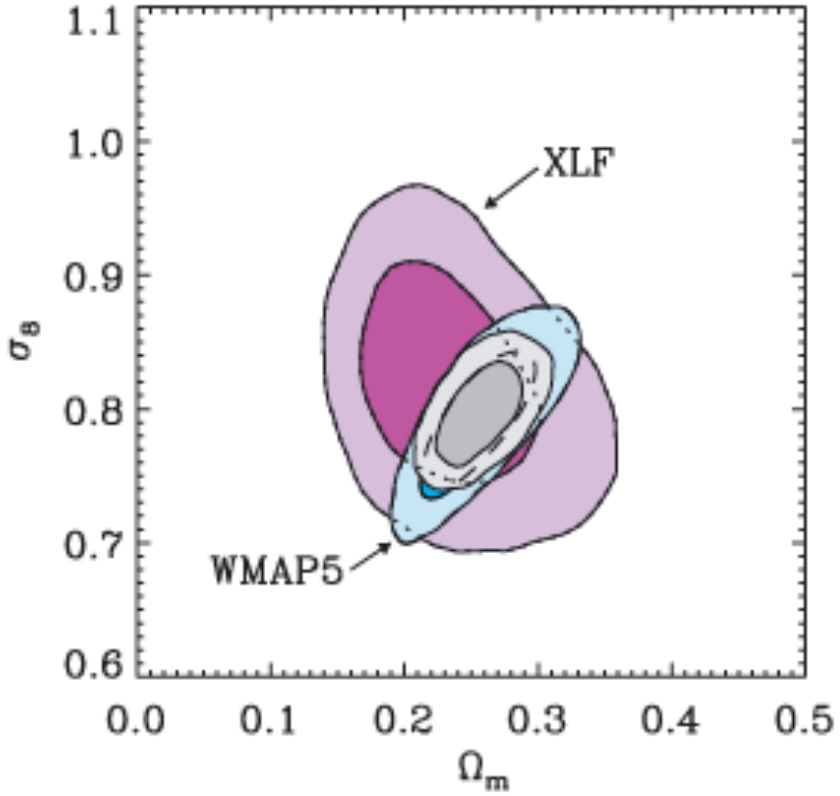

Mantz et al 10
(238 from RASS; 94 CXO)

The search for clusters: XLF

The evolution in XLF provides cosmological constraints *once a L-(T)-M correlation is adopted & N(M) is recovered*.

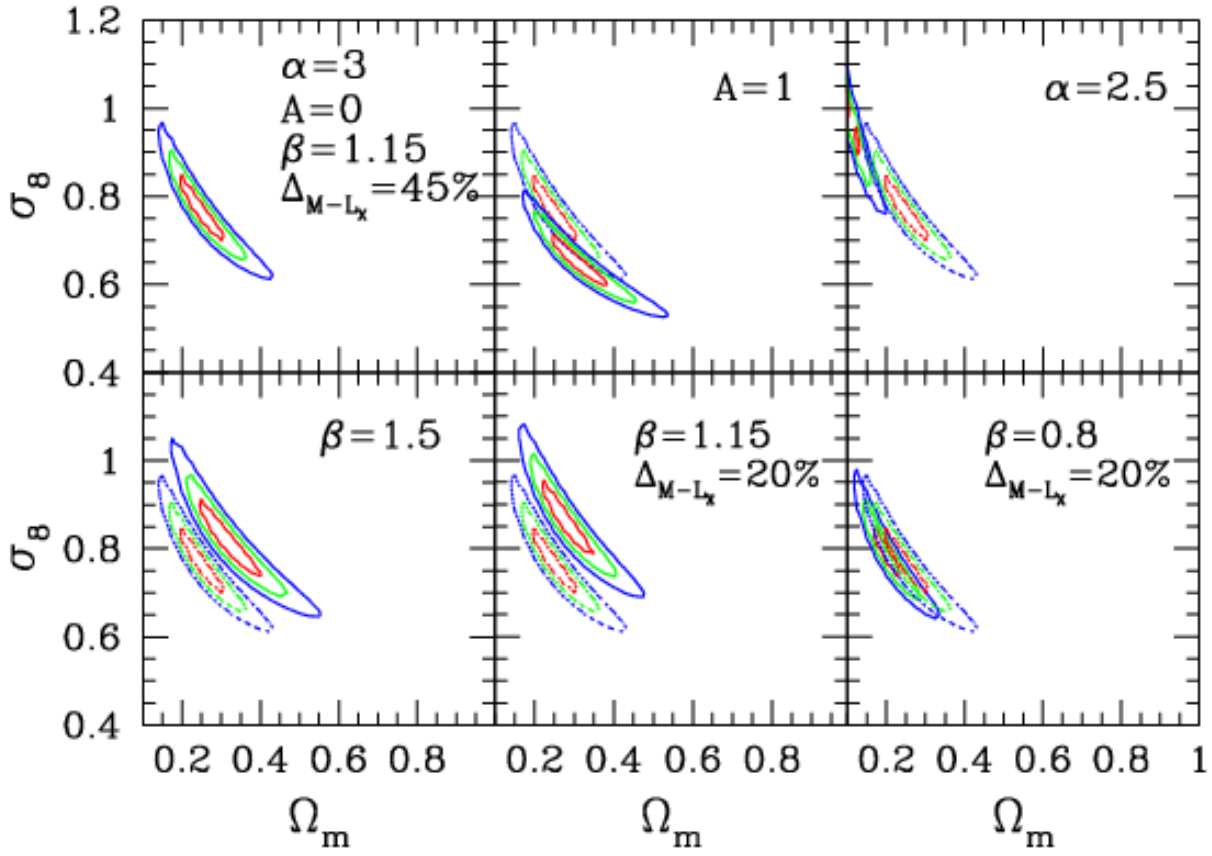

Rosati etal 03

XTF & cosmological constraints

Otherwise, but for a reduced number of objects due to the observational limitation in determining T [***5 X-ray cts to fix L, 500 to know T***…], one can derive an ***observed*** N(M) from a statistically well-defined sample of T…

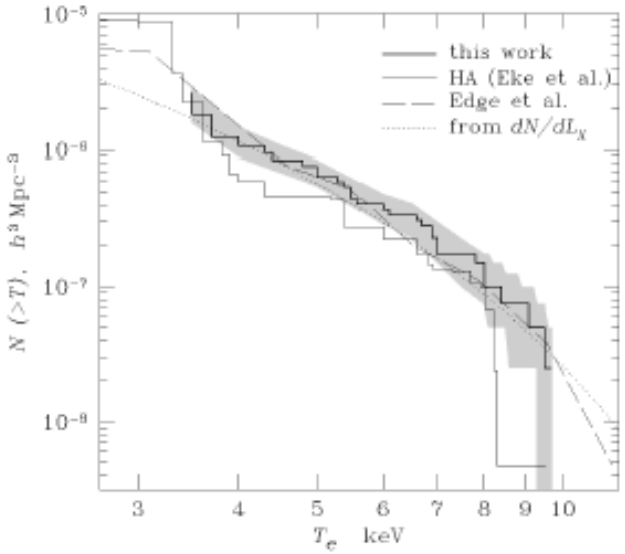

Markevitch 98

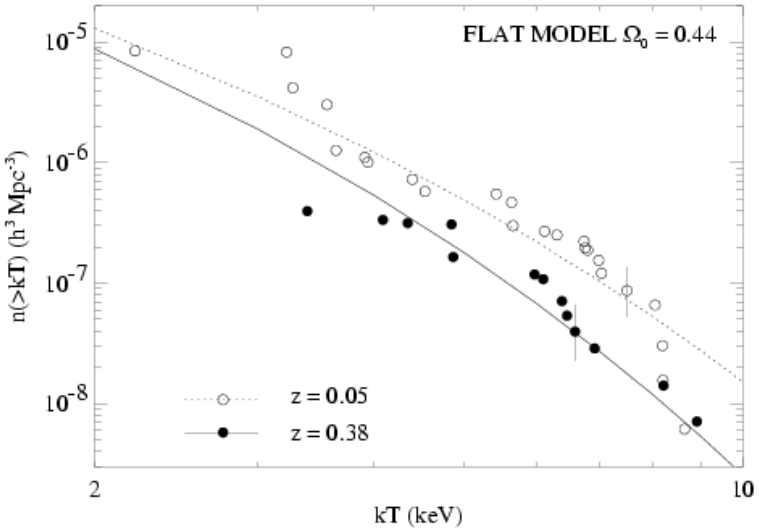

Henry 00

XTF & cosmological constraints

… and **put constraints on cosmological parameters**

by using an *adopted T-M relation*

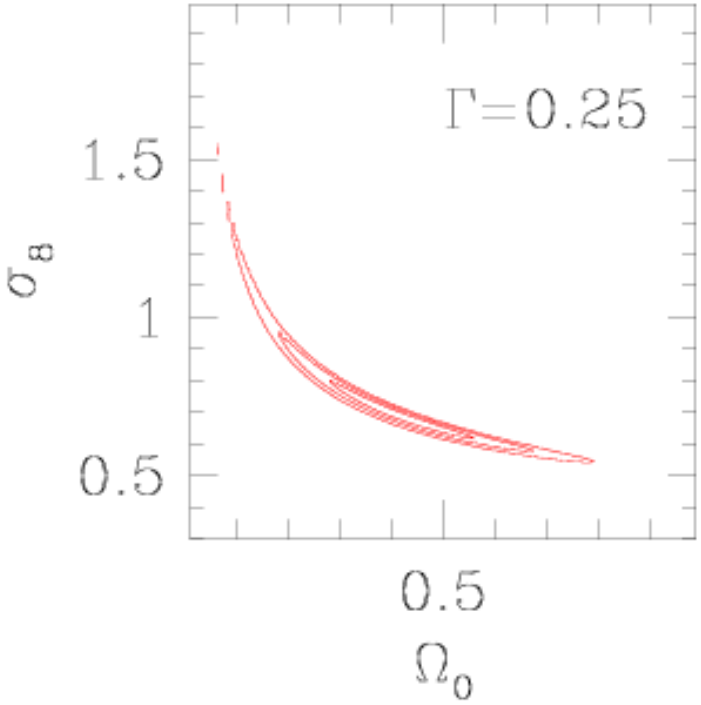

Eke etal 98

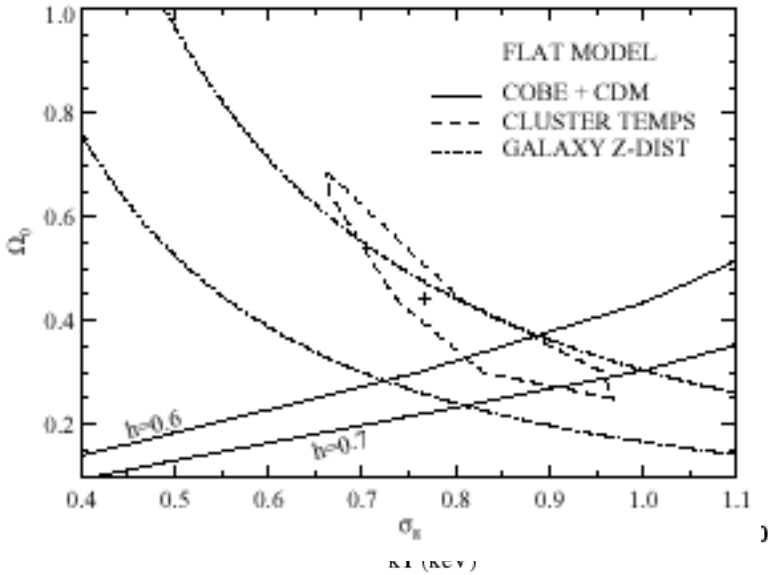

Henry 00

Sunyaev-Zel'dovich Effect: properties

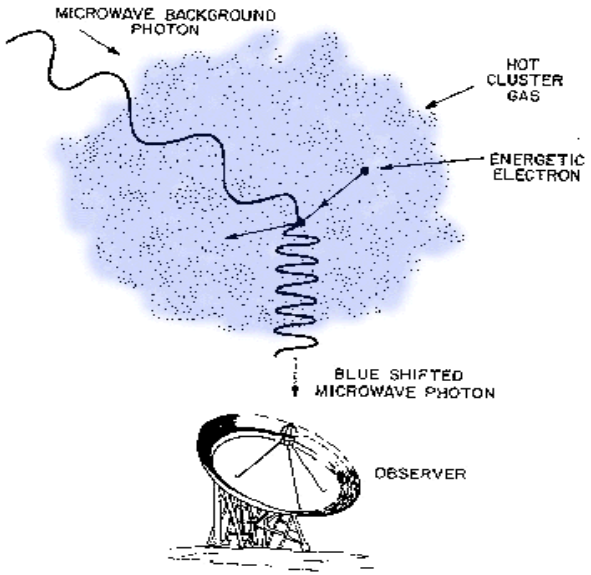

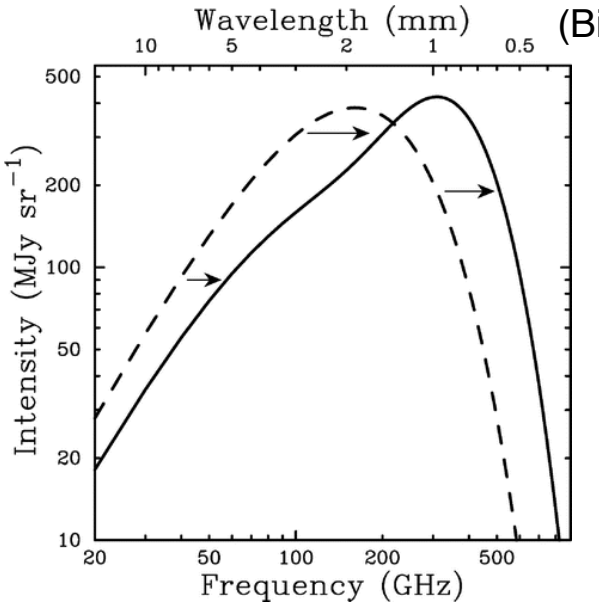

(Birkinshaw 2003)

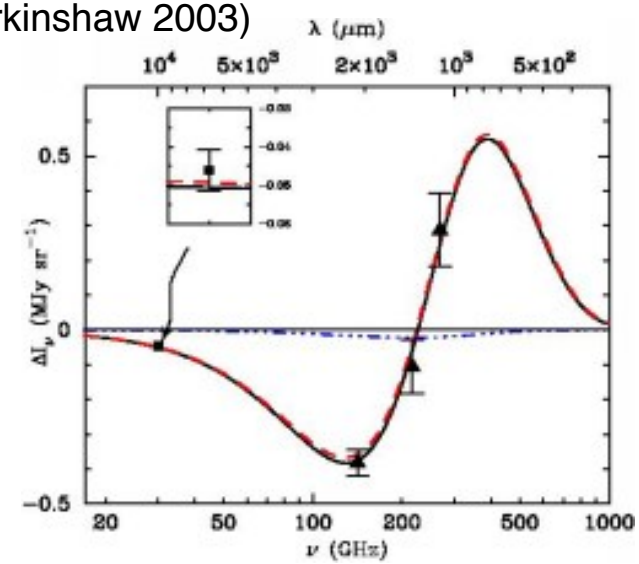

The SZ effects = inverse-Compton scattering by hot electrons on cold CMB photons, causing a distorsion of the CMB spectrum around 218 GHz (2mm)

The principal (thermal) SZ effect has an amplitude proportional to the Comptonization parameter, y_e (~10^{-4}), i.e. the integral of the pressure a.l.o.s.

The signal is due to absorption, i.e. **independent from redshift**!

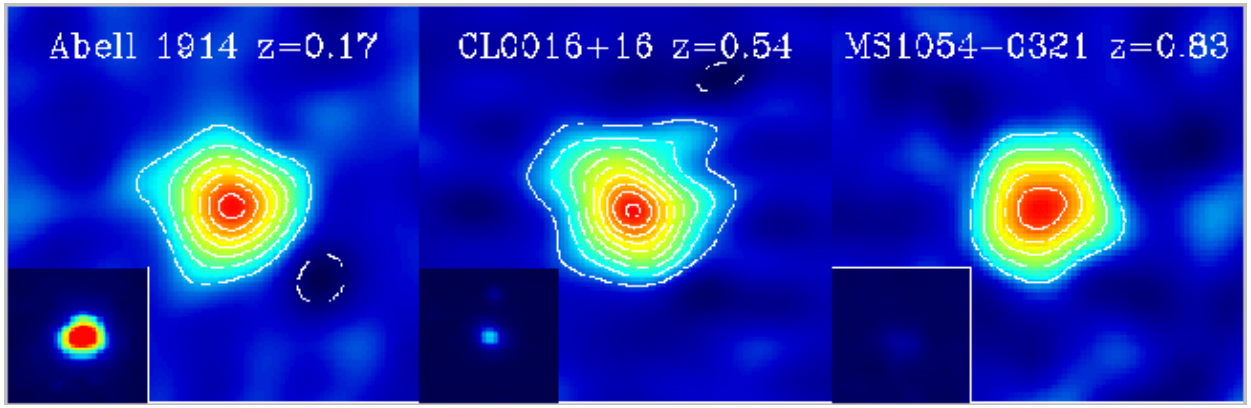

Sunyaev-Zel'dovich Effect: ongoing surveys

Atacama Cosmology Telescope ***ACT****:* located on Cerro Toco in the Atacama Desert of Chile, in the 2008 observing season ACT surveyed 455 square degrees of sky in the southern hemisphere at 148 GHz; **a sample of 23 SZ-selected clusters was optically confirmed**.

*South Pole Telescope (****SPT***; Carlstrom et al. 2009) is midway through a ~2500 deg^2 survey sensitive to galaxy clusters above ≈ 5e14 $M_\odot$ at all redshifts. **26 most significant SZ detection (12 new) in the z-range 0.1-1.13 (z_{med}~0.4) with M_{200}~1-3e15 $M_\odot$**.

Why South Pole ? At an altitude of 2800 meters above sea level, the South Pole is one of the premier locations for mm-wave astronomy. The high altitude and low temperatures ensure an atmosphere with low water-vapor content and excellent transparency.

Sunyaev-Zel'dovich Effect: ongoing surveys

Planck: ESA's mission, launched on 14 May 2009 carries a scientific payload consisting of an array of 74 detectors sensitive to a range of frequencies between roughly 25 and 1000 GHz, which scan the sky simultaneously and continuously with an angular resolution varying between ~30 / 4 arcmin (FWHM) at the lowest / highest frequencies

The Early SZ (ESZ) sample of **189 candidates** comprises high signal-to-noise clusters, from 6 to 29. Planck provides the first measured SZ signal for about 80% of the 169 ESZ known clusters. Planck further releases 30 new cluster candidates among which 20 are within the ESZ signal-to-noise selection criterion. Eleven of these 20 ESZ candidates are confirmed using XMM-Newton snapshot observations as new clusters, most of them with disturbed morphologies and low luminosities. The ESZ clusters are mostly at moderate redshifts (86% with z below 0.3) and span over a decade in mass, up to the rarest and most massive clusters with masses above 1e15 $M_{\odot}$.

The "lookback time cone" of observed clusters

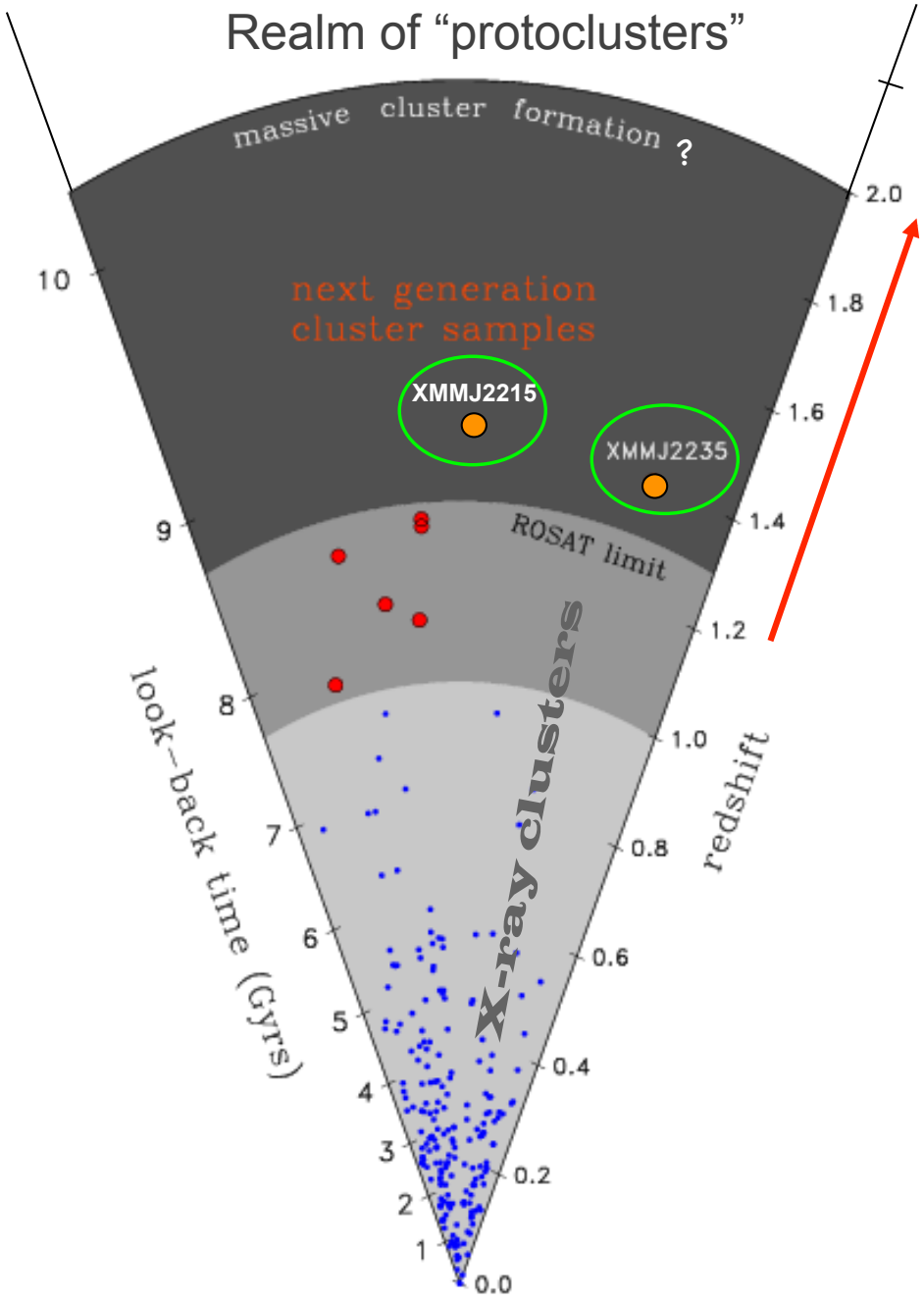

- **1<z<~2** is a critical epoch for the formation of baryonic structure (~50% of the stellar mass assembled)
- Only a few clusters at z>1 were discovered in the pre-Chandra/XMM era (+ optical surveys)
- The first massive (~10^{14} $M_{\odot}$) are thought to have *virialized* at z~2
- Several on-going surveys in X-ray (XMM) and IR(Spitzer) are now unveiling clusters out to z~1.5
- On-going large area near-IR surveys (e.g. UKIRT) and upcoming SZ surveys are expected to fill this cosmic epoch

Searching galaxy clusters: summary

- Galaxies overdensities in the optical/near-IR:

  extension to K-band (2m) increases the contrast even at high-z;
  volume ill-defined; easy to cover large areas

- X-ray selection:

  clusters are high contrast objects in the X-ray sky; L_x~M; hard to cover
  large areas; simple selection function; SB dimming limits effectivness at z>~1.5

- Search for galaxy overdensities around high-z radio galaxies or AGN:

  only method known so far to go to very high-z (up to z=4) -> proto-clusters;
  clusters might not be representative; no cosmology

- Sunyaev-Zeldovich (SZ) effect

  sensitivity is independent of redshift, high expectations in the near future
  with large areas to be covered; contamination from radio sources?

- Weak lensing shear:

  detection independent on dynamical state and baryon content in clusters.
  Shear selected cluster surveys are underway. Difficult task limited to z<0.8
  from the ground (complex selection function). It would be powerful from space.

Galaxy clusters & cosmology

- Concentration of 100-1000 galaxies
- Velocity dispersion (observed): $\sigma_v \sim 1000$ km s^{-1}
- Size: R ~ 1 Mpc $\Rightarrow$ the crossing time (lower limit to the relaxation time) is $t_{cross} = R/\sigma_v \sim 1$ Gyr < $t_H = 9.8\ h^{-1}$ Gyr
  $\Rightarrow$ clusters must be dynamically relaxed at the present
- **Mass:** assuming virial equilibrium $\Rightarrow$ $M \simeq \frac{R\sigma_v^2}{G} \simeq \left(\frac{R}{1}\right)\left(\frac{\sigma_v}{10^3}\right)^2 10^{15}\, h^{-1} M_\odot$
- Mass components: $f_{baryons} \approx$ 10-15%
  ($f_{gas} \approx$10%, $f_{gal} \approx$ a few%) $\Rightarrow$ $f_{DM} \approx$ 80-90%
- Intra-Cluster Gas: $T_X \approx$ 3-10 keV, $n_{gas} \approx 10^{-3}$ atoms/cm^3,
  Z ~ 0.3 solar $\Rightarrow$ **fully ionized plasma,** free-free bremsstrahlung + lines
  emission: $L_X \sim n_{gas}{}^2 \Lambda(T)\, V \sim 10^{43}$-$10^{45}$ erg/s

$$k_B T \simeq \mu m_p \sigma_v^2 \simeq 6 \left(\frac{\sigma_v}{10^3}\right)^2 \text{keV}$$

Optical Richness as M proxy

In the next few years, a host of large scale optical surveys (Dark Energy Survey/***DES***, Panoramic Survey Telescope & Rapid Response Systems/***Pan-STARRS***, Hyper-Suprime Camera/***HSC***, Large Synoptic Survey Telescope/***LSST***) are expected to generate galaxy catalogs spanning several thousands of square degrees to sufficient depth to reliable detect galaxies at $z \approx 1$.

These surveys will be used to optically select galaxy clusters, and in conjunction with stacked weak-lensing mass calibration, can be used to place tight constraints on cosmological parameters.

Optical Richness as M proxy

In **maxBCG cluster catalog** (Koester et al. 07, Rozo et al. 09), which is currently the best-studied optically selected cluster catalog at moderate redshifts, the scatter in mass at fixed richness (N_{200}) is $\sigma_{lnM\ lN} = 0.45 \pm 0.1$ for clusters with M_{200} >1e14/h $M_{\odot}$. Considering more carefully only red-gals can reduce the scatter by ~50% (Rykoff et al. 11).

For comparison, L_X, which is the noisiest X-ray mass estimator, has a scatter of $\sigma_{ln\ M\ lLX} = 0.25–0.32$ (Vikhlinin et al. 2009; Mantz et al. 2010).

Scatter at fixed weak lensing mass, which is also estimated to be about $\sigma_{ln\ M\ lWL} = 0.25 – 0.30$ (Becker & Kravtsov 2010).

X-ray scaling laws at a glance

✓ From hydrostatic equilibrium equation (or isothermal sphere equation): $\mathbf{M \approx \int \rho_{DM}\, r^2\, dr \propto R^3 \propto R\, T}$

✓ Thus, $\mathbf{R \propto T^{1/2}}$ **&** $\mathbf{M \propto T^{3/2}}$

✓ Assuming *brehmsstrahlung* emission & $\rho_{DM} \approx n_{gas}$,
$\mathbf{L \approx \int n_{gas}^2\, \Lambda(T)\, r^2\, dr \approx n_{gas}^2\, T^{1/2}\, R^3 \propto f_{gas}^2\, T^2 \propto f_{gas}^2\, M^{4/3}}$

✓ Considering that we generally measure these quantities at fixed overdensity Δ with respect to $\rho_{cr}(z) = 3H_z / 8\pi G$, these relations scale as ($F_z = \Delta^{1/2}\, H_z / H_0$):

- $F_z\, M \propto T^{3/2}$
- $F_z^{-1}\, L \propto T^2$
- $F_z^{-1}\, L \propto (F_z\, M)^{4/3}$

X-ray scaling laws: $L \propto T^2$

Pratt et al. (2009): to understand & kill the scatter

REXCESS: the Representative XMM Cluster Structure Survey
2<T<9 keV, selected only in L_X

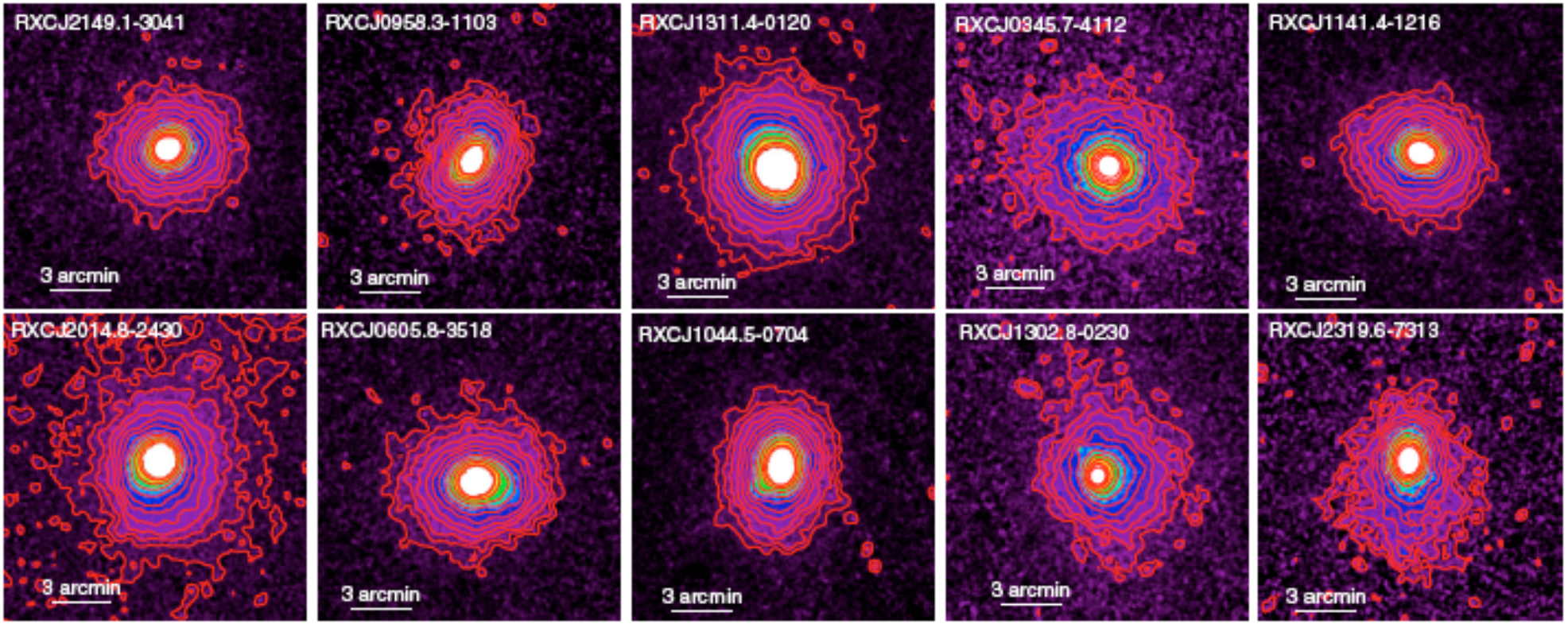

X-ray scaling laws: L ∝ T^2

Pratt et al. (2009): to understand & kill the scatter

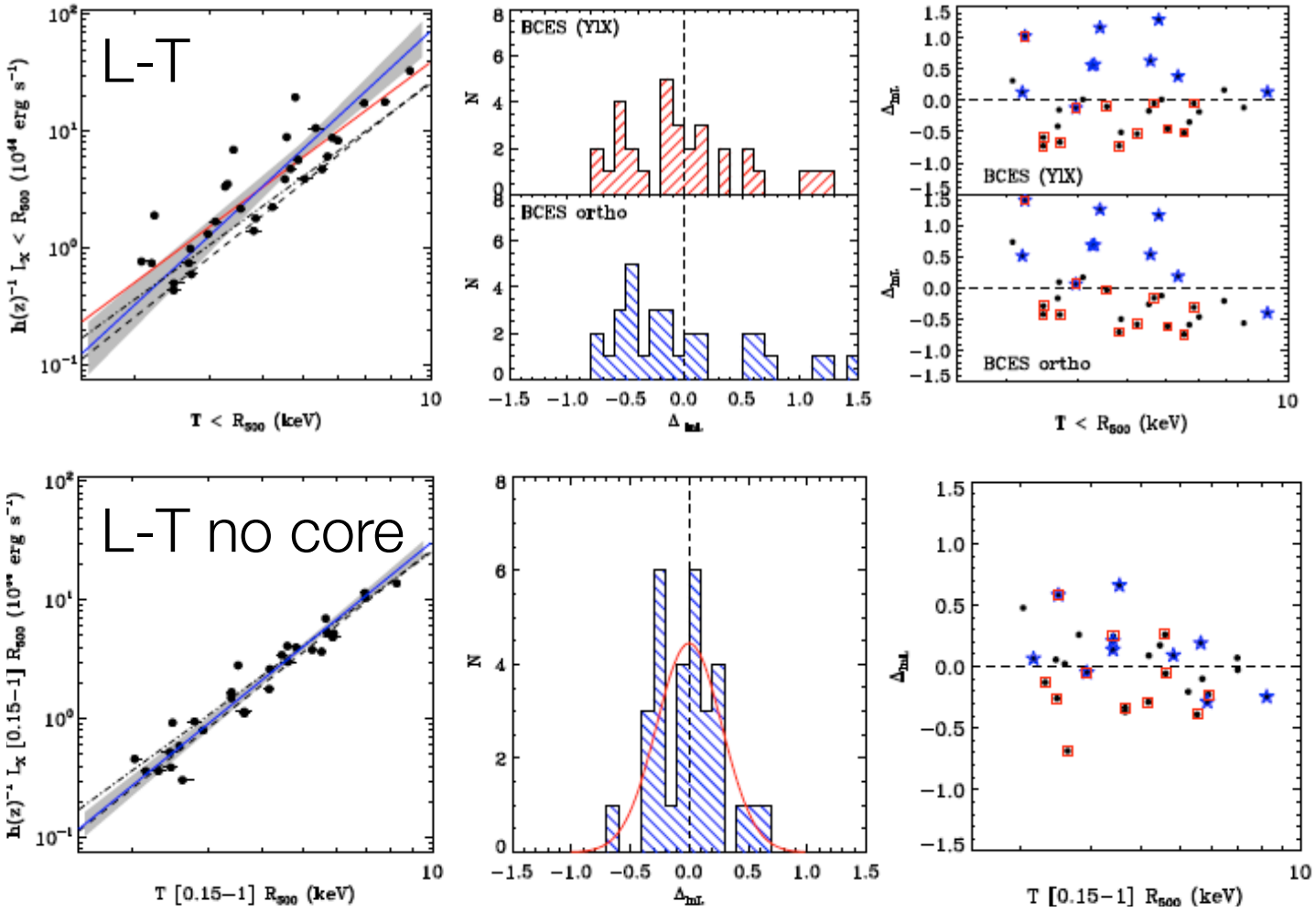

X-ray scaling laws: $L \propto T^2$

Pratt et al. (2009): to understand & kill the scatter

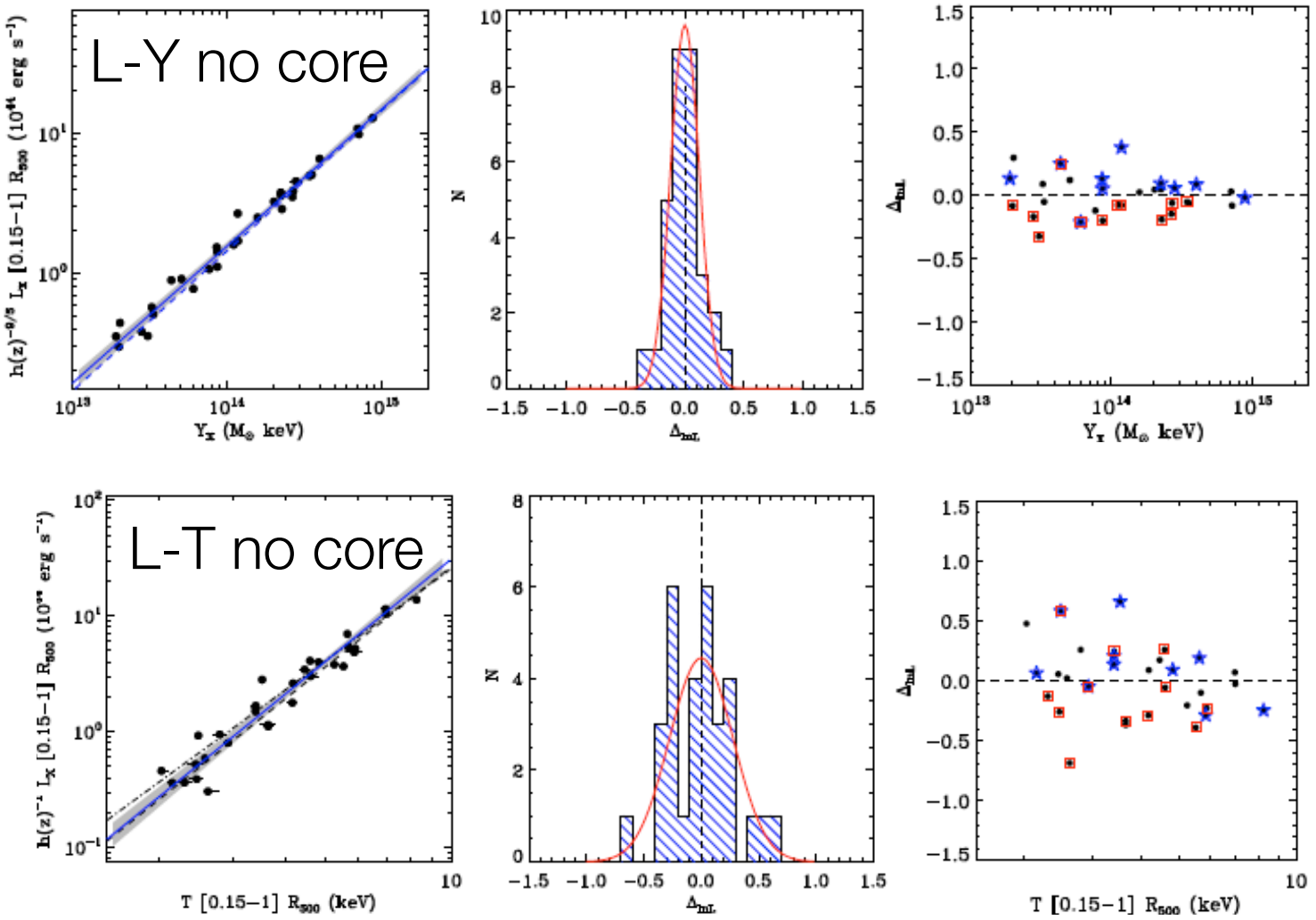

X-ray scaling laws: $L \propto T^2$

Pratt et al. (2009): relations steeper than SS predictions

$L \sim f_{gas}^2 M \Lambda(T) Q$ … not necessarily $\sim M^{4/3} \sim T^2$

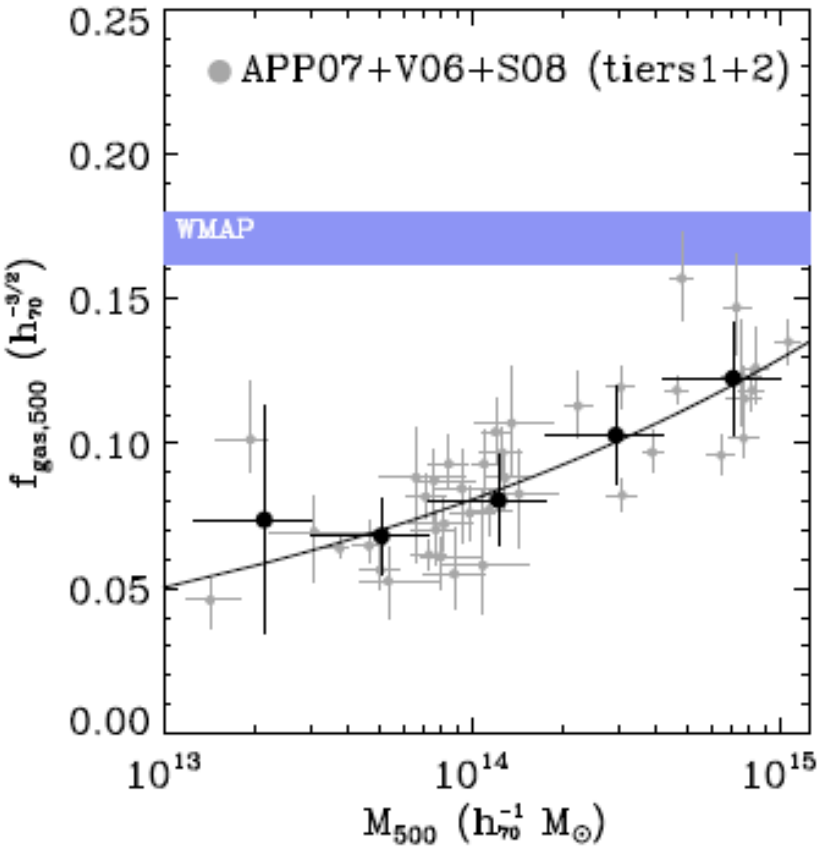

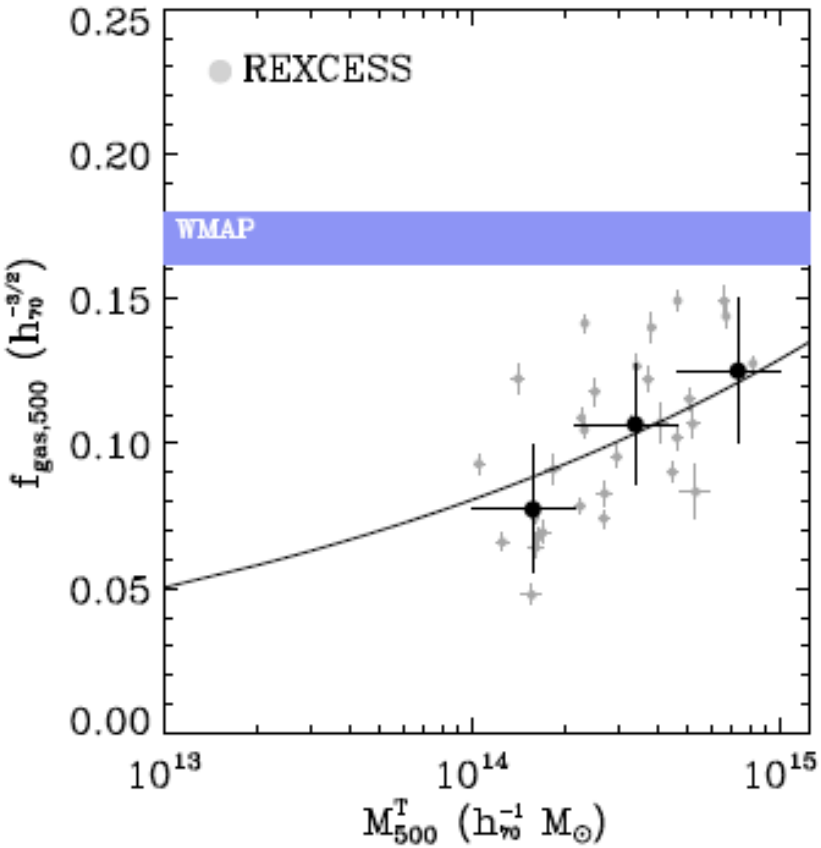

X-ray scaling laws: $M \propto T^{3/2}$

Evrard, Metzler & Navarro (1996) use gasdynamic simulations to assess the accuracy of X-ray mass estimations & conclude that within an overdensity between 500 and 2500, the masses from β-model are good. The scatter can be reduced if M is estimated from the tight M-T relation observed in simulations:

$$M_{500} = 2.22e15\ (T/10\ keV)^{3/2}\ h_{50}^{-1}\ Msun$$

β-model

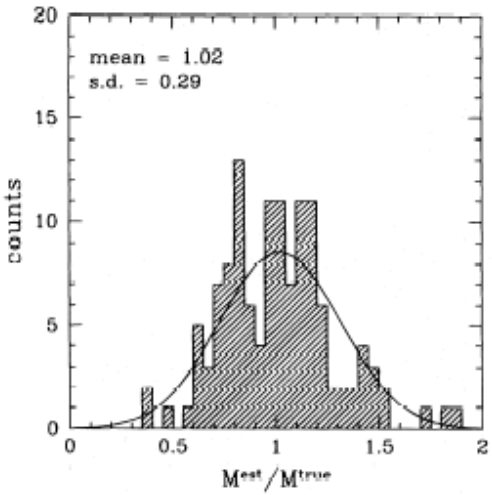

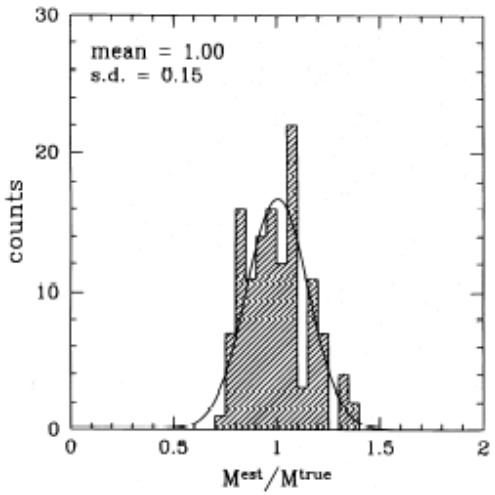

law

Estimators of X-ray total mass

from observables to M_{tot}

$$M_{500} = 5.6e14\ (T/5\ keV)^{3/2}\ \ h_{70}^{-1}\ \ M_{sun}$$

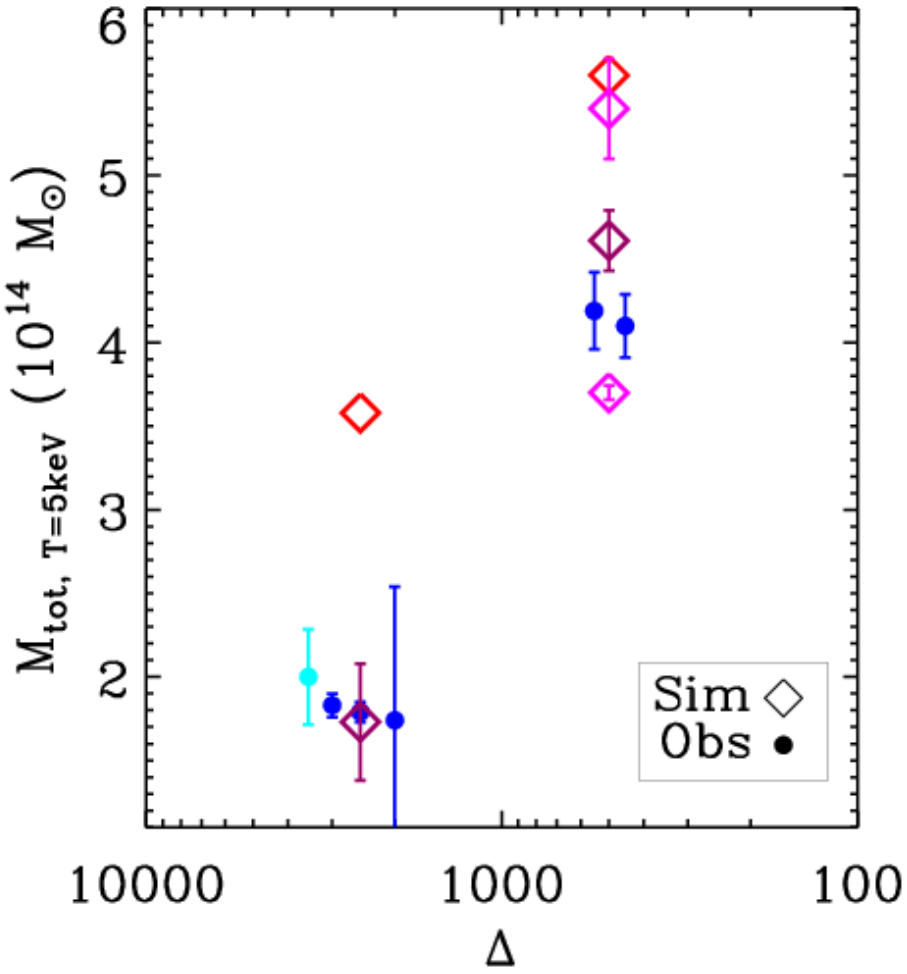

Evrard et al. 96
Borgani et al. 04
Nagai et al. 07

Arnaud et al. 05
Vikhlinin et al. 05
Ettori et al. 02
Hoekstra 07

Estimators of X-ray total mass

from observables to M_{tot}

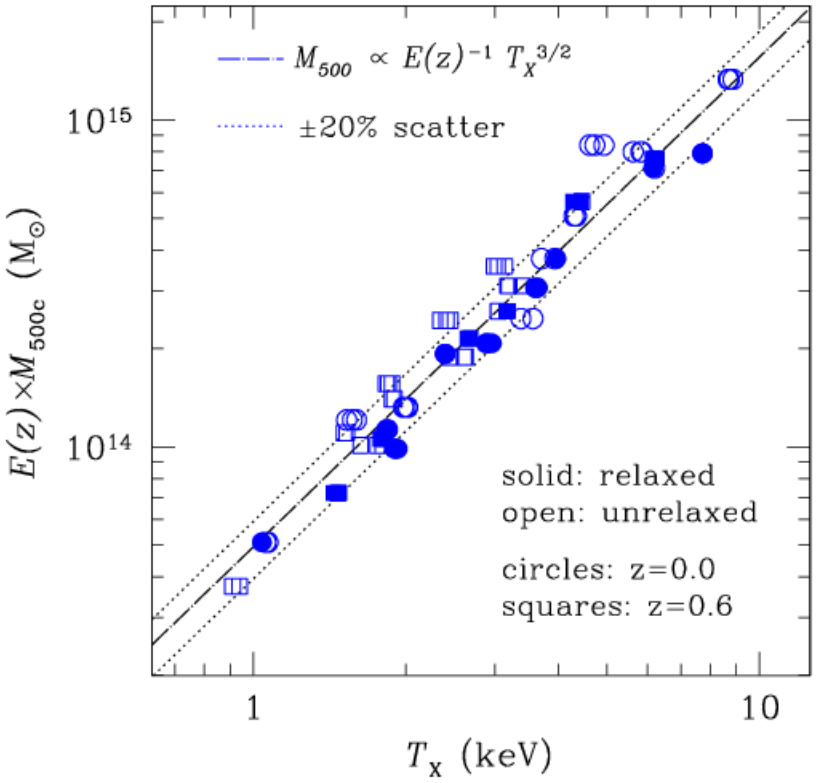

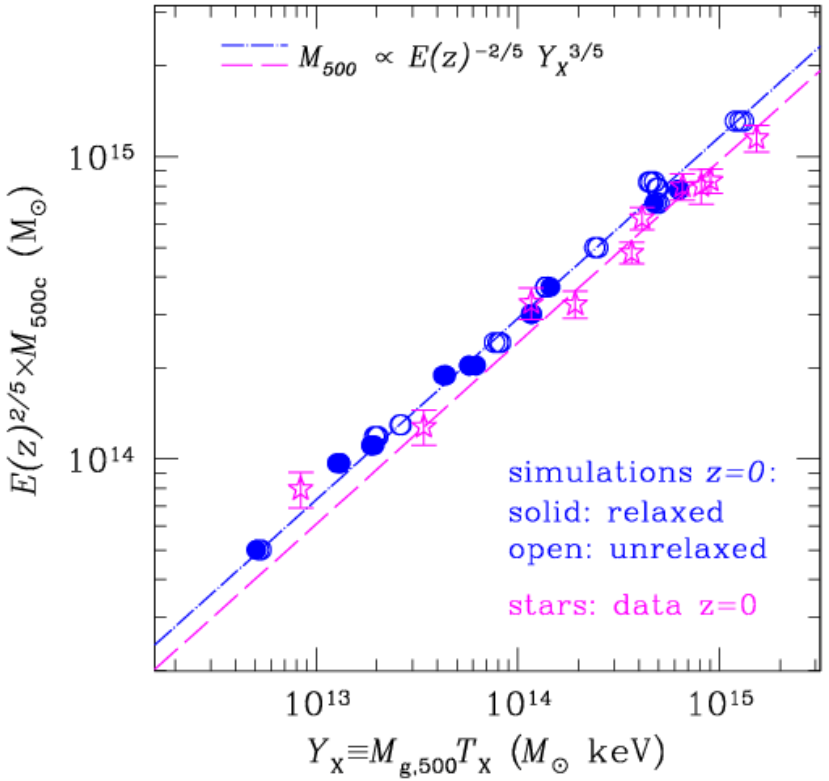

Kravtsov et al. 06 (Maughan 07)

Estimators of X-ray total mass

from observables to M_{tot}

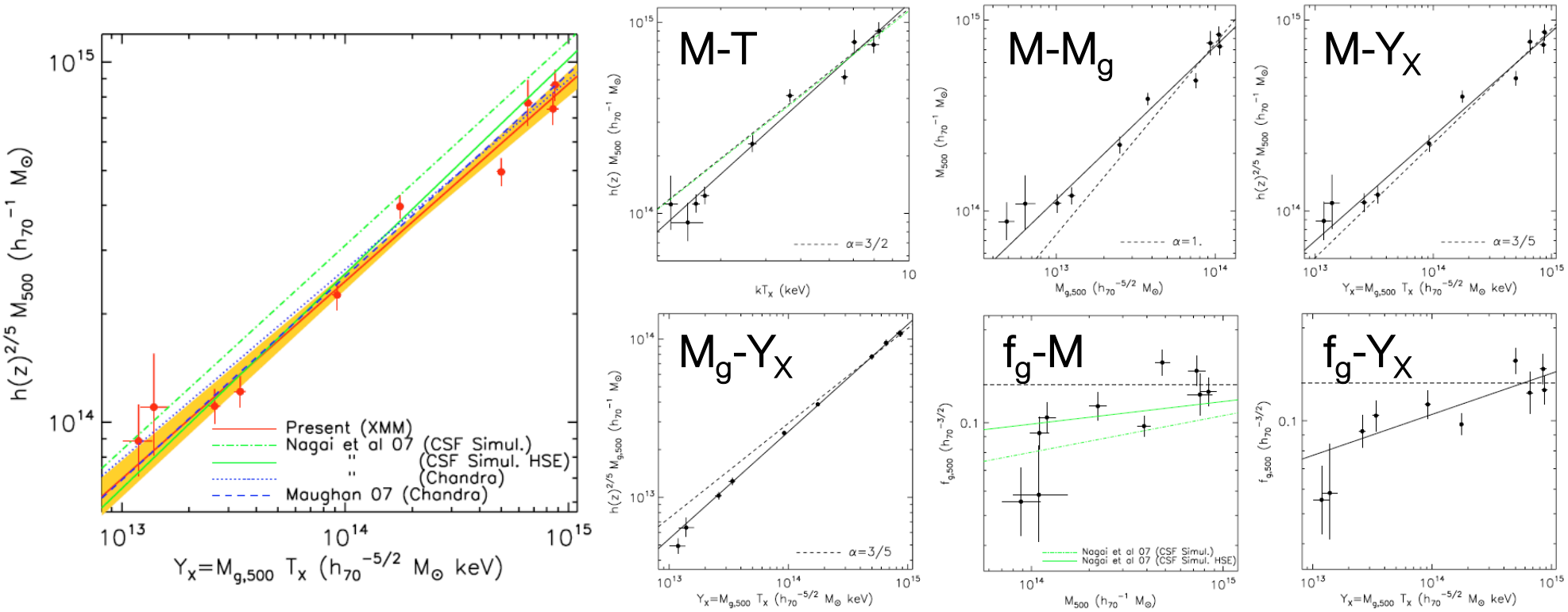

Arnaud et al. 07: correlation with mass of X-ray observables for a sample of 10 relaxed nearby systems observed with XMM

X-ray scaling laws: evolution

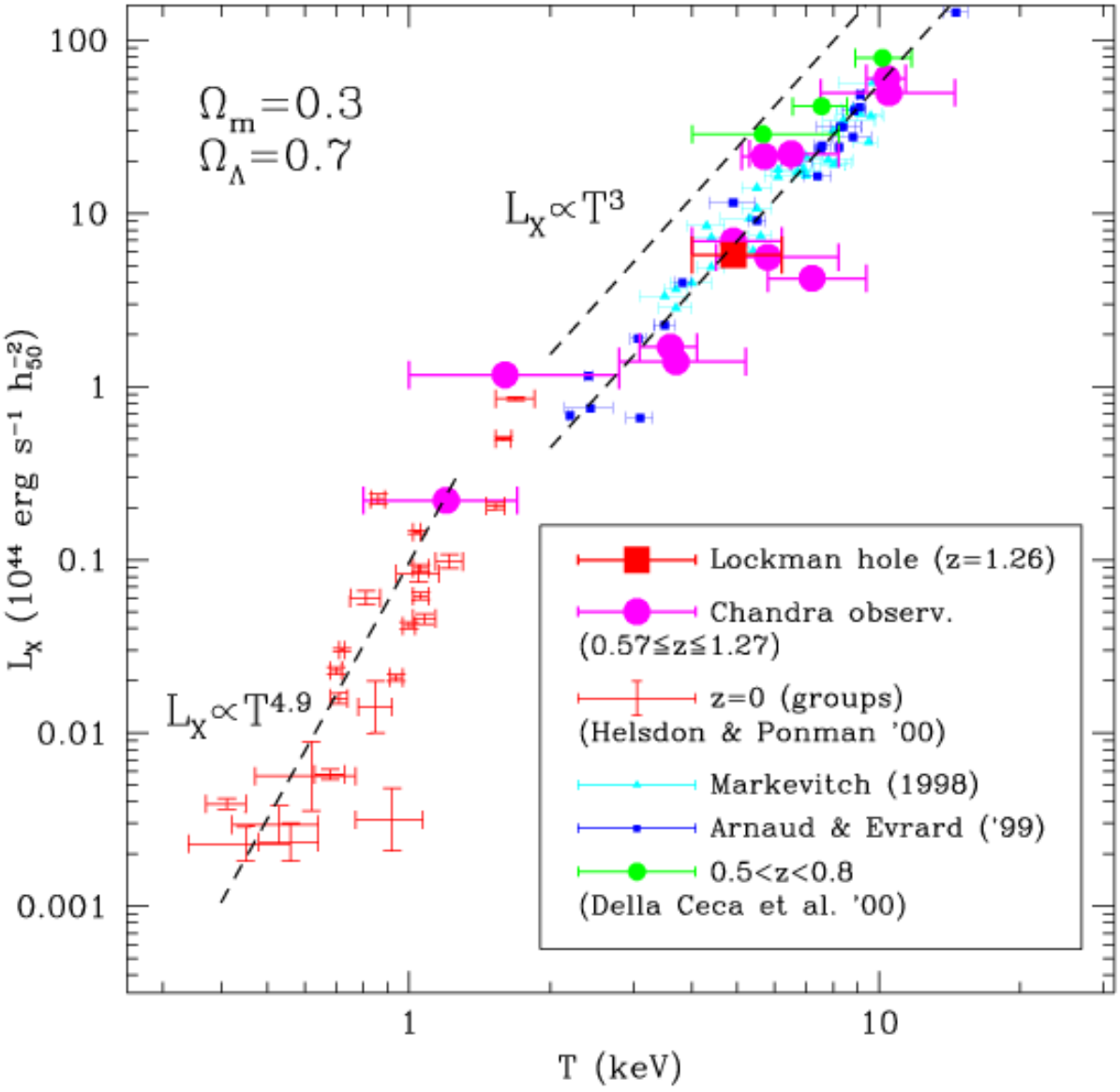

Evolution in the M-T relation

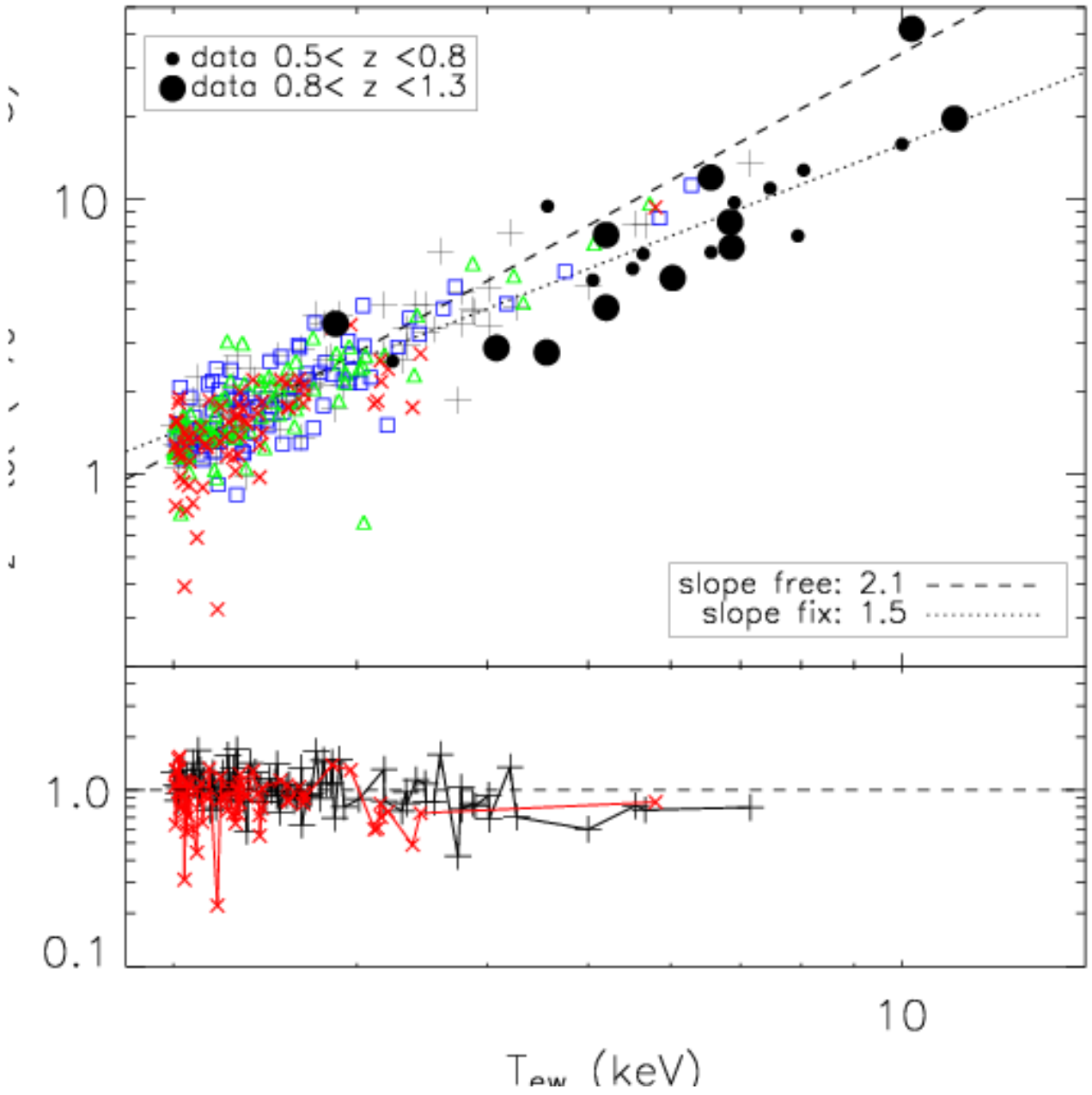

Evolution

$(1+z)^B$

Simulated

B = -0.1 ±0.1

Observed

B = -0.2 ±0.3

(Ettori et al. 04)

Evolution in the L-T relation

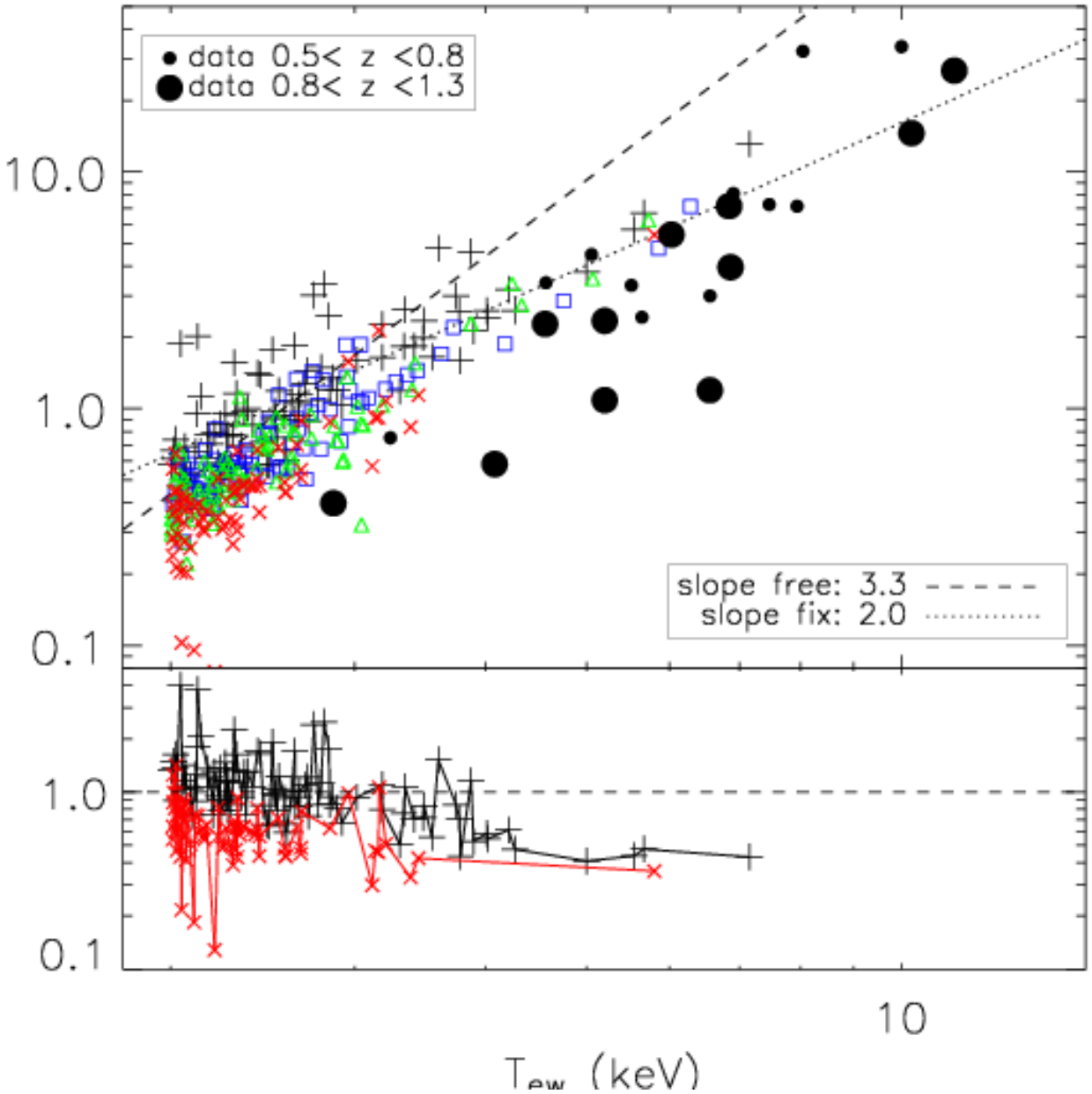

Evolution

$(1+z)^B$

Simulated

B = -0.8 ±0.1

Observed

B = -2.2 ±0.5

(Ettori et al. 04)

X-ray scaling laws: evolution

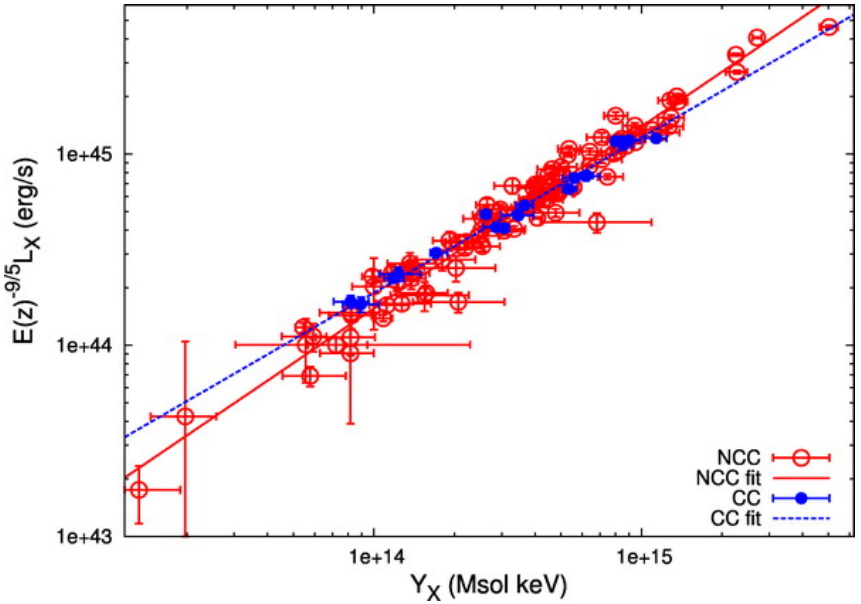

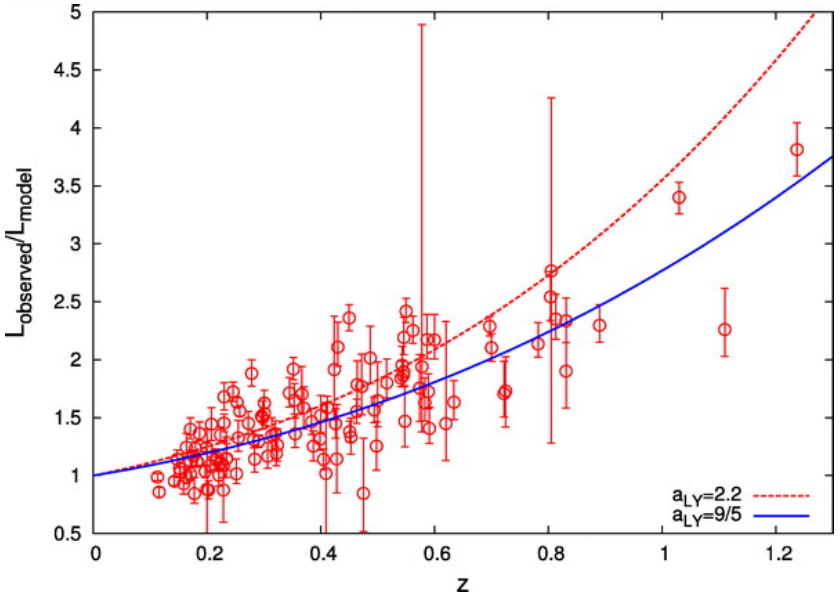

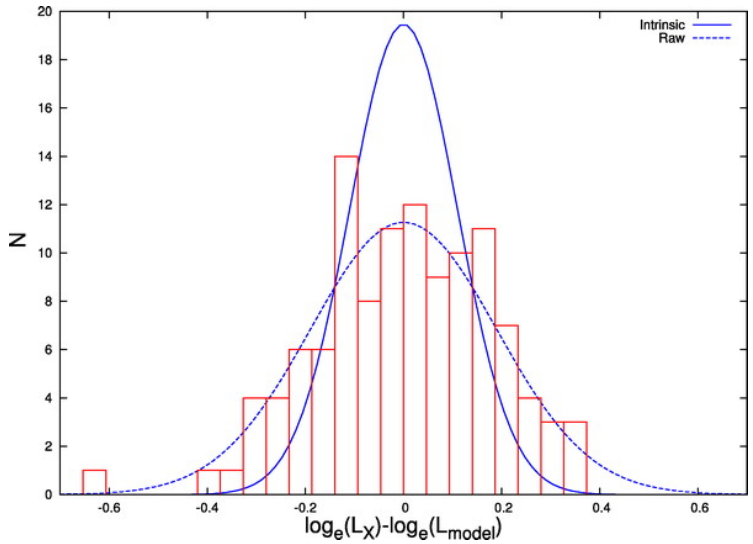

Maughan 07: 115 obj observed with CXO in 0.3<z<1.3 … L_X-Y_X relation (11% intrinsic scatter in L_X) is recovered if sufficiently large core regions ($0.15R_{500}$) are excluded; for high-redshift clusters the scatter in the *L_X-M relation remains low if cluster cores are not excluded*

Conclusions on evolution of SL

• **No evolution, *apart from self-similar expectations*, is observed in M-T & M_{gas}-T & L-Y**…
The normalization in M – T/Y_X for nearby systems is lower (by ~20%) than the one predicted from simulations including cooling & galaxy feedback.

• **Negative evolution in L-T**: i.e. a slight decrease in L for given T at higher z is observed (cores not excised).
Note that *the entropy at 0.1 R_{200} is measured higher in systems at higher redshift,* with an apparent correlation between high-Fe / low-S systems (see also the observed higher metallicity in low-T clusters in Tozzi et al. 03).

From observed Galaxy Clusters to Cosmology: the mass proxies

Stefano Ettori
(INAF-OA Bologna)

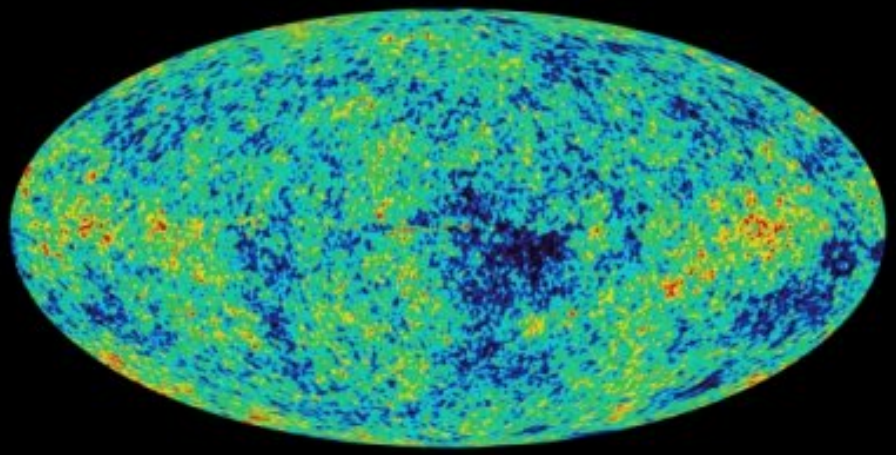

WMAP

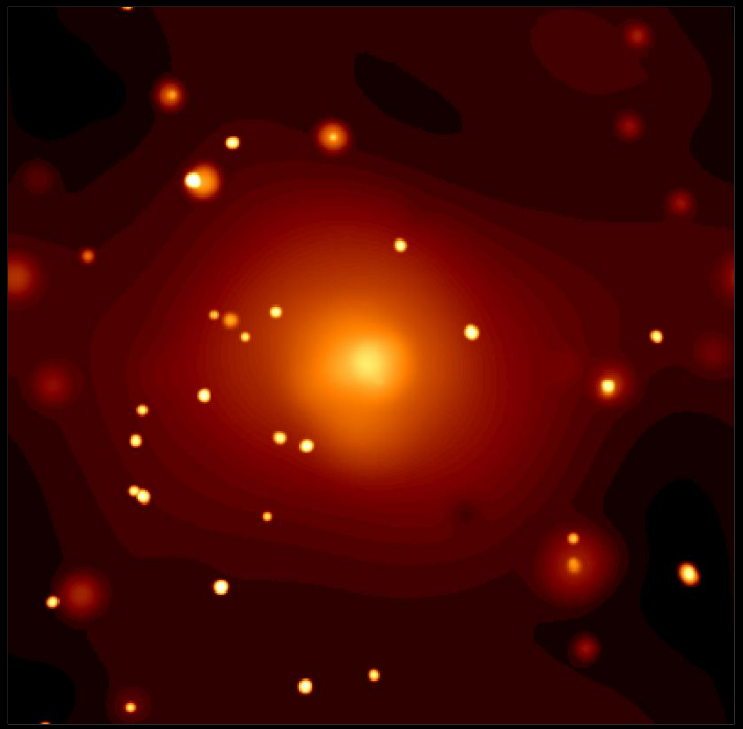

rxj1252 (z=1.24)

Dark Matter & X-ray clusters

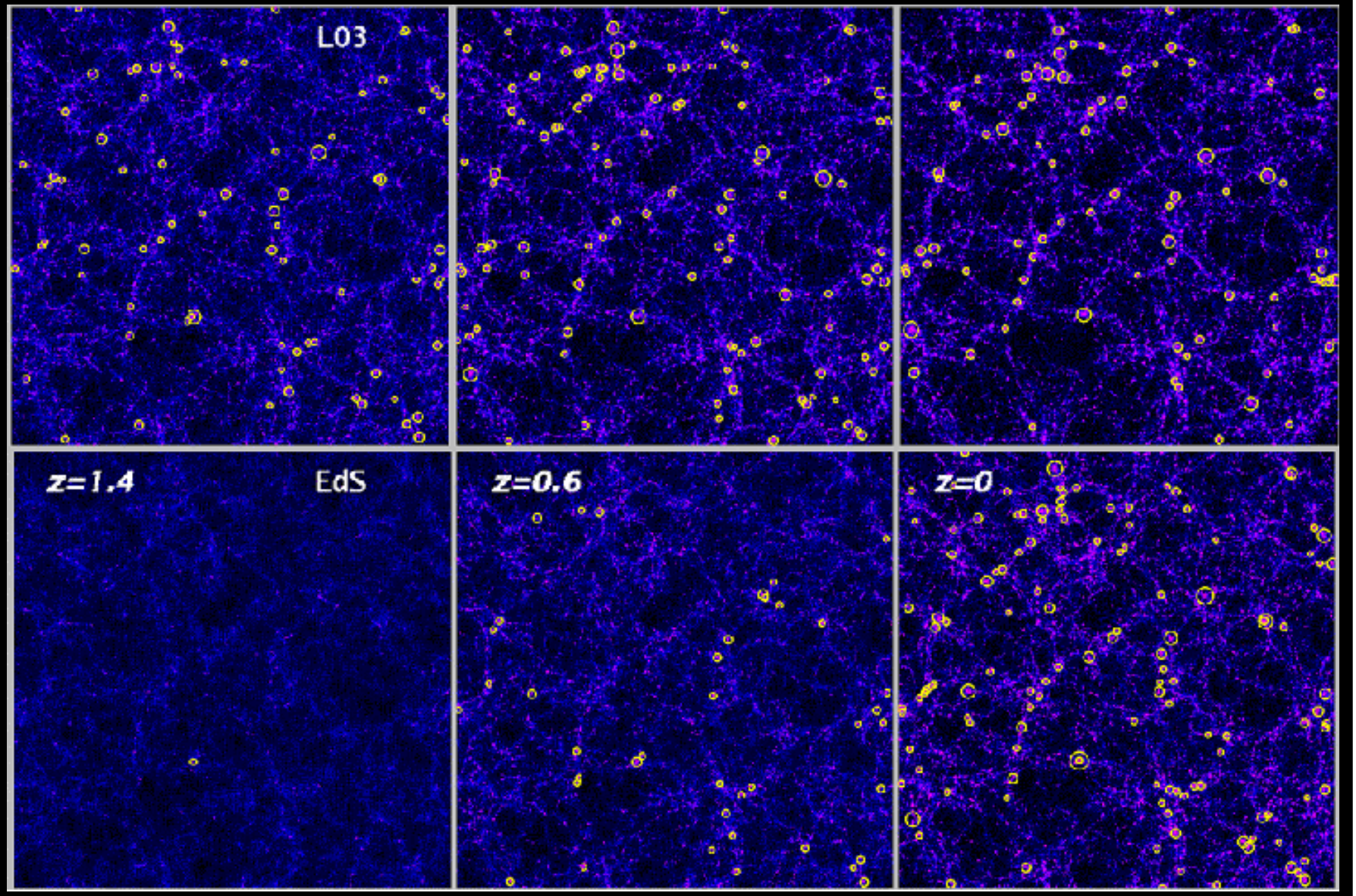

Ω_m=0.3
=1- Ω_Λ

EdS

(*Borgani & Guzzo 2001*) Normalized to space density at z=0;
circles: clusters with T>3 keV & $\propto$T

ICM at R_{200}: *S_b of simulated clusters*

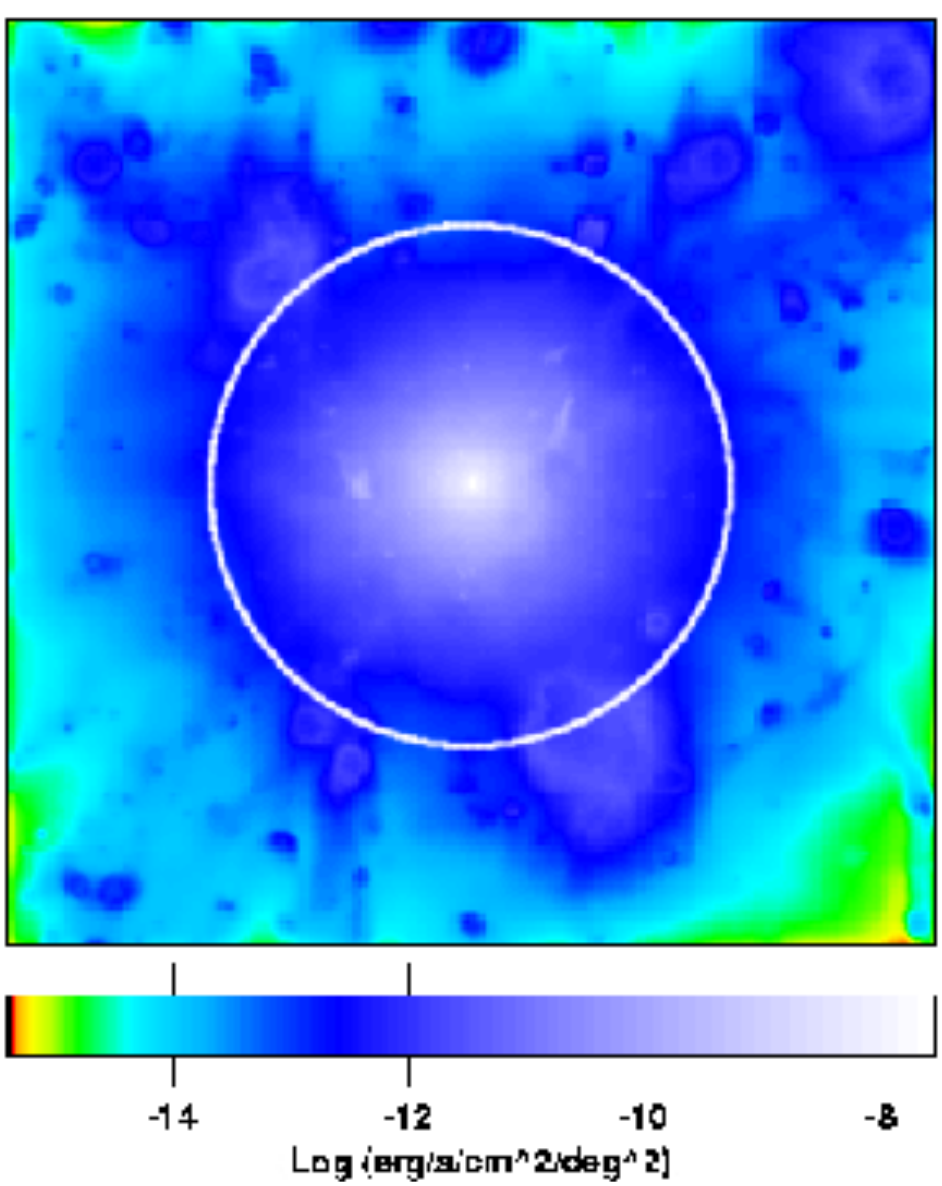

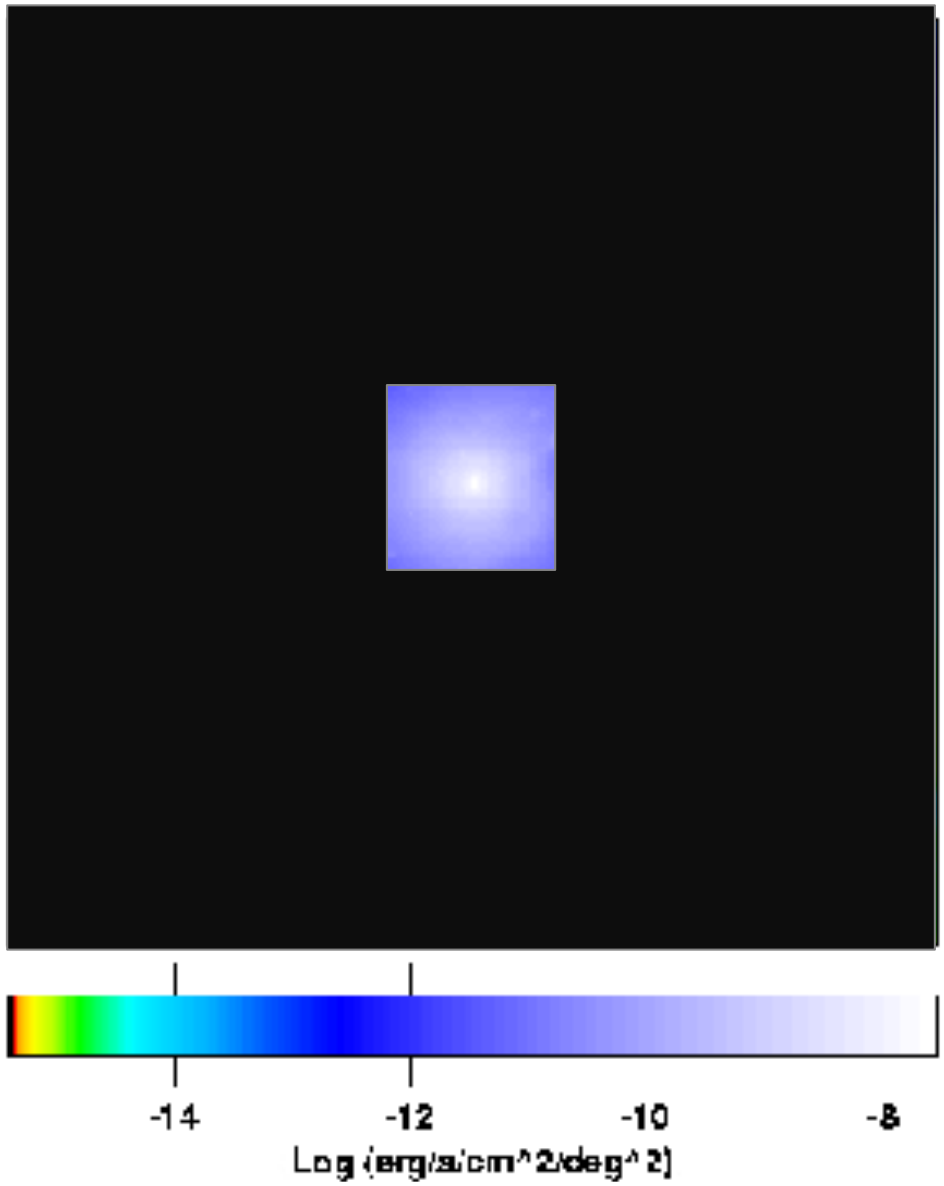

X-ray observables

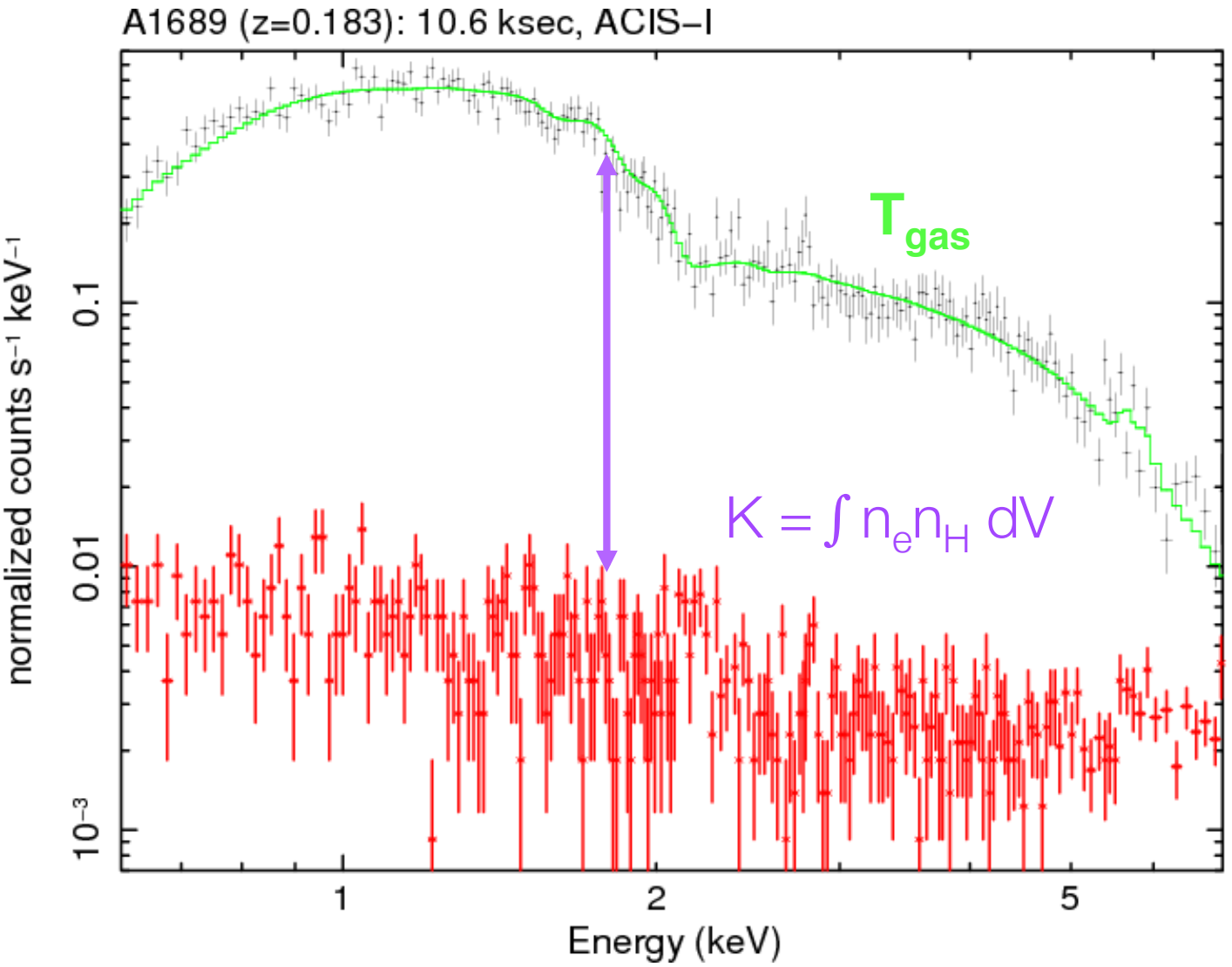

- few tens of counts to have detection and estimate of the gas density ($L_x \sim n_{gas}^2$)
- few thousands of cts to measure properly T_{gas}

X-ray total mass

Total mass from X-ray is determined by assuming
1. spherical symmetry, 2. hydrostatic equilibrium

$$\frac{d\Phi}{dr} = \frac{G M_{tot}(<r)}{r^2} = -\frac{1}{\rho_{gas}} \frac{dP_{gas}}{dr}$$

X-ray total mass

Total mass from X-ray is determined by assuming
1. spherical symmetry, 2. hydrostatic equilibrium

$$M_{tot}(<r) = -\frac{kT_{gas}(r)\ r}{G\mu m_p}\left(\frac{\partial \ln n_{gas}}{\partial \ln r} + \frac{\partial \ln T_{gas}}{\partial \ln r}\right)$$

- ✓ direct application of HEE on deprojected T and n_{gas}
- ✓ HEE with functional forms of T and n_{gas} (β-model)
- ✓ Use of analytic mass models (e.g. NFW, RTM profiles)

by fitting either T_{deproj} from inversion of HE to deprojected values or M(<r) from functional forms +HEE

X-ray total mass in 7 steps

Step 1: define a grid in {c, rs}

Step 2: define a functional form for

$M(<r) = K * f(x) * r_s^3 * m(c)$

where $m(c) = \delta/3 * c^3 / (\log(1+c) - c/(1+c))$

$f(x) = \log(x + \sqrt{1+x^2}) - x/\sqrt{1+x^2}$ [Isothermal]

$= \log(1+x) - x/(1+x)$ [NFW]

$= \ldots$

Step 3: at each resolved r, estimate $dP = -M/r^2 * n_e * dr$

Step 4: define P_{out}

Step 5: $P(r) = P_{out} - \mathrm{Sum}(\mathrm{Reverse}(dP))$

Step 6: $T_{fit} = P(r) / n_e$

Step 6bis: project T_{fit} in the observed annulus

(e.g., with Mazzotta's rule)

Step 7: $\chi^2(c, rs) = \mathrm{Sum}((T_{fit} - T_{xspec})^2 / err^2)$

Structure of CDM halos

(Navarro, Frenk, White 1996, 1997)

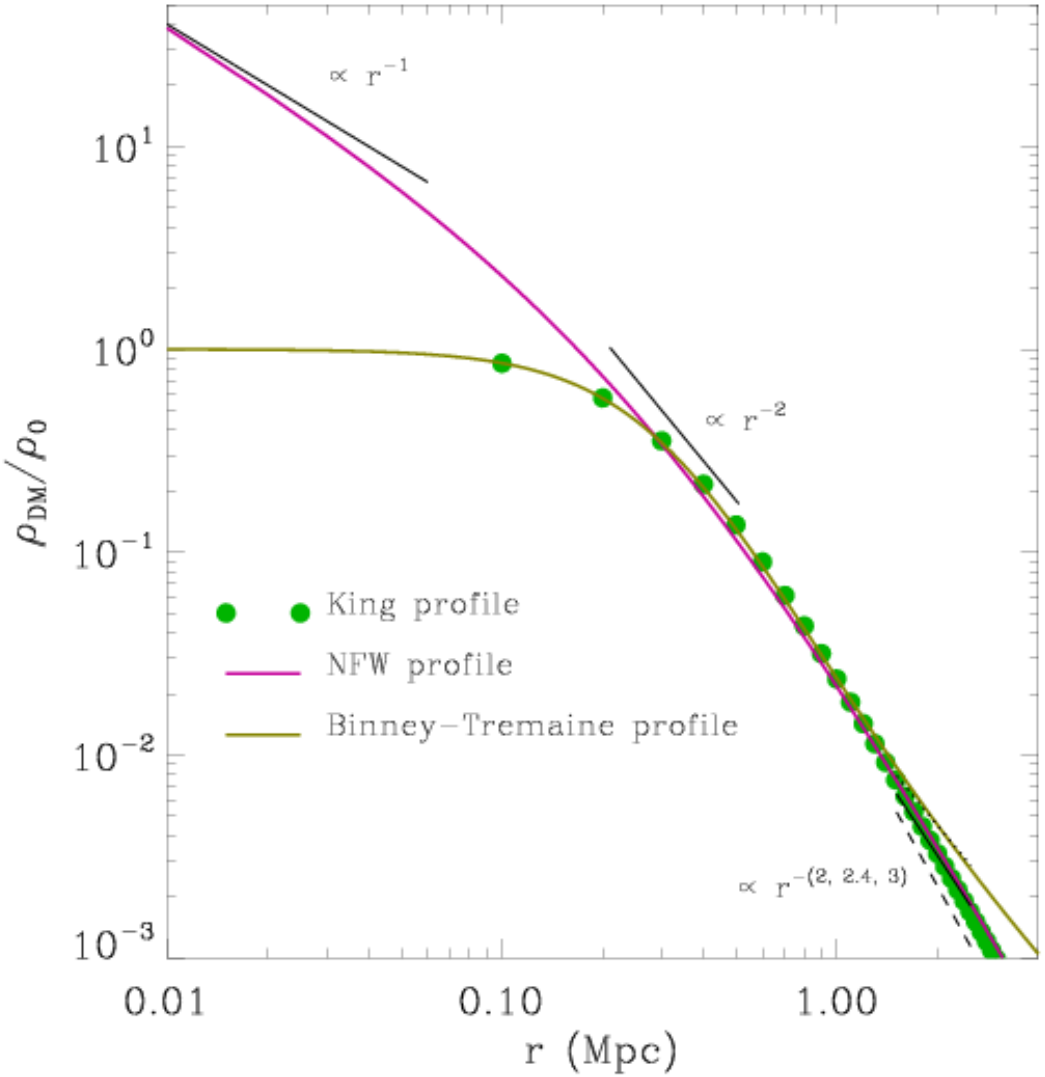

The **NFW profile** is an approximation to the equilibrium configuration produced in simulations of collisionless DM particles

$$\frac{\rho_{DM}}{\rho_0} = \left(\frac{r}{r_s}\right)^{-1}\left(1+\frac{r}{r_s}\right)^{-2}$$

$$\rho_0 = \rho_c \delta_c$$

$$\delta_c = \frac{200}{3}\frac{c^3}{\ln(1+c) - c/(1+c)}$$

$$R_{200} = M_{200} / (\rho_c V_{200}) = c \times r_s$$

Example of M_{tot} estimate

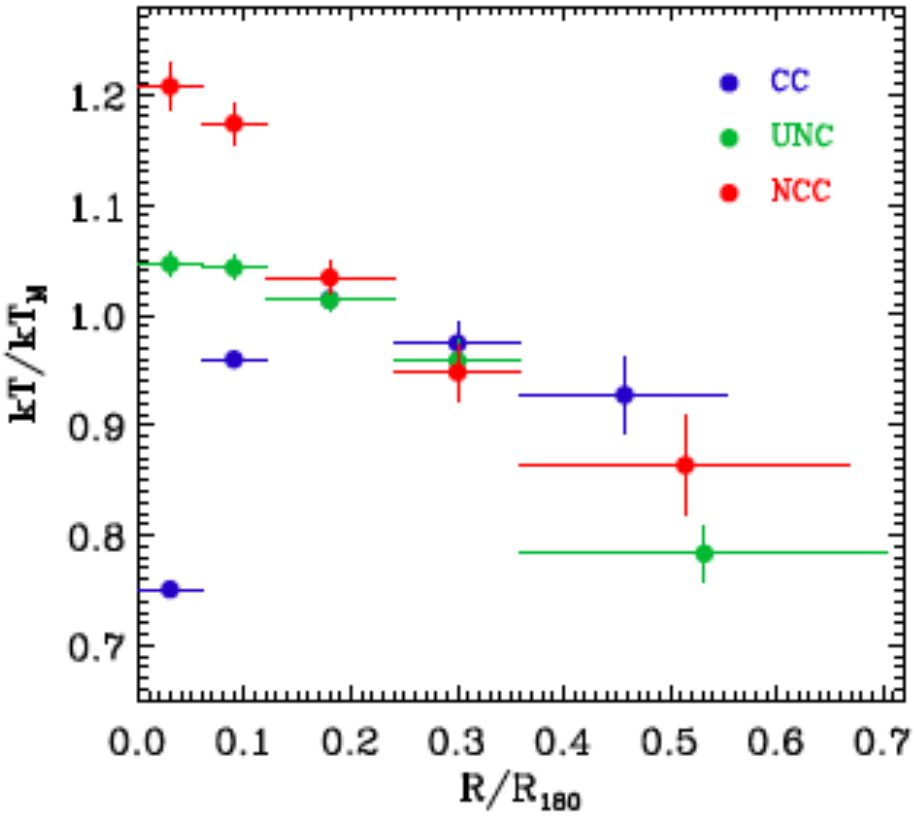

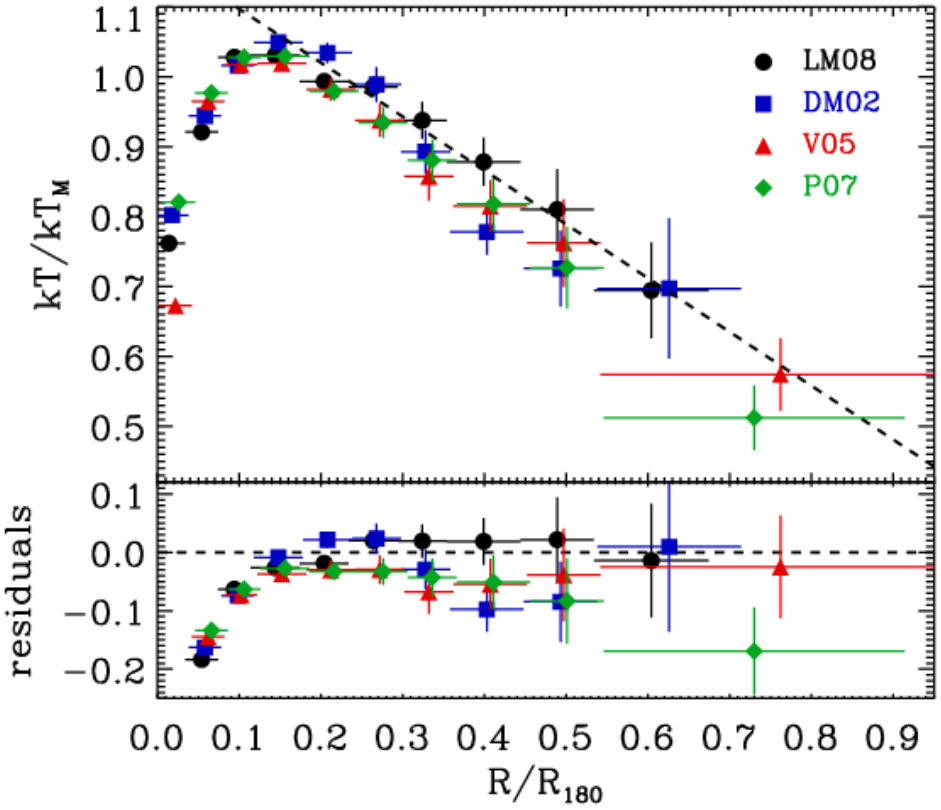

44 X-ray luminous galaxy clusters, relaxed (=CC) & not (=NCC), observed with *XMM-Newton* in the z-range 0.1–0.3

Example of M_{tot} estimate

Spatial analysis of the XMM S_b to recover n_{gas}

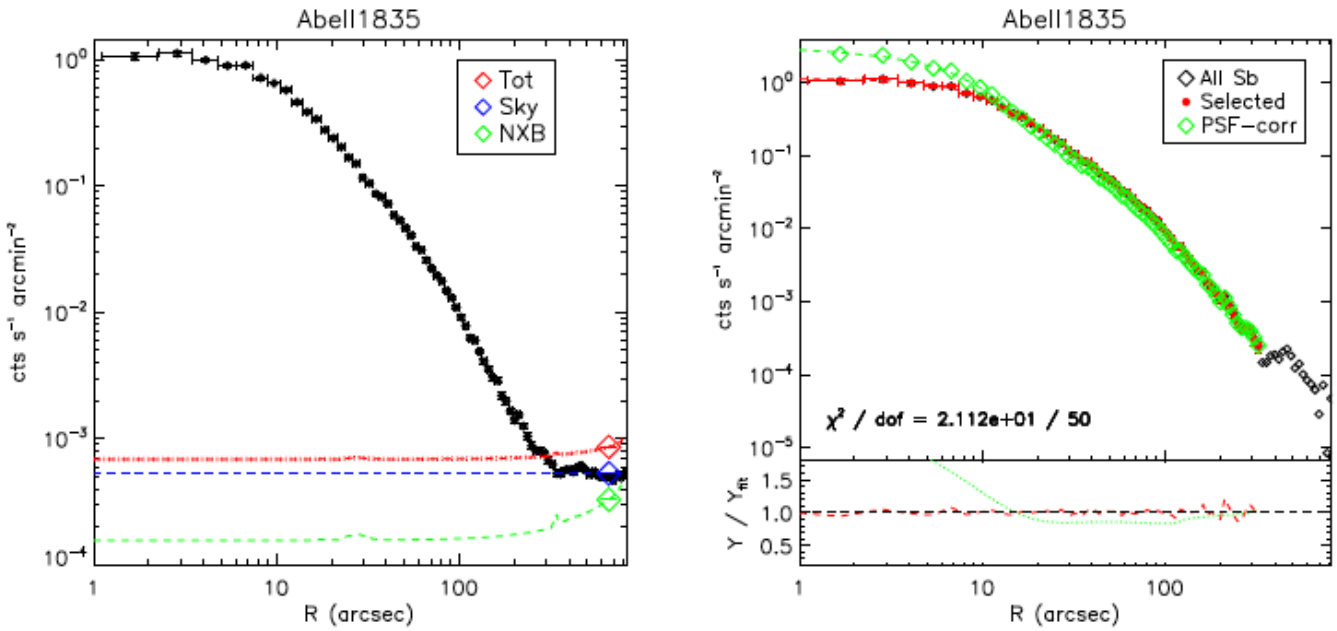

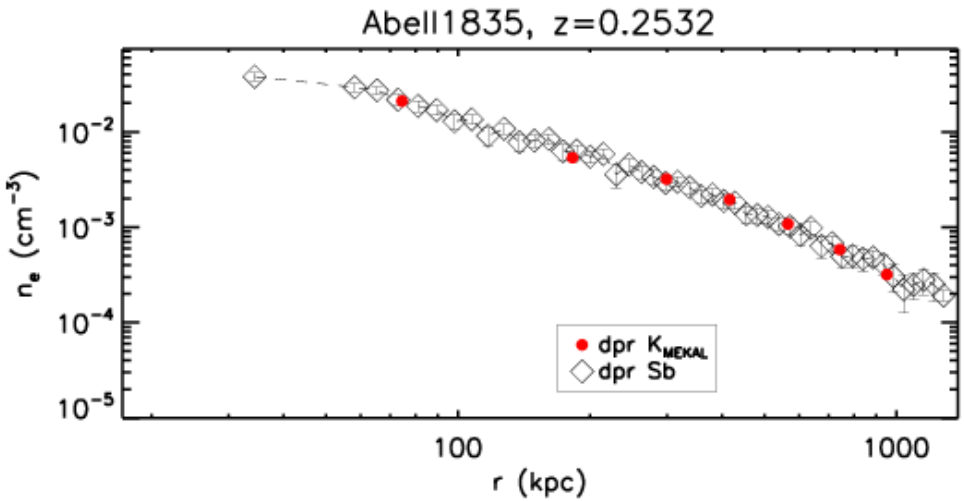

Example of M_{tot} estimate

We use n_{gas} & T_{gas} +NFW to constrain $\{r_s, c\}$

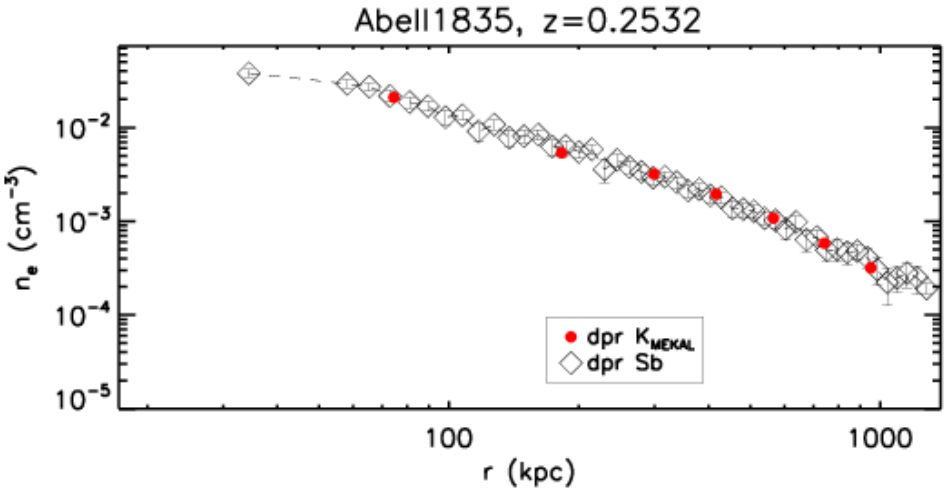

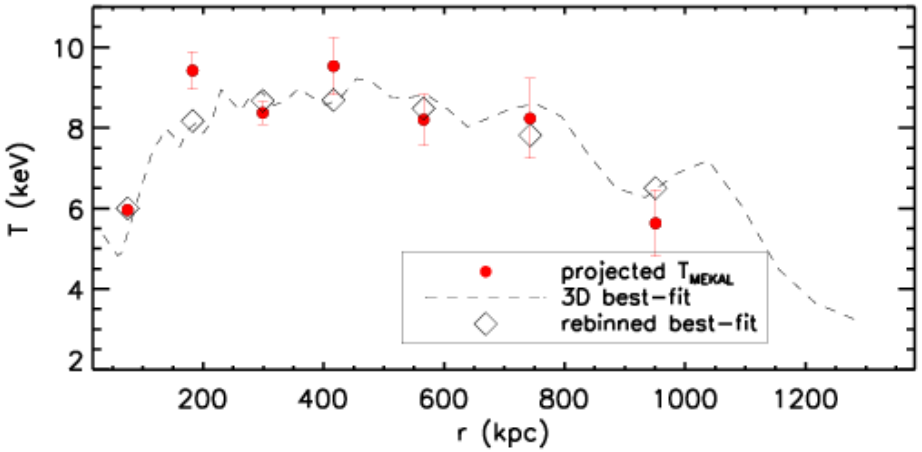

$$M_{\rm DM}(<r) = M_{\rm tot}(<r) - M_{\rm gas}(<r) = 4\pi\, r_{\rm s}^3\, \rho_{\rm s}\, f(x),$$

$$\rho_{\rm s} = \rho_{c,z}\frac{200}{3}\frac{c^3}{\ln(1+c) - c/(1+c)}$$

$$f(x) = \ln(1+x) - \frac{x}{1+x} \qquad (1)$$

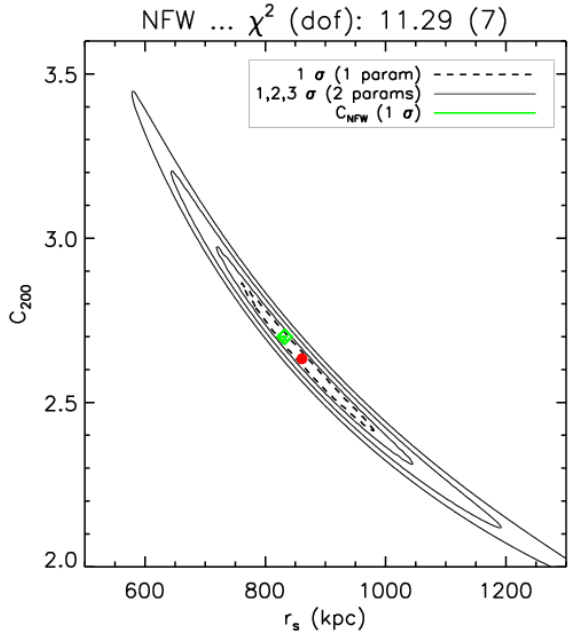

X-ray vs Optical mass: *VT*

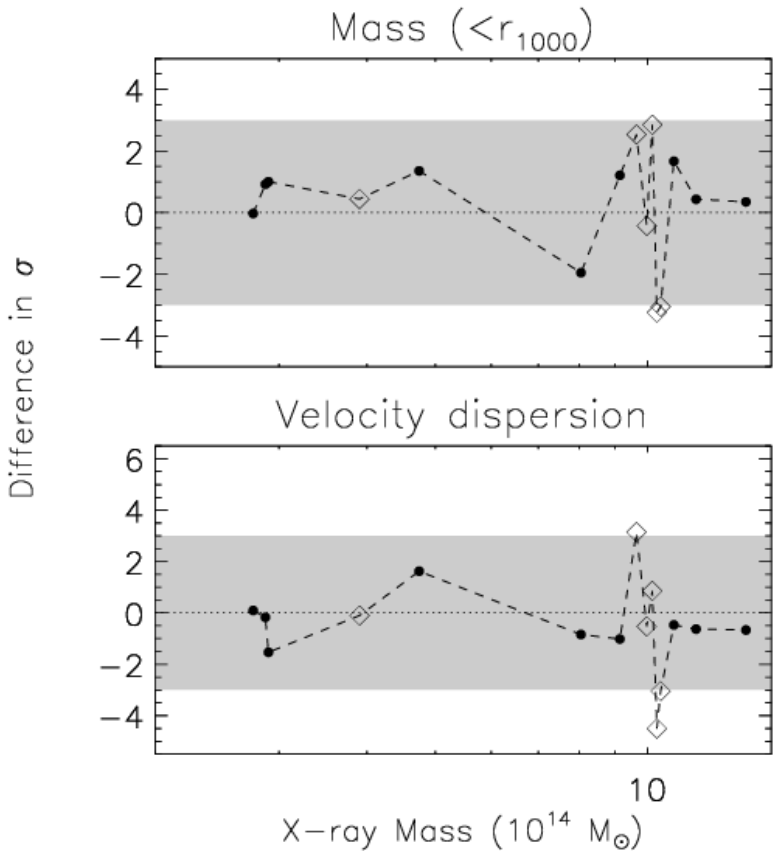

z<0.1: Ettori, De Grandi, Molendi 02

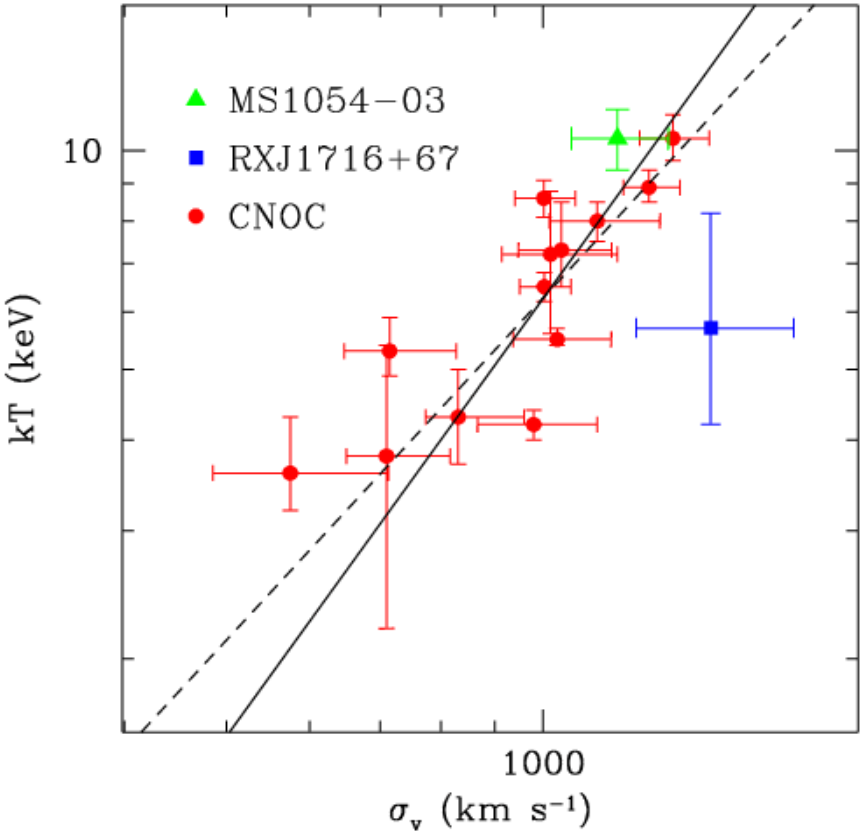

z>0.15
(Rosati etal 03; *solid line:* β=1, *dashed*: low-z from Wu etal. 99)

X-ray vs Optical mass: *lensing*

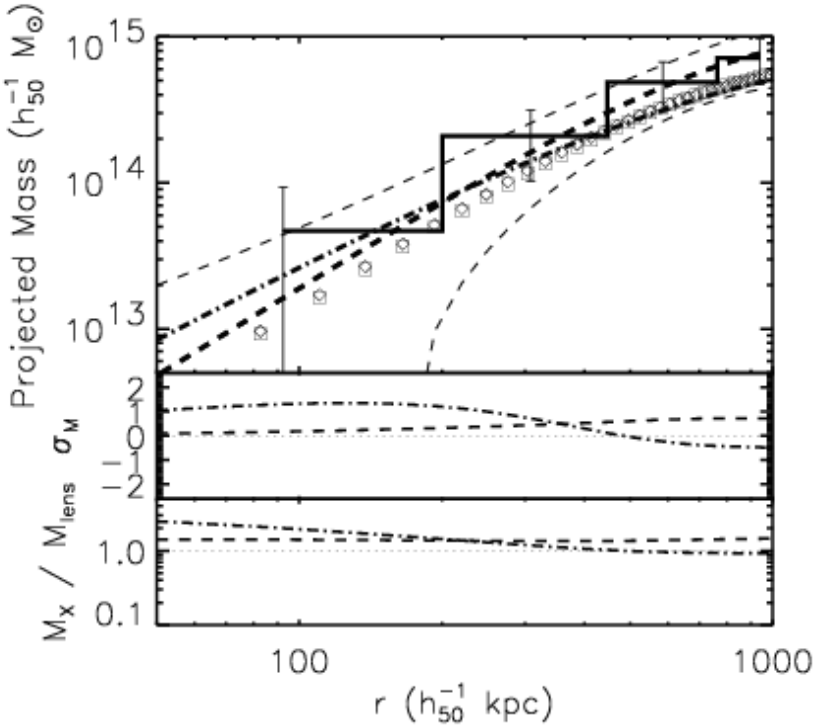

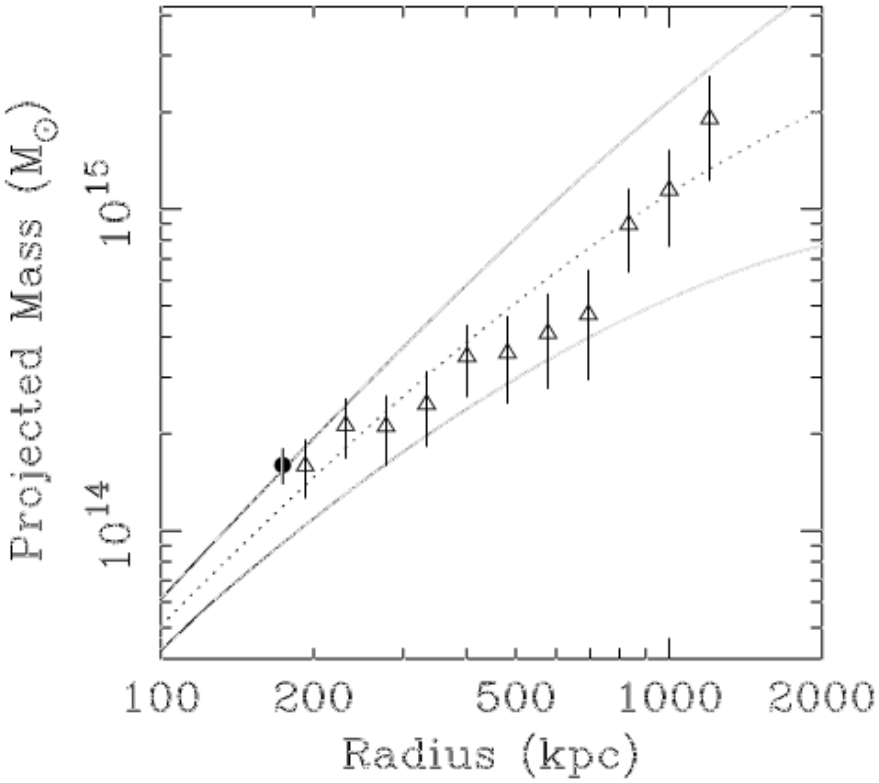

MS1008 (z=0.31, Ettori & Lombardi 03)

A2390 (z=0.23, Allen, Ettori, Fabian 01)

X-ray total mass: *MS2137*

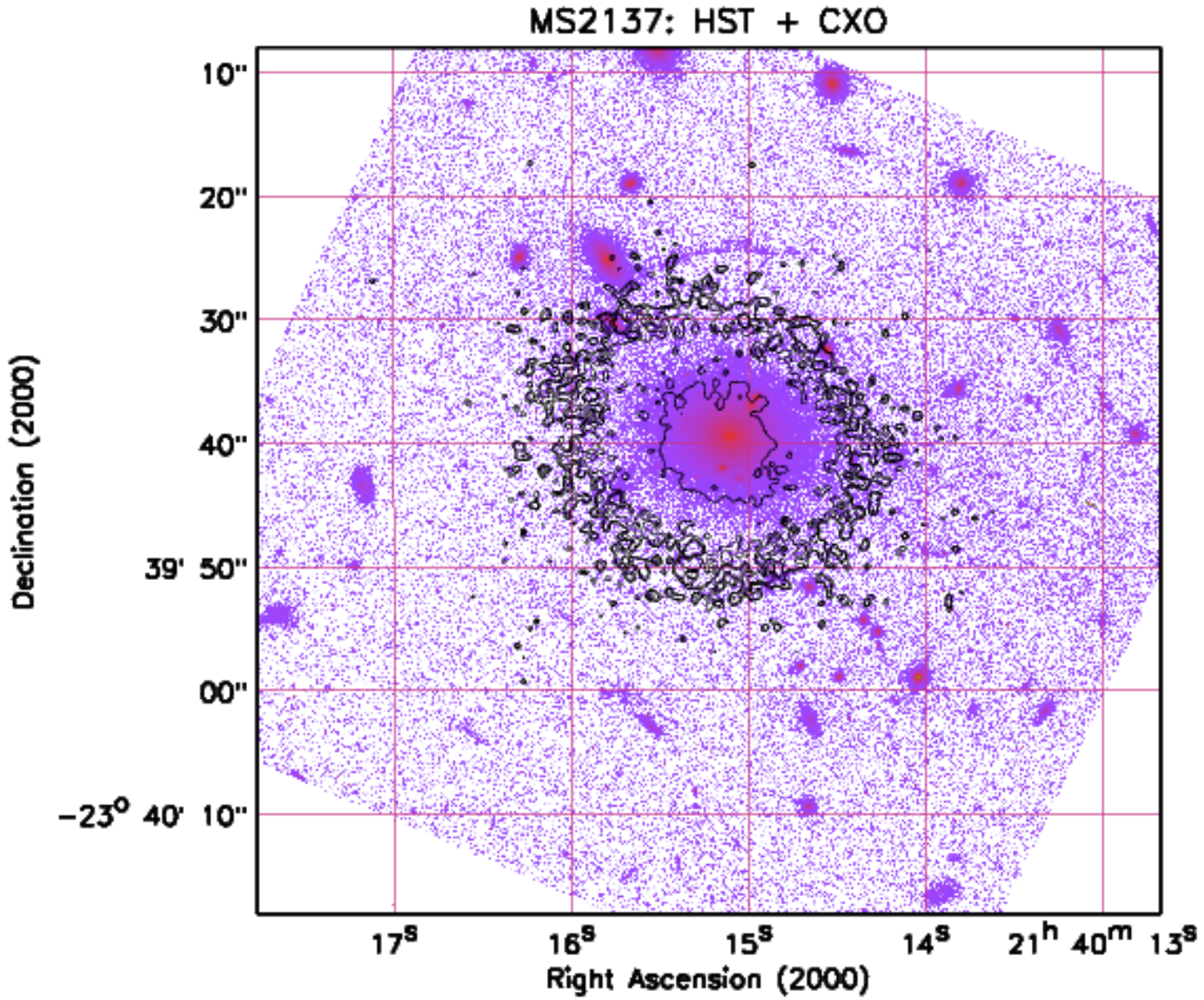

The case of MS2137

(Donnarumma et al. 2008)

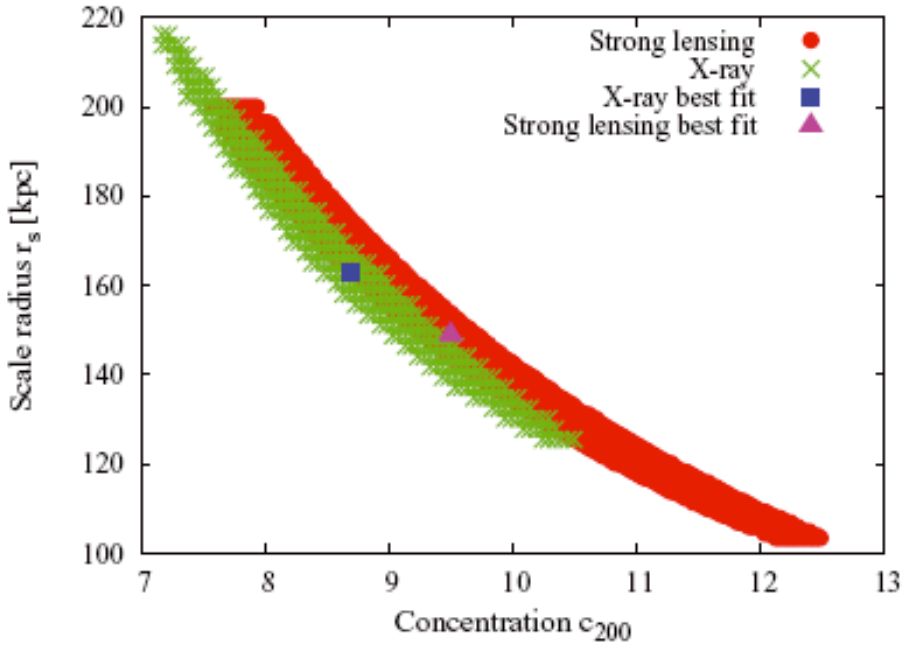

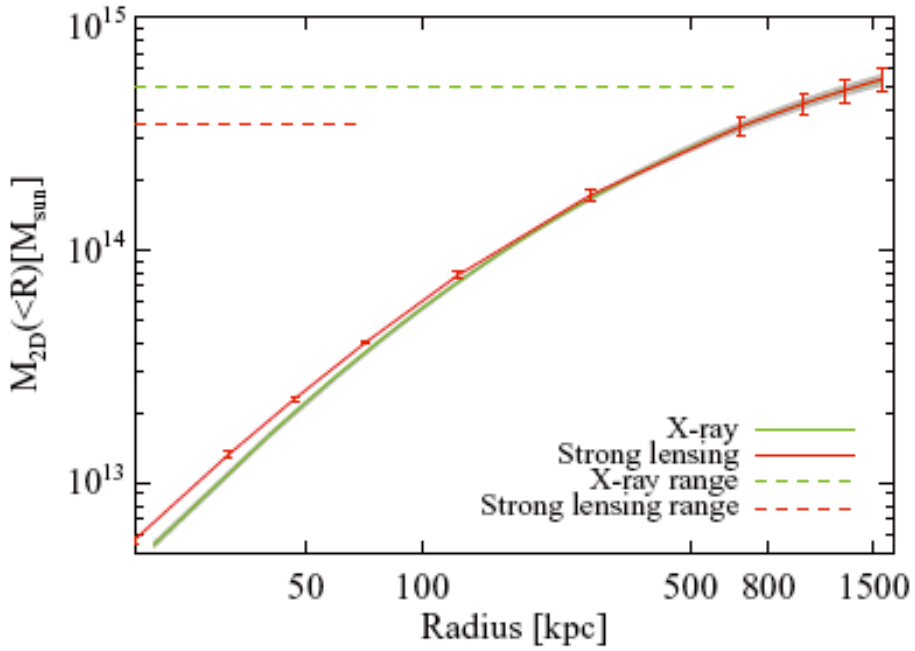

X-ray vs Optical mass

$M_X \approx M_{lensing}$ within 15% implies

$$\frac{G\,M_X}{r^2} = -\frac{d(P_{therm} + P_{NO-therm})}{dr}\frac{1}{\rho_{gas}}$$

$P_{NO\text{-}therm} \approx 0$

Moreover, the difference btw M_X and true Mass **cannot be larger than ~20%** as proved in cosmological studies [e.g. $f_{bar} = (M_{gas}+M_{star})/M_{tot} = \Omega_b / \Omega_m$] & hydrodynamical simulations…

X-ray vs lensing mass: *simulations*

M_X / X-MAS & M_{lens} / SkyLens

both convolve hydro simulations with observational setup

(work with E. Rasia & M. Meneghetti;
see also Nagai, Kravtsov, et al.)

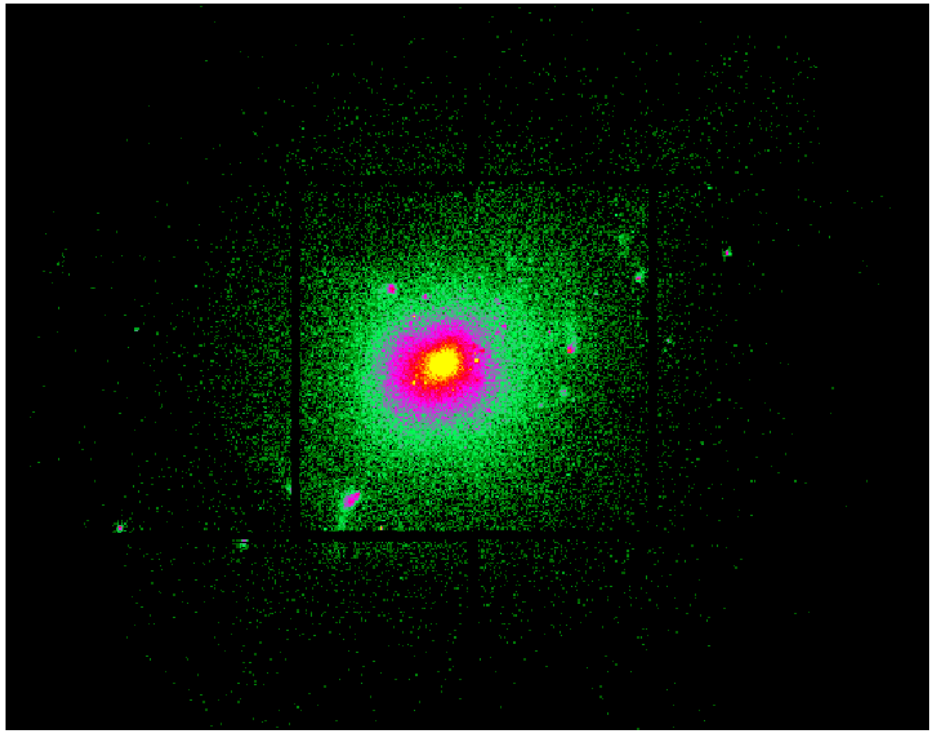

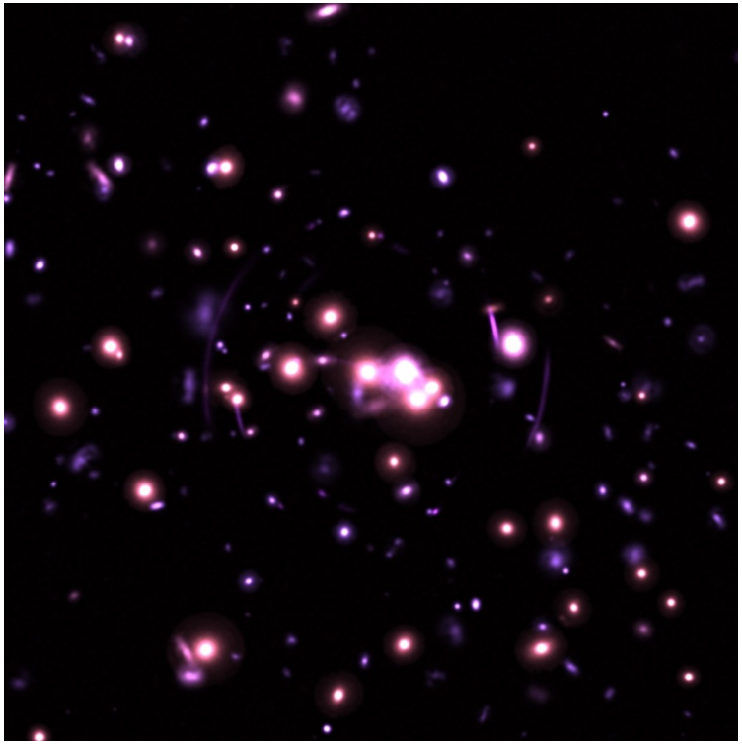

X-ray vs lensing mass: *simulations*

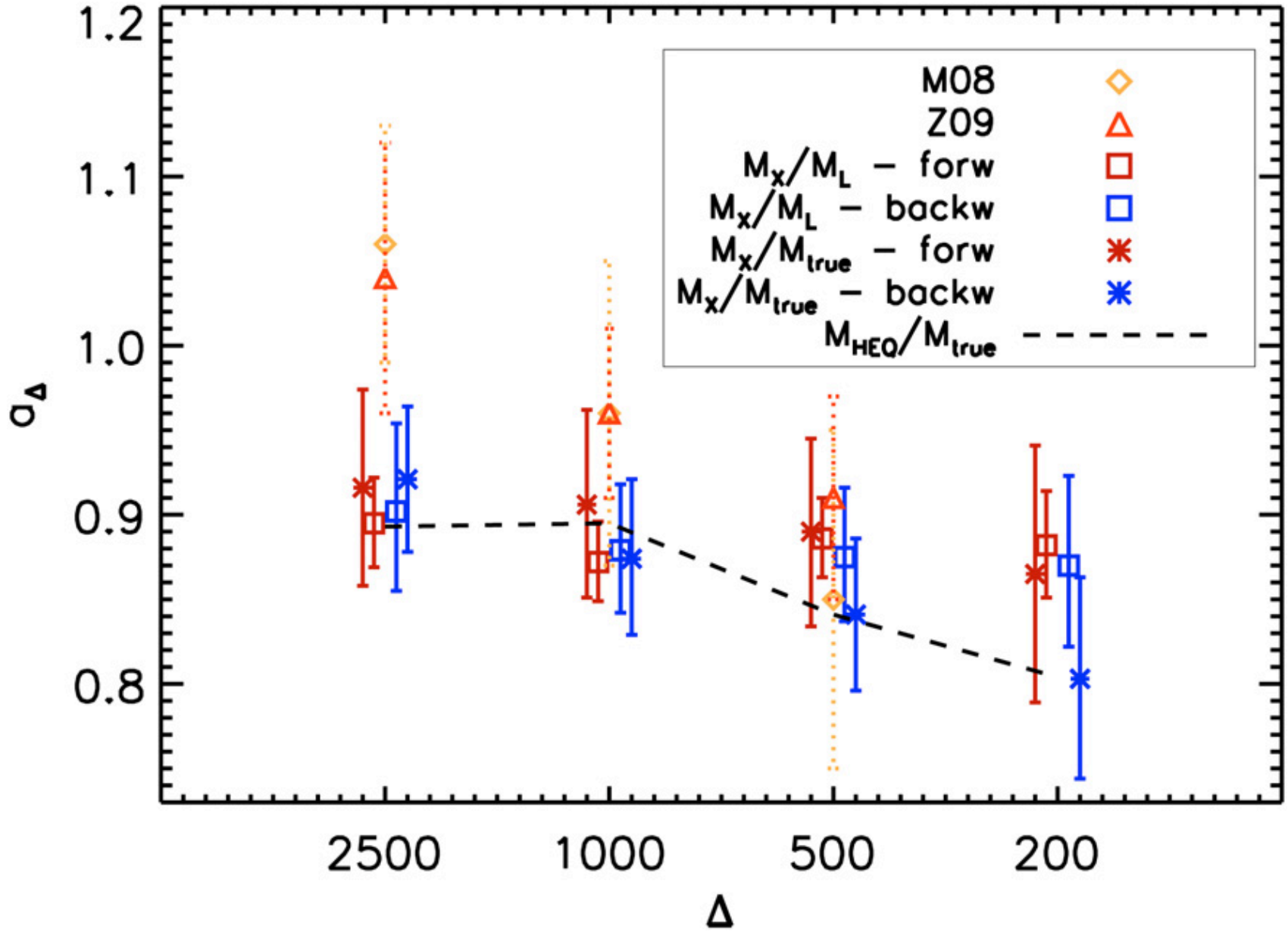

Conclusions on estimate of the X-ray M_{tot}

- Hydrostatic equilibrium holds locally: look for relaxed regions also in merging systems

- At least two main ways (one ***forward***, one ***backward***) to apply HEE: pro/contra, no systematic is evident btw them, not thermalized ICM is missed

Results on {c, M_{DM}, f_{gas}}

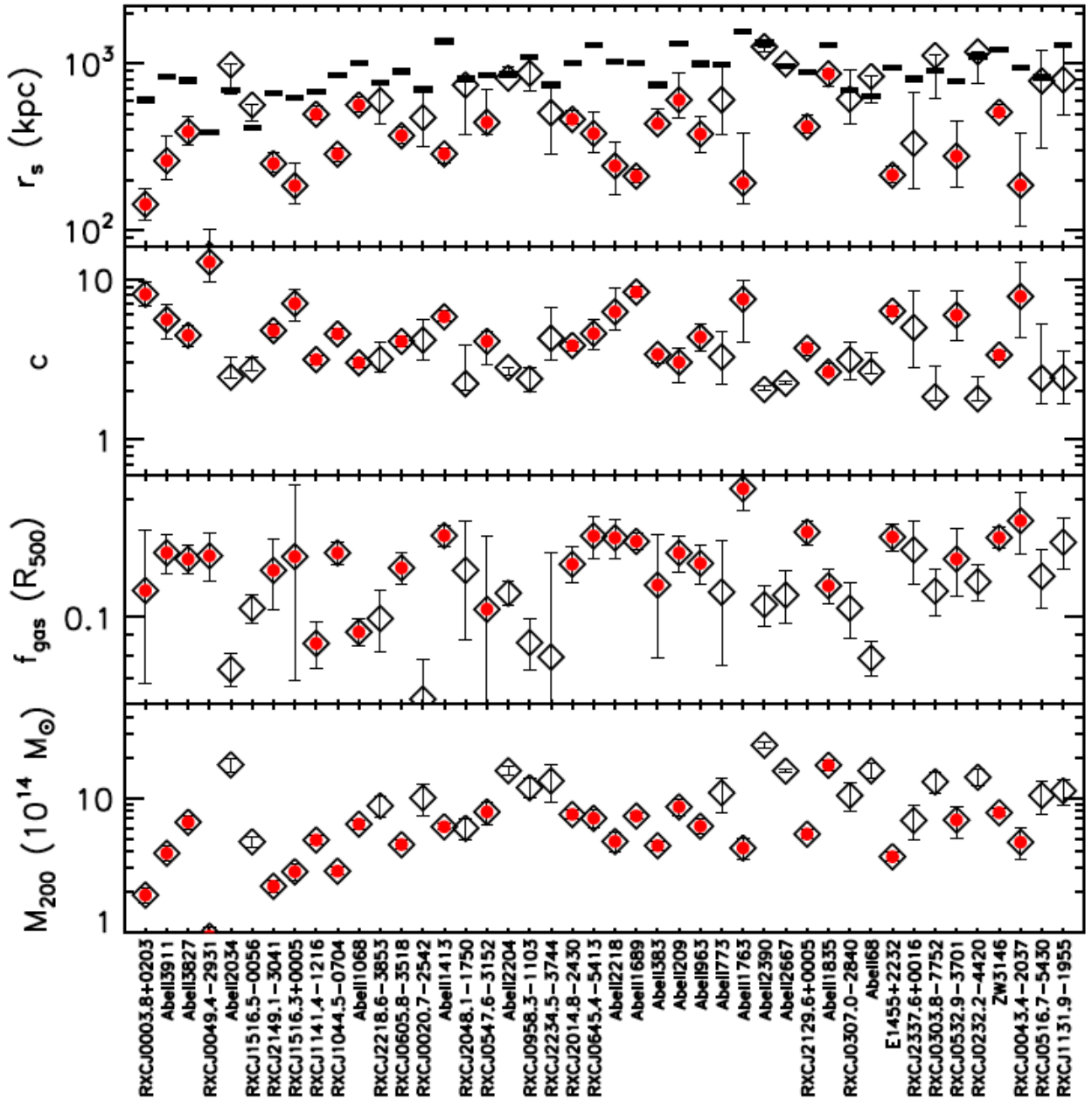

$c=R_{200}/r_s$

$f_{gas}=M_{gas}/M_{tot}$

$M_{200}=200\rho_c(z)\ V$

$V = 4/3\pi R_{200}^3$

Gas mass fraction

To constrain the cosmological model

$$\Omega_m + \Omega_\Lambda + \Omega_k = 1$$

We combine a **dynamical** and a **geometrical** method

(see also Allen et al, Blanchard et al., Ettori et al, Mohr et al) :

1. baryonic content of galaxy clusters is representative of the cosmic baryon fraction Ω_b / Ω_m (White et al. 93)
2. f_{gas} is assumed constant in cosmic time in very massive systems (Sasaki 96, Pen 97)

Gas mass fraction: the method

(see e.g. Allen et al. 08, Ettori et al. 09)

$$\chi^2 = \sum_{i=1}^{N_{dat}} \frac{(f_{bar,i}/b_i - \Omega_b/\Omega_m)^2}{\varepsilon^2}$$

- $\mathbf{b_{500}}$ = 0.874 (±0.023)
  = 0.923 (±0.006) +0.032 (±0.010) z

- $\Omega_b h^2$ = 0.0189 ±0.0010 (PN, Burles et al. 01)

- H_0 = 72 ± 8 km/s/Mpc (Freedman et al. 2001)

- $f_{bar,\,i} = f_{cold,\,i} + f_{gas,\,i}$

$f_{cold} = (0.18 - 0.012\, T_{gas})\, f_{gas}$ (Lagana et al. 2008) = 0.1-0.2 f_{gas}

Gas mass fraction: the method

(see e.g. Allen et al. 08, Ettori et al. 09)

$$\chi^2 = \sum_{i=1}^{N_{dat}} \frac{(f_{bar,i}/b_i - \Omega_b/\Omega_m)^2}{\varepsilon^2}$$

- $\mathbf{b_{500}}$ = 0.874 (±0.023)
  = 0.923 (±0.006) +0.032 (±0.010) z

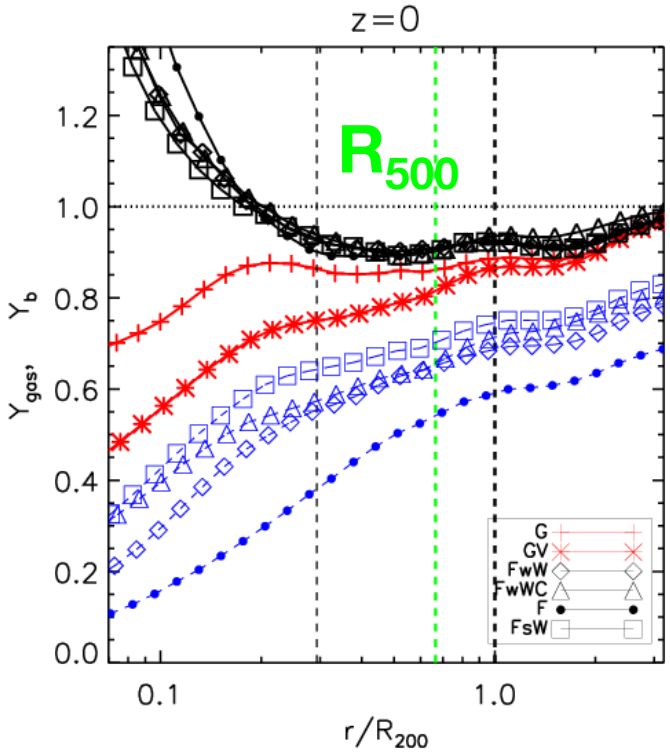

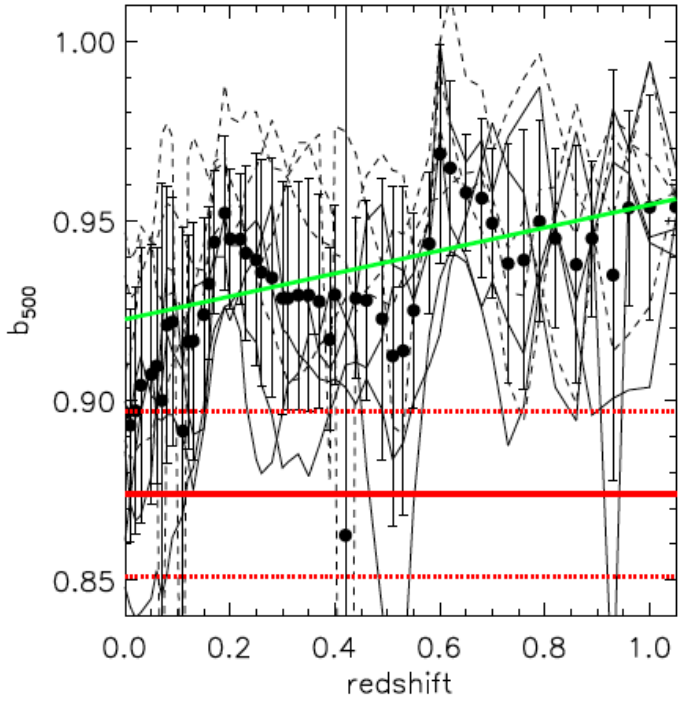

The cosmological dependence

$f_{gas}(<R_{500}) = M_{gas}/M_{tot} \propto n_{gas}R^3/R \propto d_{ang}(\Omega_m, \Omega_\Lambda, w)^{3/2}$

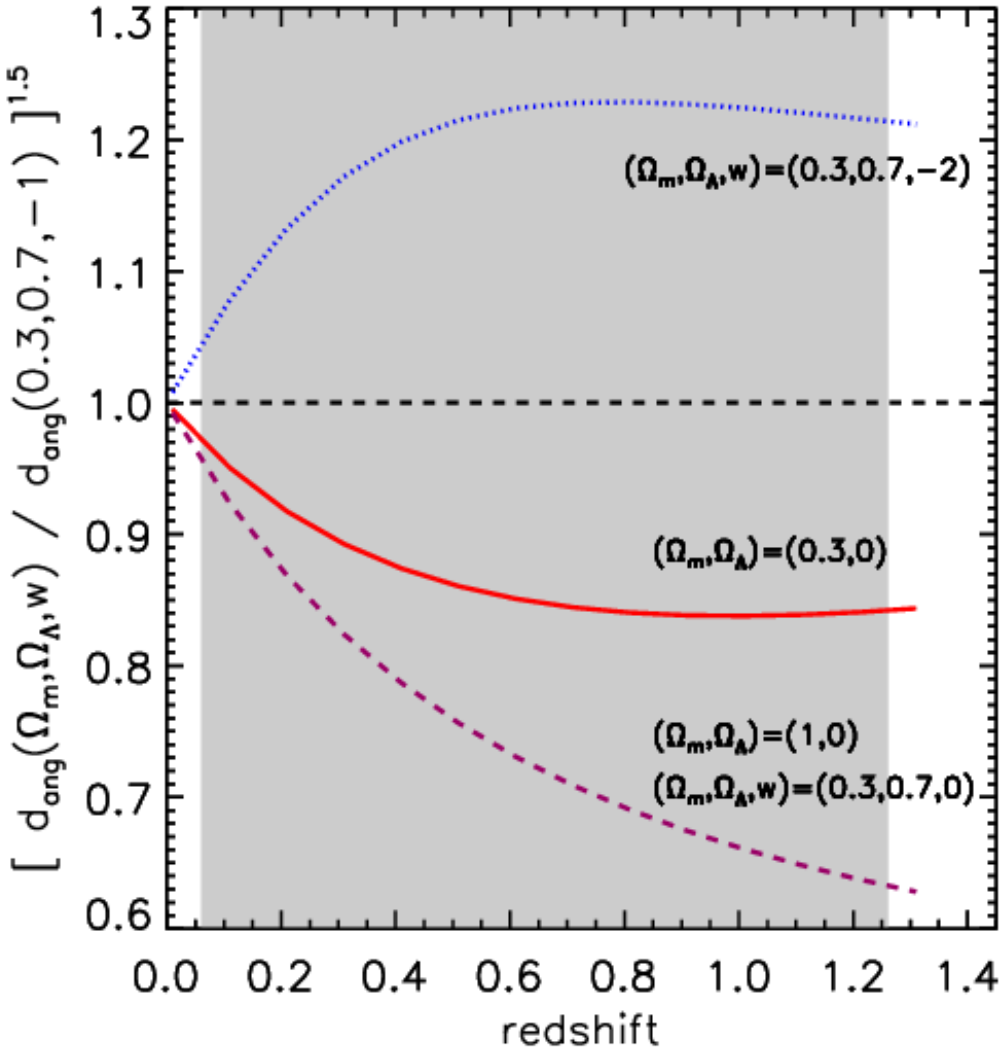

500 relaxed hot (T>5 keV) obj with f_{gas} estimate precise at 5% level provides a FoM_{DETF} [~$1/(\sigma_{w0}\,\sigma_{wa})$, $w=w_0+w_a(1-a)$] ~**15-40** *(Rapetti et al. 08)*, comparable to:

ground-based SNIa … 8-22
Space-based SNIa … 19-27
Ground-based BAO … 5-55
Space-based BAO … 20-42
Space-based clusters cts … 6-39

Gas mass fraction

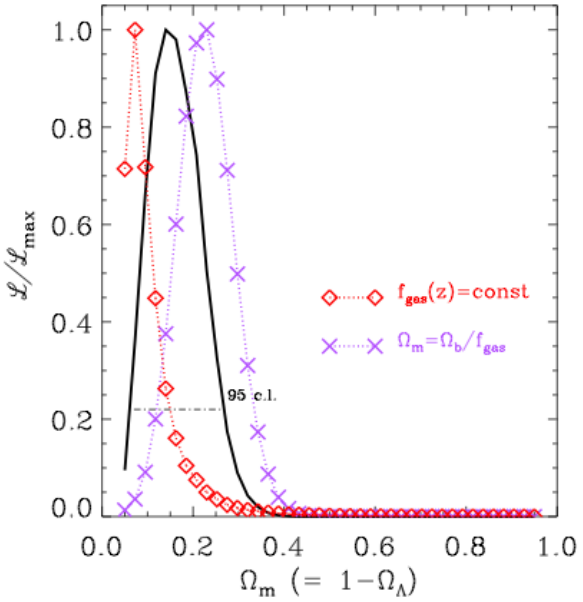

Ettori & Fabian (1999):
36 obj observed with ROSAT/PSPC
with L_x>1e45 erg/s @z=0.05-0.44

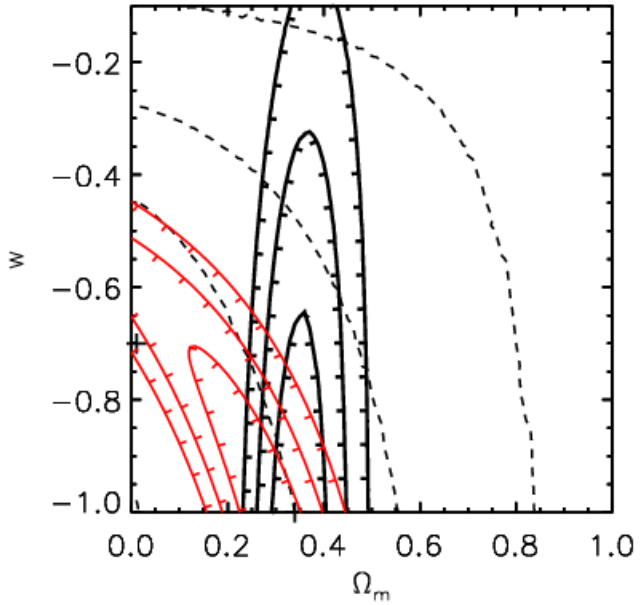

Ettori, Tozzi, Rosati (2003):
8 obj observed with Chandra
@z=0.7-1.3 +local f_{gas} estimate
from BeppoSAX mass profiles

Gas mass fraction

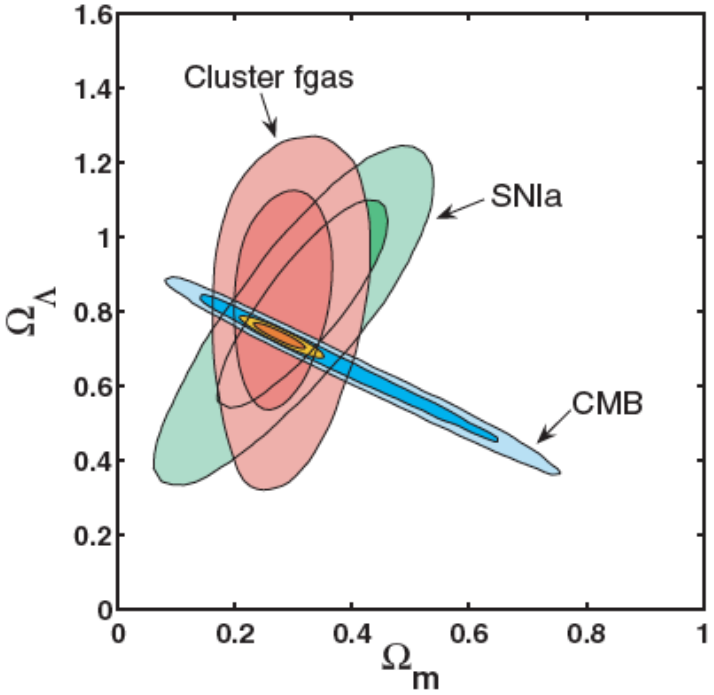

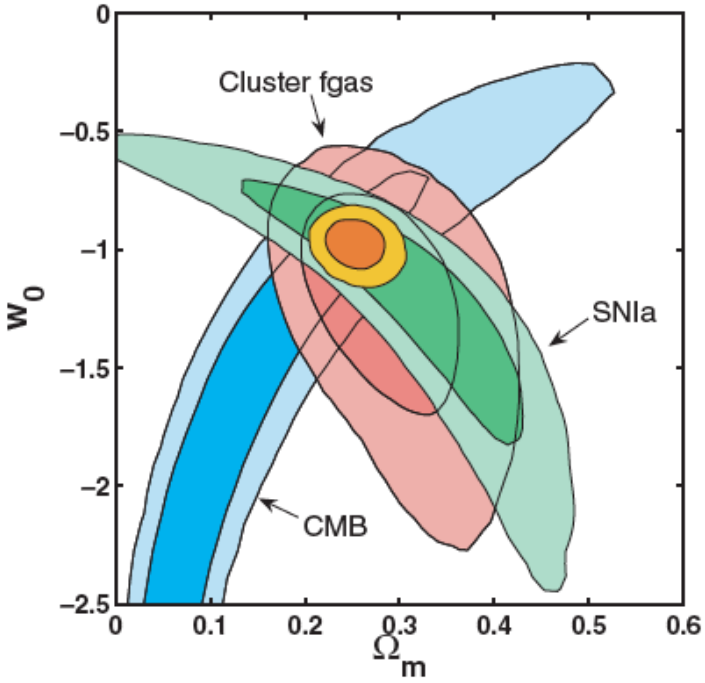

Allen et al. (2008):
42 obj with T>5 keV observed with Chandra @z=0.05-1.1

➔ $\varepsilon_{\Omega m}$~20%, ε_w~30% , Ω_Λ>0 @99.99% l.c.

Dark energy with GC: results

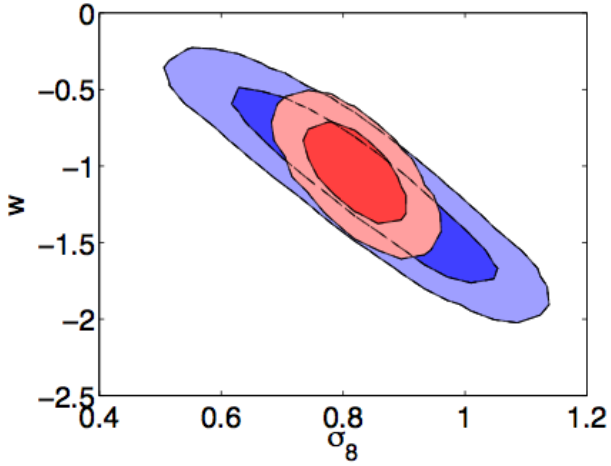

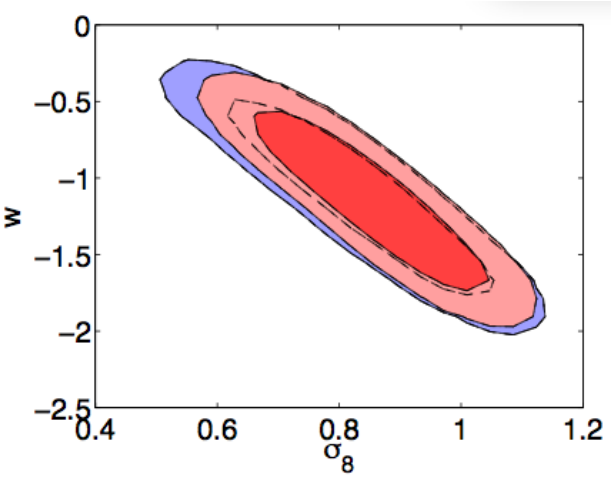

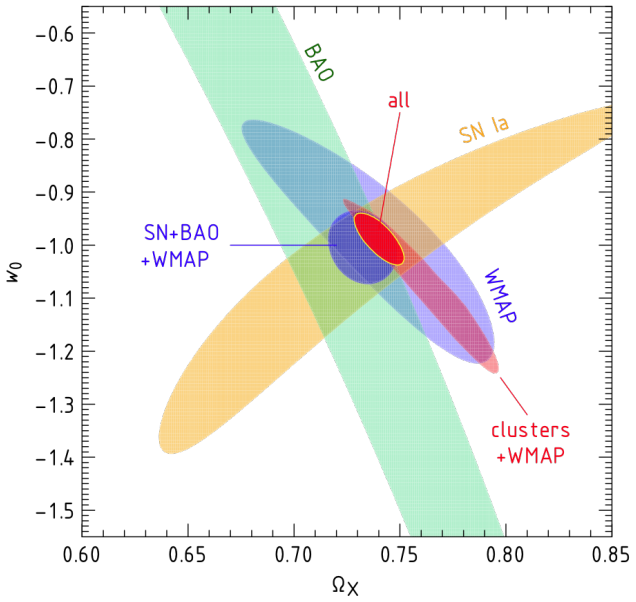

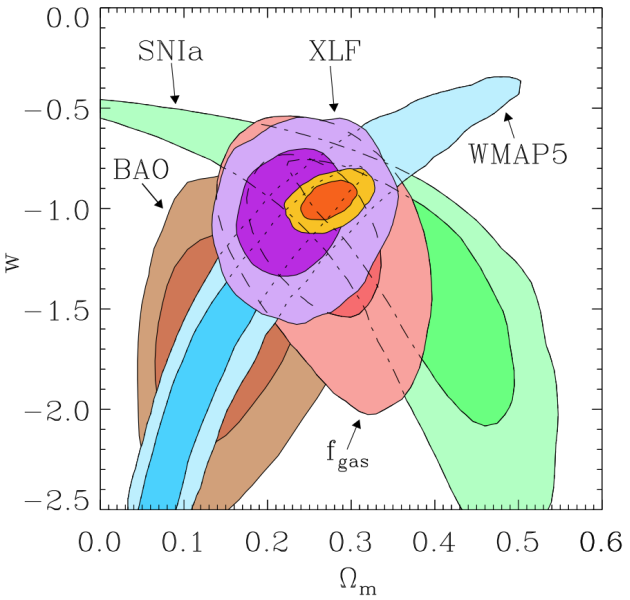

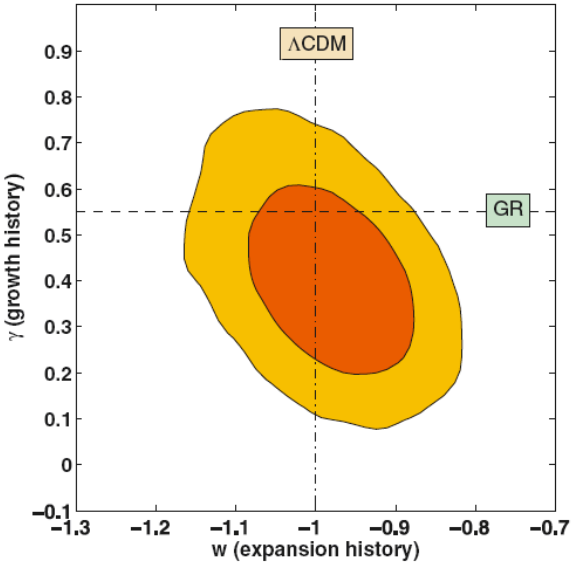

Constraints from X-ray data

Vikhlinin et al. (2009): from 37 clusters @<z>=0.55 (400 deg^2 survey) & 49 brightest z~0.05 … 3 M-proxies: T measured in 0.15-1 R_{500}; $M_{gas}(<R_{500})$; $Y_X = T \times M_{gas}$ … $w_0 = -1.14 \pm 0.21$

Mantz et al. (2010): 238 obj from RASS with CXO follow-up of 94 of these … $M_{gas}(<R_{500})$ as M-proxy … $w_0 = -1.01 \pm 0.20$

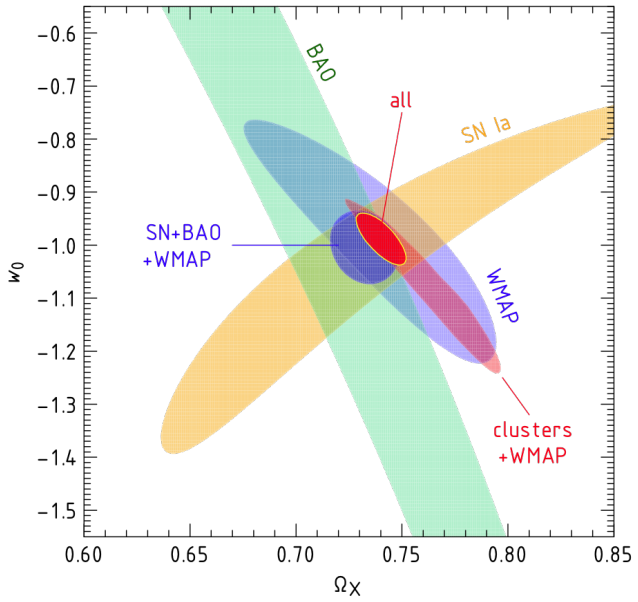

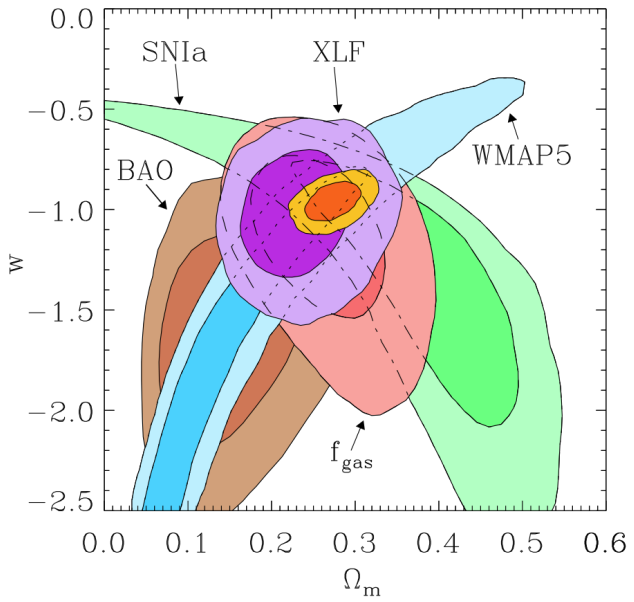

Constraints from X-ray data

Vikhlinin et al. (2009): a case study.

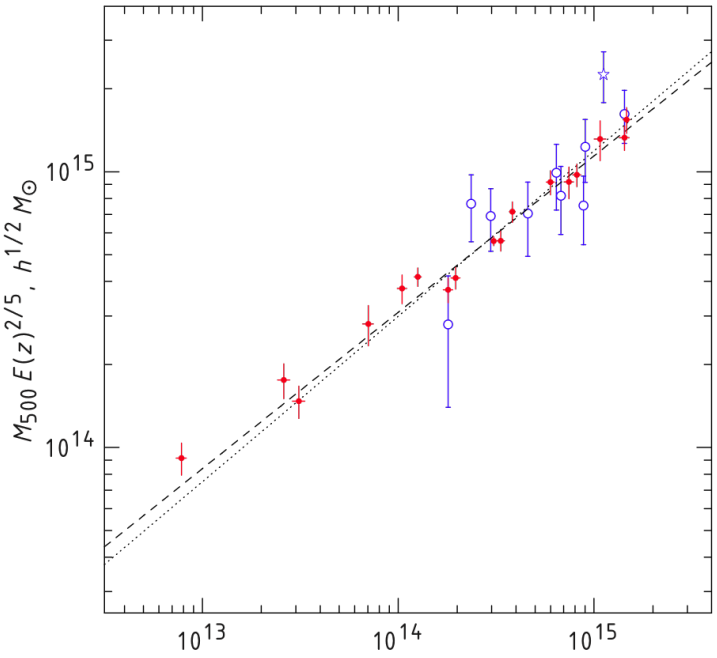

17 local relaxed clusters with estimated M_{hyd} from Chandra data are used to calibrate the scaling relations

Table 3
Calibration of Mass-observable Relations

Relation	Form	$M_0, f_{g,0}$	α
$M_{500} - T_X$	$M_{500} = M_0 (T/5\,\mathrm{keV})^\alpha\, E(z)^{-1}$	$(3.02 \pm 0.11) \times 10^{14}\, h^{-1}\, M_\odot$	1.53 ± 0.08
$M_{500} - T_X$	$M_{500} = M_0 (T/5\,\mathrm{keV})^\alpha\, E(z)^{-1}$	$(2.95 \pm 0.10) \times 10^{14}\, h^{-1}\, M_\odot$	1.5, fixed
$M_{500} - M_{\mathrm{gas}}$	$f_g = f_{g,0} + \alpha \log M_{15}$	$(0.0764 \pm 0.004)\, h^{-1.5}$	0.037 ± 0.006
$M_{500} - Y_X$	$M_{500} = M_0 (Y_X/3 \times 10^{14}\, M_\odot\,\mathrm{keV})^\alpha\, E(z)^{-2/5}$	$(5.77 \pm 0.20) \times 10^{14}\, h^{1/2}\, M_\odot$	0.57 ± 0.03
$M_{500} - Y_X$	$M_{500} = M_0 (Y_X/3 \times 10^{14}\, M_\odot\,\mathrm{keV})^\alpha\, E(z)^{-2/5}$	$(5.78 \pm 0.30) \times 10^{14}\, h^{1/2}\, M_\odot$	0.6, fixed

Constraints from X-ray data

Effective survey volume: being X-ray flux limited sample, one needs to compute the survey volume V as function of mass M passing through the estimated luminosity L. Cosmology appears in the K-correction K(z), in the volume-redshift relation dV/dz, in the luminosity distance d_L. Note that in a f-limited sample, average L of selected obj is > than L in parent population inducing overestimates of V (*Malmquist bias*).

$$V(L) = \int_{z_1}^{z_2} A(f_x, z) \frac{dV}{dz} dz, \qquad f = \frac{L}{4\pi\, d_L(z)^2} K(z),$$

$$V(M) = \int_{z_1}^{z_2} dz \int_L A(f_x, z) \frac{dV}{dz} P(L|M, z) dL,$$

$$P(\ln L|M) \propto \exp\left(-\frac{(\ln L - \ln L_0)^2}{2\sigma^2}\right),$$

where

$$L_0 = A(z)\, M^{\alpha}.$$

Constraints from X-ray data

Effective survey volume

$$V(M) = \int_{z_1}^{z_2} dz \int_L A(f_x, z) \frac{dV}{dz} P(L|M, z) dL,$$

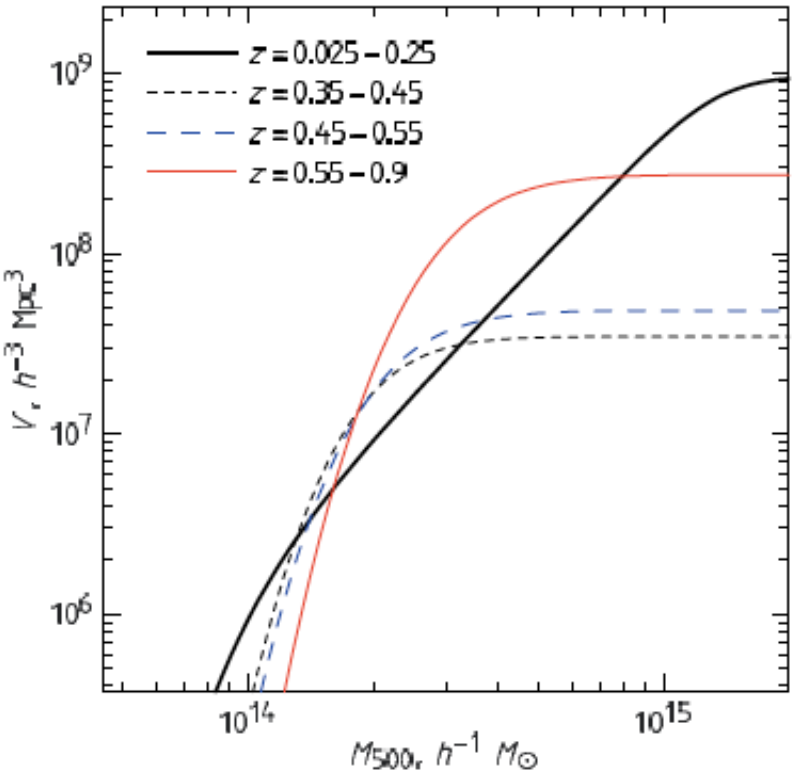

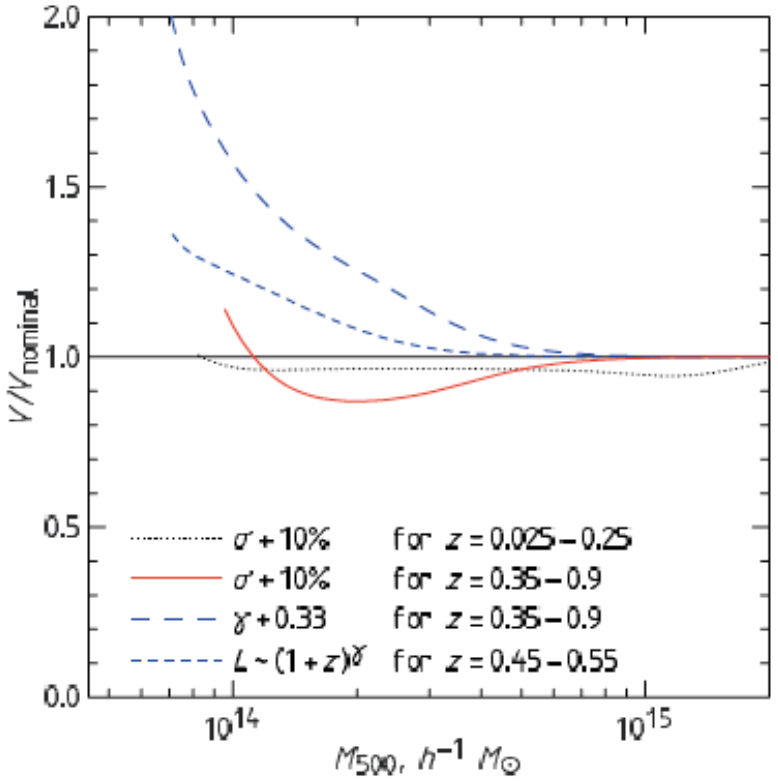

It takes ~20s CPU time to: re-estimate M, re-fit L-M, re-compute V for a new combination of cosmological parameters

Constraints from X-ray data

Finally, for each combination of interesting parameters (Ω_m Ω_Λ w σ_8 … power spectrum tilt, neutrino massess…) the mass function N can be evaluated and the the likelihood function can be estimated (e.g. Cash 1979)

$$N(>M) = \sum_{M_i > M} V(M_i)^{-1}.$$

$$\ln L = \sum_i \ln p\left(M_i^{\rm est}, z_i\right) + \sum_i \ln M_i^{\rm est} - \int\int_{M,z} p(M^{\rm est}, z)\, dM^{\rm est}\, dz.$$

$$\chi^2 = -2 \ln L$$

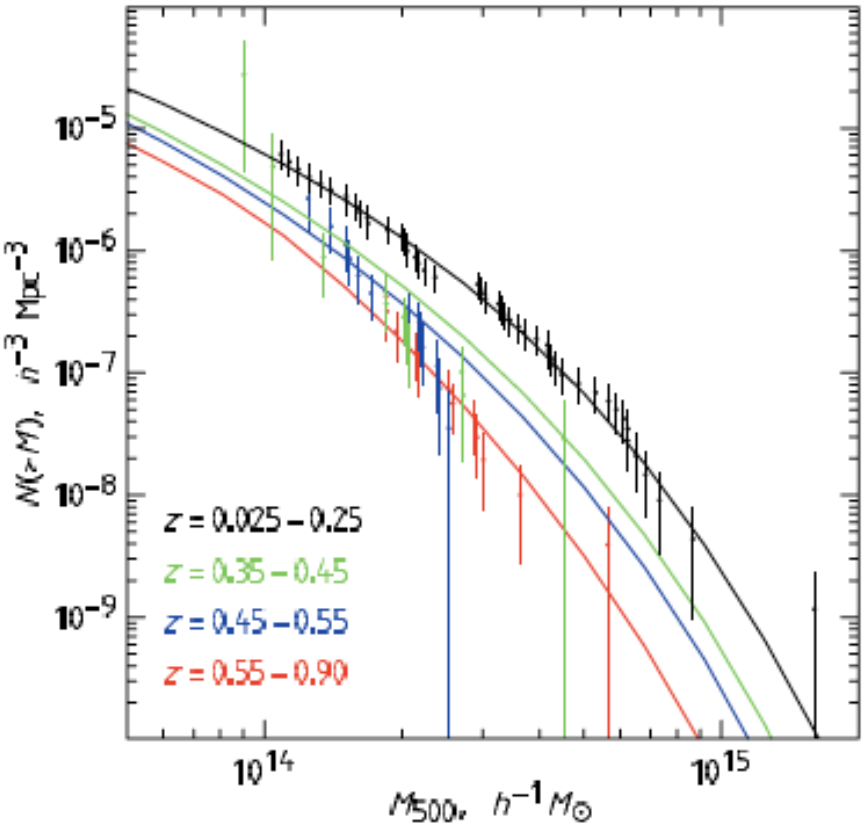

Constraints from X-ray data

Finally, for each combination of interesting parameters (Ω_m Ω_Λ w σ_8 … power spectrum tilt, neutrino massess…) the mass function N can be evaluated and the the likelihood function can be estimated (e.g. Cash 1979)

$$N(>M) = \sum_{M_i > M} V(M_i)^{-1}.$$

$$\ln L = \sum_i \ln p\left(M_i^{\rm est}, z_i\right) + \sum_i \ln M_i^{\rm est} - \int\int_{M,z} p(M^{\rm est}, z)\, dM^{\rm est}\, dz.$$

$\chi^2 = -2 \ln L$

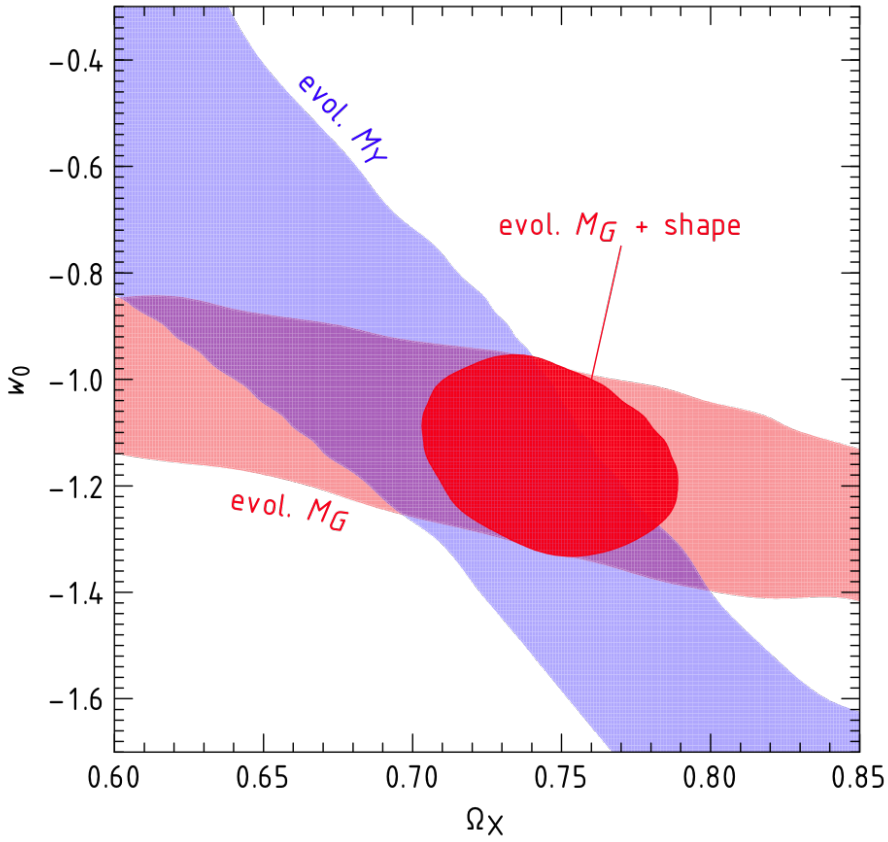

Testing GR with X-ray GC

Rapetti et al. (2008-2010): use M10 sample to constrain the growth index γ: $d(\ln\delta) = \Omega_{m,z}^{\gamma} d(\ln a)$

Schmidt et al. (2009): use V09 sample to constrain the modified action f(R) model with simulation-calibrated cluster abundance

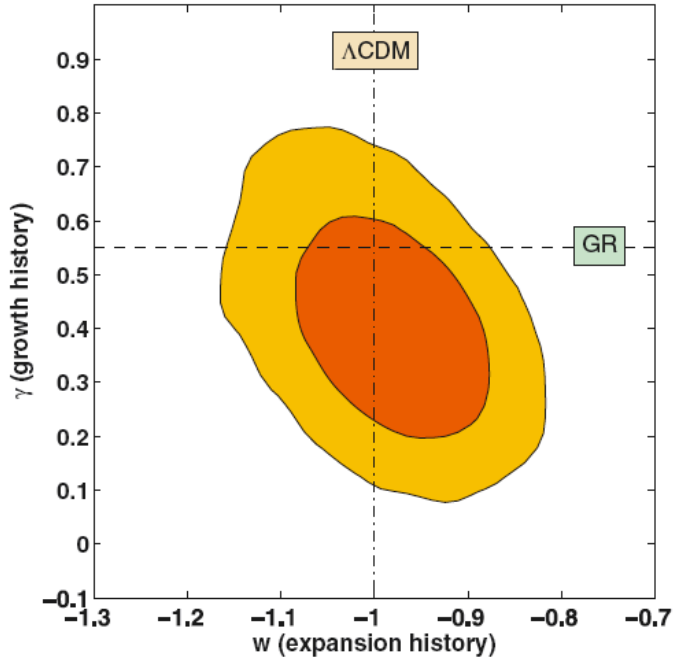

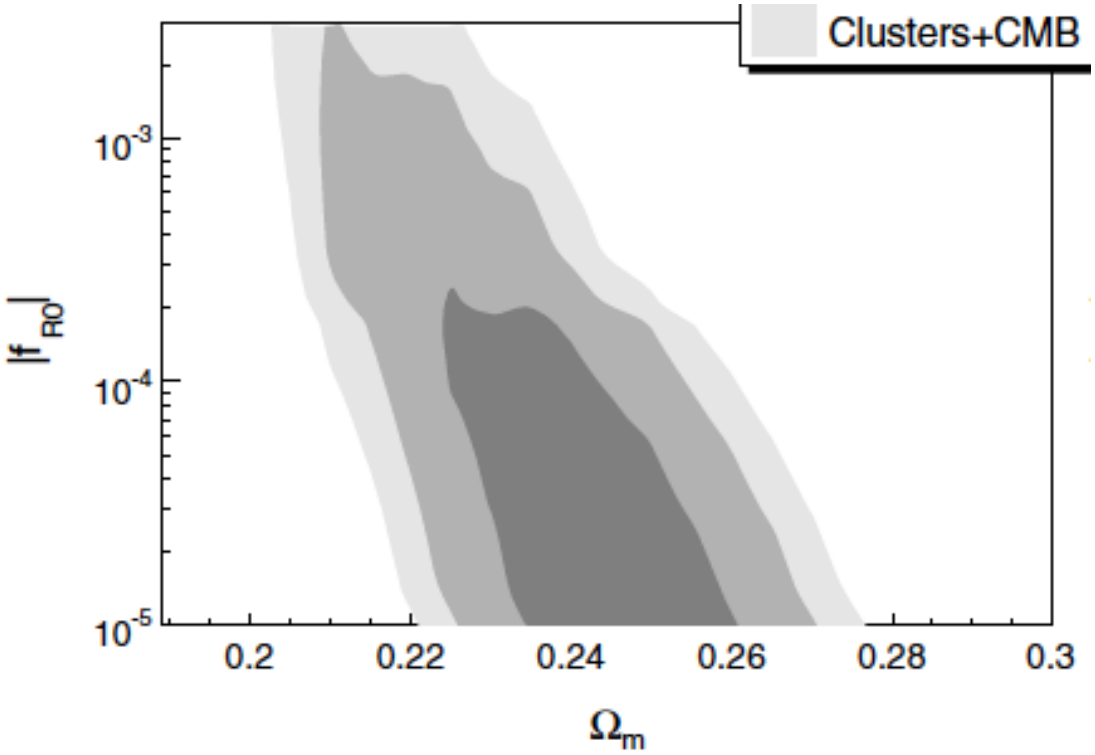

Constraints from optical data

Rozo et al. (2009): using 10,800 clusters in the maxBCG catalog extracted from ~7,000 deg^2 surveyed with SDSS in the z-range=0.1-0.3 & M-range=7e13-1.2e15/h … M-proxy: N_{200} =num.of red-sequence gals in a region with gal-overdensity of 200 … $\sigma_8 (\Omega_m/0.25)^{0.41} \approx 0.832 \pm 0.033$

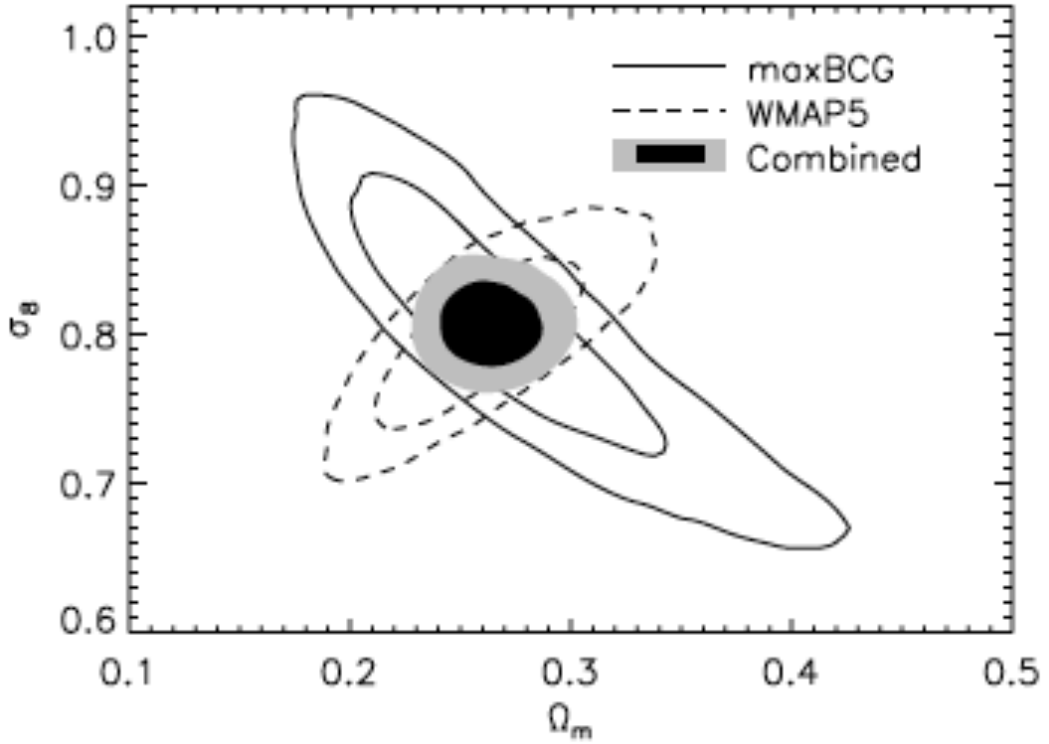

Constraints from SZ data: *ACT*

Atacama Cosmology Telescope ***ACT****:* surveyed 455 deg^2 at 148 GHz; a sample of 23 SZ-selected clusters was optically confirmed. *Sehgal et al. (2011)* make use of the subsample of 9 clusters with high-significance SZ detections (S/N> 5) to obtain cosmological parameter constraints.

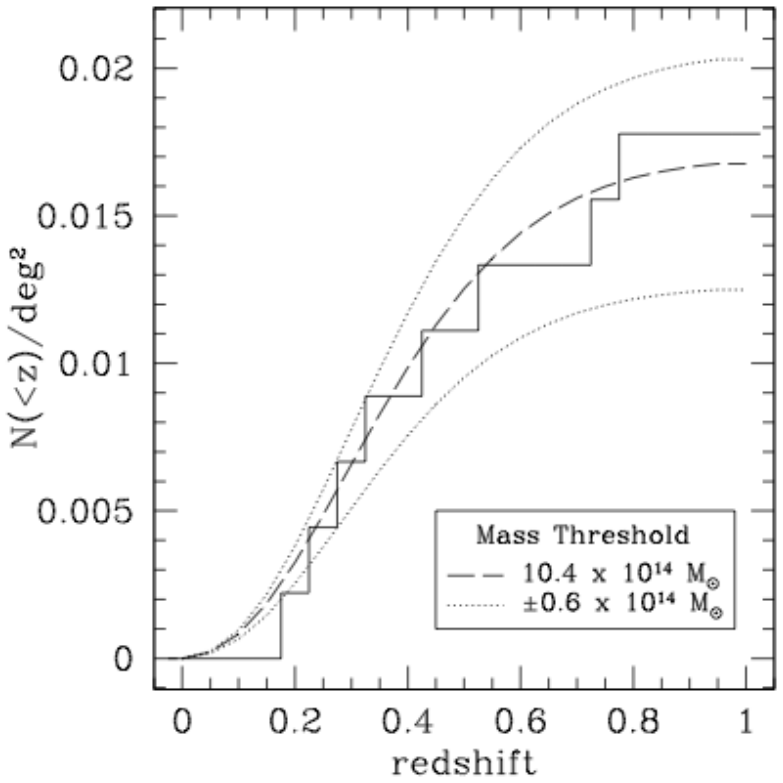

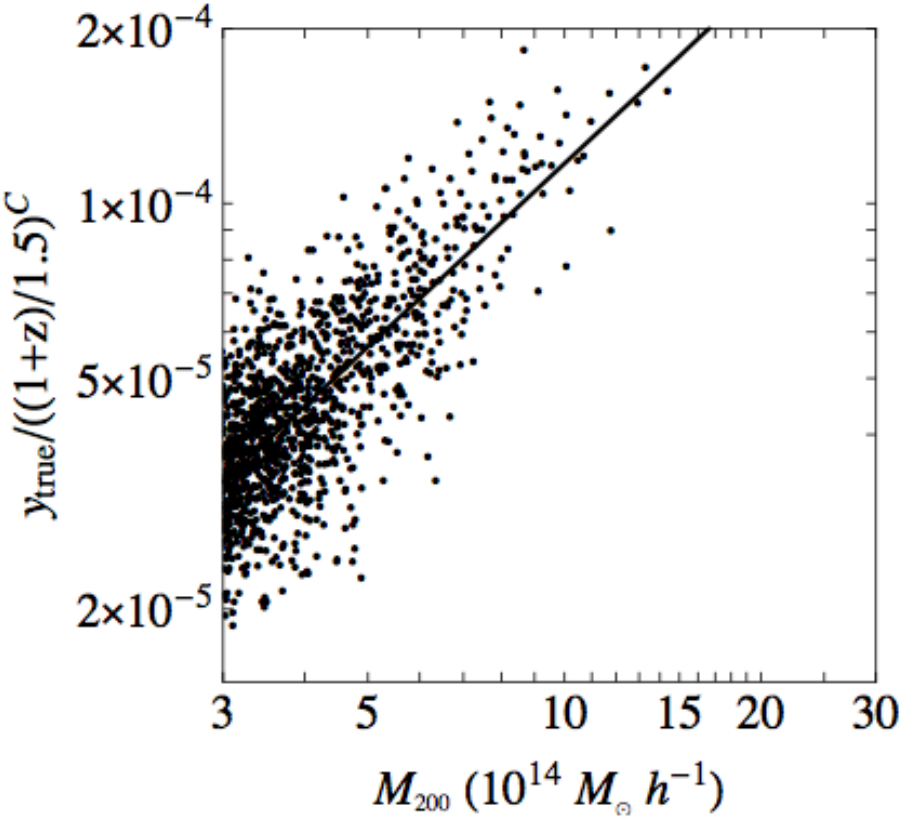

Constraints from SZ data: *ACT*

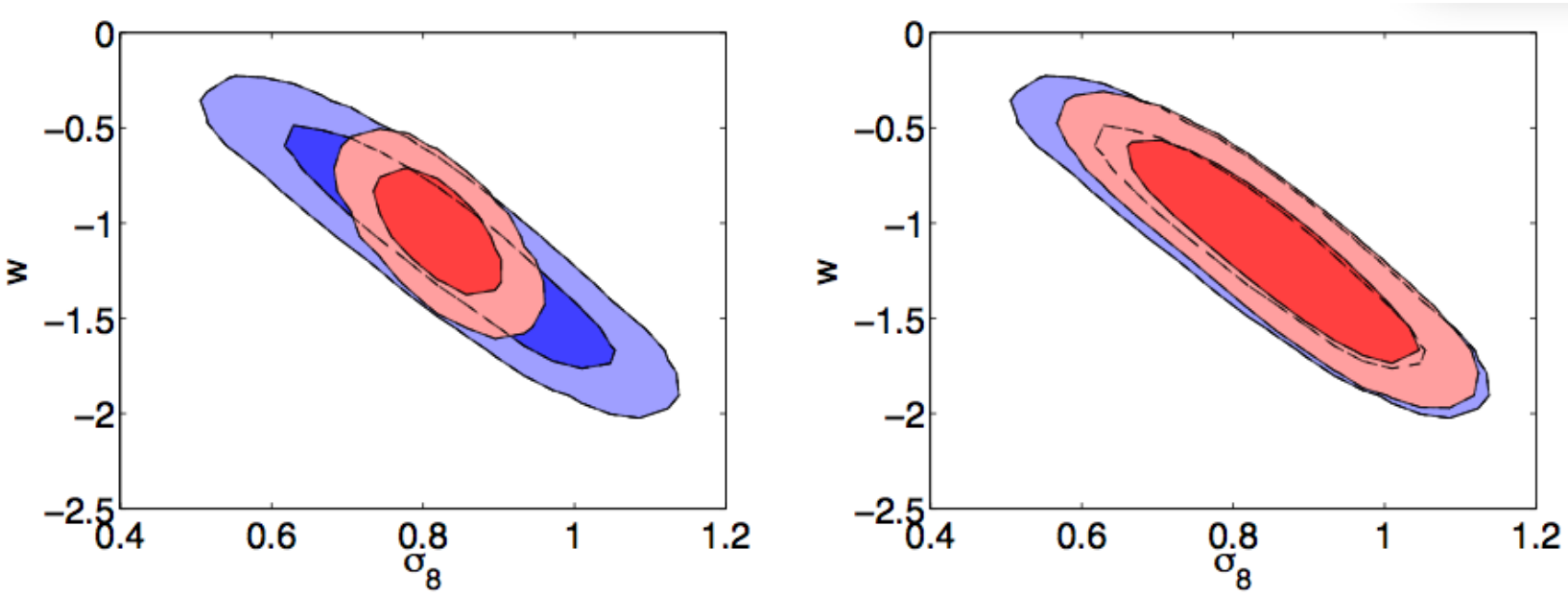

Blue contours: from WMAP7 alone

Red contours: including SZ clusters & fixing the parameters in the mass-observable relation (left), marginalizing over (right)

Constraints from SZ data: *SPT*

SPT (*Williamson et al. 11; see also Vanderlinde et al. 10*): 26 most significant SZ detection (12 new) in the z-range 0.1-1.13 (z_{med}~0.4) with M_{200}~1-3e15 $M_{\odot}$.

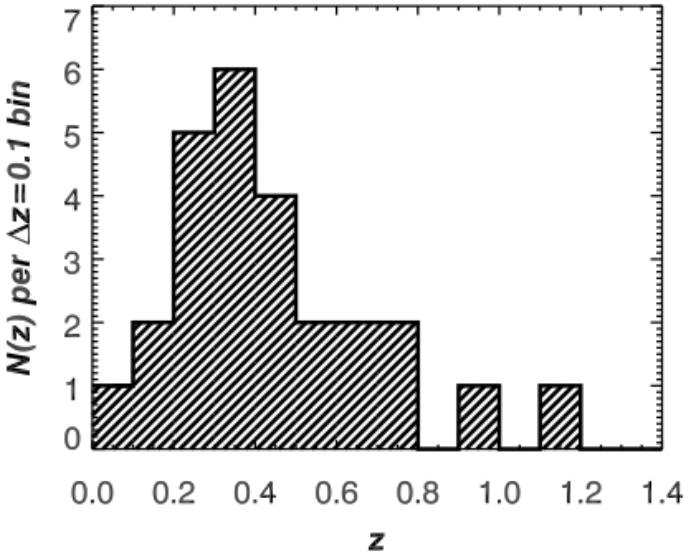

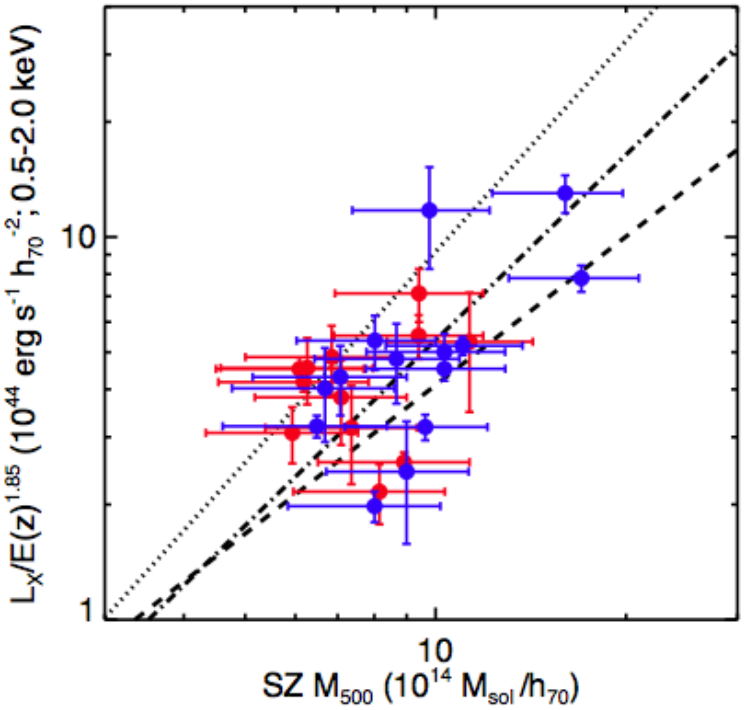

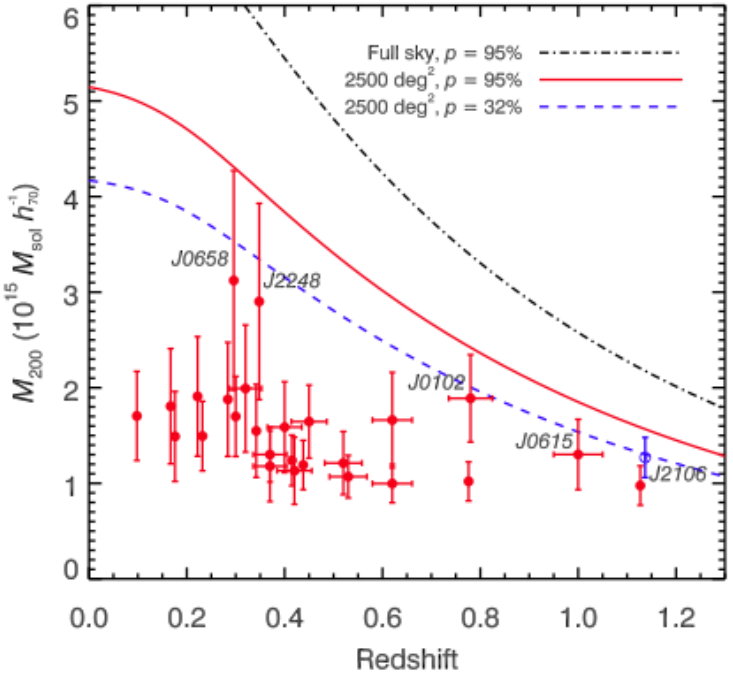

Constraints from SZ data: *Planck*

Planck: the Early SZ (ESZ) sample of 189 candidates comprises high signal-to-noise clusters, from 6 to 29. Planck provides the first measured SZ signal for about 80% of the 169 ESZ known clusters. Planck further releases 30 new cluster candidates among which 20 are within the ESZ signal-to-noise selection criterion. Eleven of these 20 ESZ candidates are confirmed using XMM-Newton snapshot observations as new clusters, most of them with disturbed morphologies and low luminosities. The ESZ clusters are mostly at moderate redshifts (86% with z below 0.3) and span over a decade in mass, up to the rarest and most massive clusters with masses above 1e15 $M_{\odot}$.

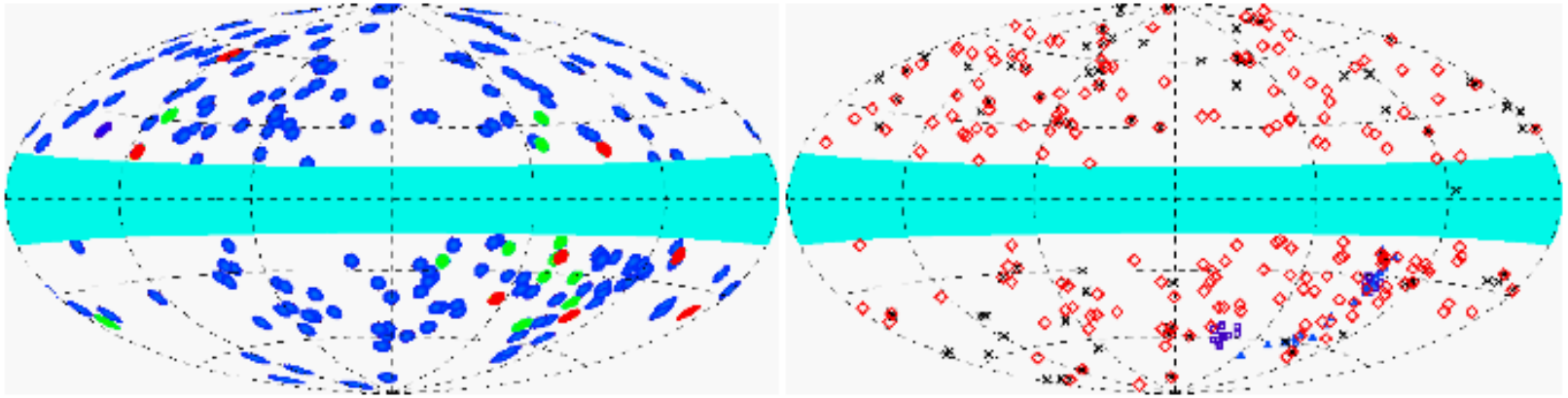

Fig. 3. Distribution of ESZ clusters and candidate clusters on the sky (Galactic Aitoff projection). Left panel: In blue are ESZ clusters identified with known clusters, in green the ESZ confirmed candidates, and in red the ESZ candidate new clusters yet to be confirmed. Right panel: In red diamonds the ESZ sample, in black crosses the compilation of SZ observations prior to 2010, in dark blue triangles ACT clusters from Menanteau et al. (2010), in purple squares SPT clusters from Vanderlinde et al. (2010). The blue area represents the masked area of $|b| < 14$ deg.

Constraints from SZ data: *Planck*

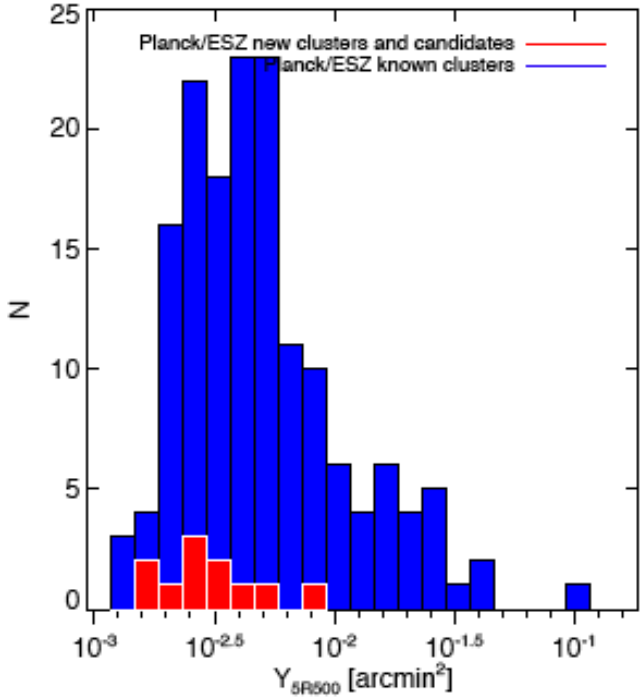

Y_X / L ➔ M

(still lack a selection function and thus an estimate of the cosmological volume sampled… more by 2013)

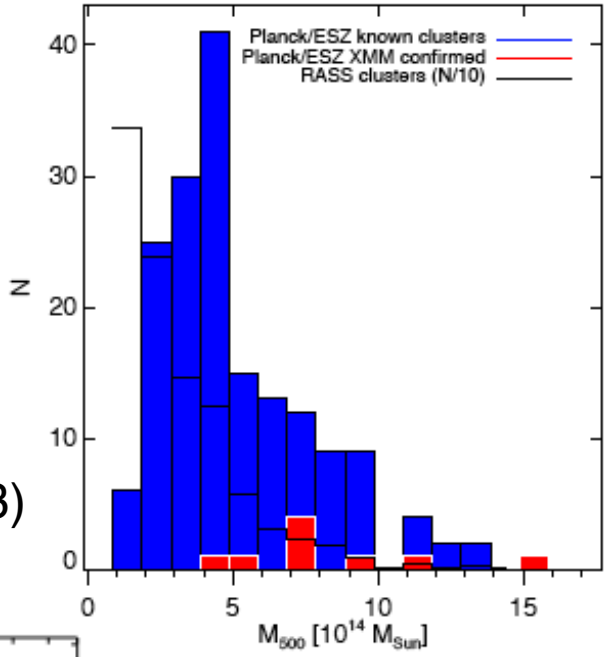

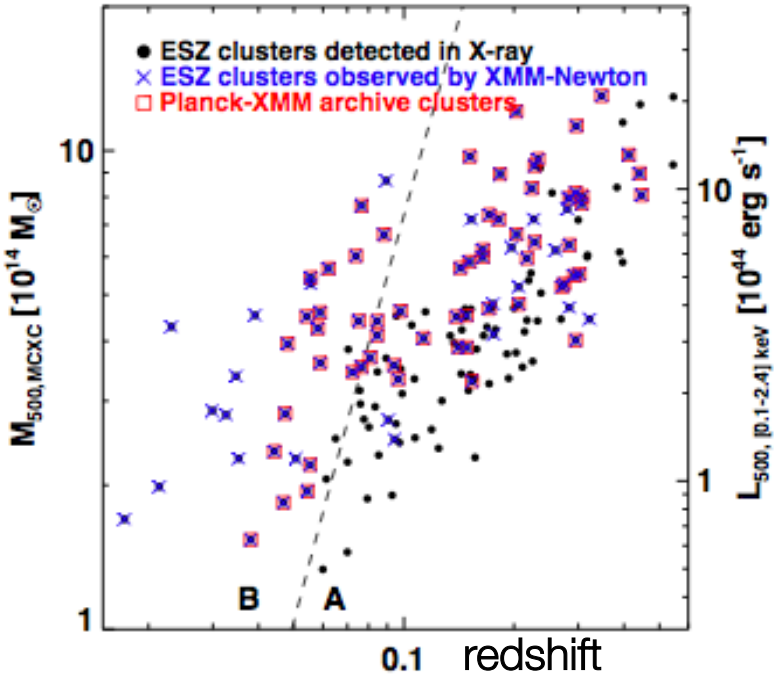

Dark energy with GC: note

Optical: constraints only on "local" cosmology ($\sigma_{8,}$ Ω_m; *no on w*) using 1e4 clusters

X-ray: constraints also on w_o(~20% at 1 σ) using 90-240 well-studied obj (*properties known for 1743 clusters, Piffaretti et al. 10*)

SZ: present surveys provide 20-190 detections; no significant constraints yet available